Wave transmission at various types of low-crested structures using neural networks

A joint master thesis about improving the prediction of the wave transmission coefficient with help of artificial neural networks and a homogeneous database

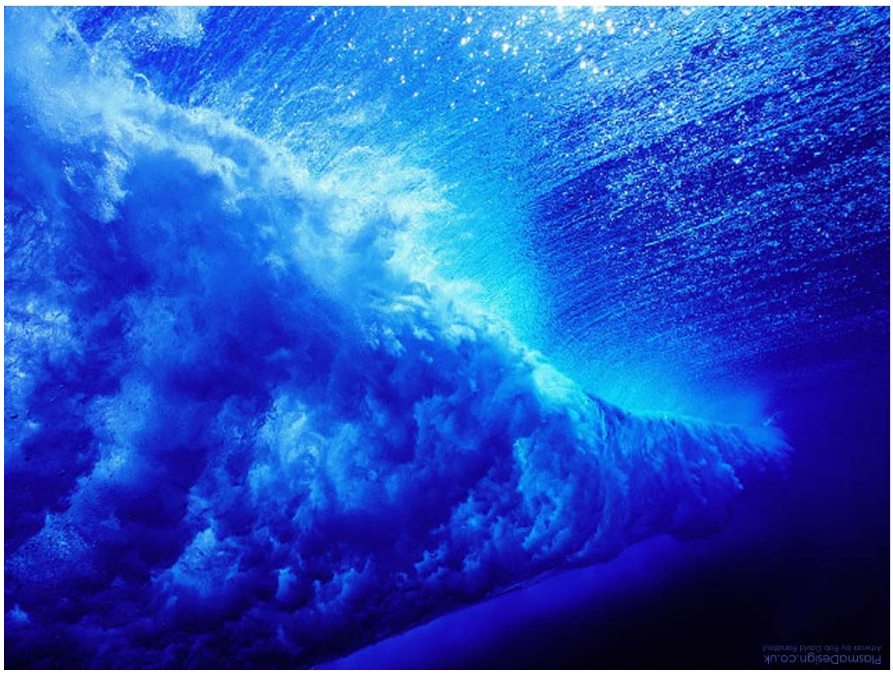

September 2005

M.Sc. Thesis
R.P. van Oosten
J. Peixó Marco

Delft University of Technology
Faculty of Civil Engineering and Geo Sciences

Table of contents

List of Tables

List of figures

List of Symbols

Symbol	Definition	Unit
α_f	Structure front side slope angle	[°]
α_B	Structure angle of the berm	[°]
$\alpha_{d\ f}$	Structure front slope angle downward of the berm	[°]
$\alpha_{u\ f}$	Structure front slope angle upward of the berm	[°]
$\alpha_{excl\ f}$	Structure mean front slope angle, without contribution of the berm	[°]
$\alpha_{incl\ f}$	Structure mean front slope angle, with contribution of the berm	[°]
$\alpha_{u\ b}$	Structure back slope angle upward of the lee side	[°]
A_c	Structure armour crest freeboard	[m]
β	Angle of wave attack with respect to the normal on a structure	[°]
B	Structure berm width (horizontal)	[m]
B_t	Width of the toe of the structure	[m]
B_h	Width of the horizontally schematized berm	[m]
CF	Complexity factor	[-]
D_{n50}	Nominal diameter, $(M/\rho)^{1/3}$	[m]
$\eta(t)$	Surface elevation with respect still water level	[m]
ξ	Surf similarity parameter, $(\tan \alpha / s_0^{0.5})$	[-]
f_p	Spectral peak frequency	[H_z]
g	Gravitational acceleration (=9.81)	[m/s^2]
G_c	Width of the armour crest of the structure	[m]
γ_f	Roughness / permeability factor for the structure	[-]
h	Water depth at the toe of a structure	[m]
h_t	Water depth on the toe of the structure	[m]

h_b	Water depth on the berm of a structure	[m]
$H_{1/3}$	Significant wave height derived from time domain analysis (=H_s)	[m]
H_{m0}	Significant wave height based on wave energy spectrum, $(m_0)^{1/2}$	[m]
$H_{m0\ deep}$	Significant wave height from spectral analysis determined at deep water	[m]
$H_{m0\ toe}$	Significant wave height from spectral analysis at the toe of the structure	[m]
$H_{mo\ trans}$	Significant wave height from spectral analysis behind the structure determined at one wave length distance from the structure	[m]
H_{rms}	Mean quadratic wave height (= $\sqrt{\sum_{i=1}^{N}\frac{H_i^2}{N}}$ with H_i the individual wave heights from time series	[m]
H_s	Significant wave height, average of highest 1/3 of all waves	[m]
K_t	Wave transmission coefficient ($H_{m0\ trans}$ / $H_{mo\ toe}$)	[-]
L_0	Deep water wave length based on $T_{m-1,0}$ = $gT^2_{m1,0}$ / 2π	[m]
m_n	$\int_{f_1}^{f_2} f^n S(f) df = n^{th}$ moment of spectral density f_1 = min(1/3.f_p, 0.05 full scale) f_2 = 3.f_p	[m^2/s^n]
m	Slope of foreshore	[-]
N_{ow}	Number of overtopping waves	[-]
N_w	Number of incident waves	[-]
P(x)	Probability distribution function	[-]
p(x)	Probability density function	[-]
P	Notional permeability factor (Van der Meer 1988a)	[-]
p_f	Ratio of nominal core diameter over nominal armour diameter	[-]
P_{ow}	Probability of overtopping per wave (=N_{ow} / N_w)	[-]
q	Mean overtopping discharge per meter structure width	[m^3/m/s]
R	Correlation coefficient	[-]
R_c	Crest freeboard of the structure	[m]
RF	Reliability Factor	[-]
RMSE	Root mean square error	[-]
s_0	Wave steepness (=H_{m0} / L_0)	[-]
S(f)	Spectral wave density	[m^2/H_z]
$T_{1/3}$	Significant wave period derived from time domain analysis (=T_s)	[s]
$T_{m-1,0}$	Spectral mean wave period	[s]
$T_{m-1,0\ deep}$	Mean period from spectral analysis in deep water	[s]

$T_{m0,2}$	Spectral mean wave period	[s]
$T_{m\ deep}$	Mean period from spectral analysis or from time domain analysis determined at deep water	[s]
$T_{m\ toe}$	Mean period from spectral analysis or from time domain analysis at the toe of the structure	[s]
T_p	Spectral peak wave period	[s]
$T_{p\ deep}$	Peak period from spectral analysis determined at deep water	[s]
$T_{p\ toe}$	Peak period from spectral analysis determined at the toe of the structure	[s]
T_s	Significant wave period	[s]
W_c	Total width of the crest of the structure	[m]
WF	Weight factor	[-]

Abbreviation	**Definition**
aNN	Artificial neural network
B_n	n^{th} bias unit
H_n	n^{th} hidden unit
i	Number of input parameter
I_i	i^{th} input unit
L	number of aNN's which have been generated by means of bootstrap resampling
N	number of tests of the ROD
MLP's	Multilayer perceptrons
n	Number of neuron in the hidden layer
O_j	j^{th} output unit
RBF's	Radial basis functions
ROD	Reduced original database
TF	Transfer function
W_{ni}	Weight parameter from the I_i to H_n

Preface

The report in front of you is the result of our joint master thesis, which we have worked on for over seven months. During this period we have proven to ourselves that with a lot of patience, joy, knowledge and some fine humor, a thankful result can be obtained. In advance of this thesis a lot of elements of the subject were new for both of us, but in a relative short period of time we managed ourselves to get familiar with it. Reinoud has mainly been focusing on the composure of the homogeneous database and analyzing the database. At the same time Jordi made the right architecture of the neural network and programming of the prediction model. We both have carried out all elements of the study where the homogeneous database and neural network are combined.

We want to thank the committee members of this thesis for their supervision and guidance:

Prof. Dr. Ir. M.J.F. Stive (TU Delft)
Prof. Dr. R. Babuška (TU Delft)
Ir. H.J. Verhagen (TU Delft)
Dr. Ir. J.W. van der Meer (Infram)
Dr. Ir. M.R.A. van Gent (WL | Delft Hydraulics)
Dr. Ir. H. Verhaeghe (Ghent University)

In particular we want to thank J.W. van der Meer, M.R.A. van Gent and H.J. Verhagen for their advice and helpful support during the whole thesis. We acknowledge their contribution to this final report.

The authors,

Ing. R.P. van Oosten
J. Peixó Marco

Delft, 07 September 2005

"We believe that if men have the talent to invent new machines that put men out of work, they have the talent too to put those men back to work."

(John Fitzgerald Kennedy (1917-1963), U.S. Democratic politician, President of the U.S. speech, Sept. 27, 1962, Wheeling, West Virginia)

Summary

Introduction

Wave transmission is often an important criterion in the design of a low-crested breakwater structure and influences early decisions on the type of the structure and the applied construction material. In design stages classical formulae are used to predict the wave transmission coefficient K_t [-]. The finished European Union funded project DELOS was focused on wave transmission and an extensive database on low-crested rubble mound structures was generated. During DELOS, a new empirical wave transmission formula was found (Van der Meer et al., 2004), but still showed a considerable scatter, probably due to a limited number of parameters included.

Another recently finished EU-project, named CLASH was concentrating on wave overtopping (high-crested structures). An extensive homogeneous database was composed (Verhaeghe et al., 2003). Homogeneous means that every available dataset was screened carefully before the data was included to the database. A new aspect of this database was that the geometry of every type of structure could be described by a limited number of parameters (toe, berm, crest, slopes, etc.). The second part of CLASH involved the development of a prediction tool, using neural networks in combination with resampling techniques. This kind of neural networks is difficult to make, but easy to use for people in this field of interest. The use of the database on its own and the neural network for wave overtopping have been shown already (Van der Meer et al., 2005)

This paper concentrates on wave transmission and is based on both European Union projects DELOS and CLASH. The main objectives of this study are:

- Screening the existing wave transmission database of DELOS in order to make it homogeneous and collecting new datasets to add to the DELOS database.
- Developing a prediction model based on neural networks according to the existing CLASH method.
- Using the homogeneous database and prediction model to analyze the influence of various parameters for wave transmission and comparing this with the existing DELOS empirical formulae.
- Making the prediction method available to users in the field of coastal engineering.

For wave transmission a simple neural network has already been tested for some DELOS datasets and promising results were obtained (Panizzo et al., 2003). The present study aims to improve the prediction of the wave transmission coefficient with the successful methods of CLASH. Till present, the last two mentioned objectives have not often been applied by developers of a neural network and this is certainly new in this field.

Homogeneous database

The DELOS database includes 2,337 wave transmission tests and is made homogeneous according to the CLASH-work database during this study. Another 1,597 tests have been added to the database to a total of 3,934 tests. The database consists of a variety of tested breakwater structures: mound structures (permeable and impermeable) as well as smooth structures (impermeable). All these structures have their own characteristics and behave differently for wave transmission. An important

issue is to use parameters that represent the characteristics of those structures. This is found possible with a selection of parameters of the CLASH-database (Steendam et al., 2004 and Verhaeghe et al., 2003).

For each test, imposed hydraulic and structural parameters have been determined. The database consists of 19 structural parameters and 10 hydraulic parameters, describing the available tests. Missing hydraulic parameters are calculated with the numerical wave model SWAN (Booij et al., 1999) and the empirical model of Battjes and Groenendijk (2000). Depending on the reliability of the measurements a 'reliability-factor' is assigned, ranging from 1 (very reliable) to 4 (unreliable). Test reports have been examined in order to judge the reliability. Also a 'complexity-factor' is assigned, depending on the difficulty of describing / characterizing the considered test section with the structural parameters, ranging from 1 (simple section) to 4 (very complex section).

Prediction model architecture

The empirical formulae of DELOS (Briganti et al., 2003 and Van der Meer et al., 2004) contain a limited number of parameters. In the present study more parameters have been introduced found important for wave transmission. The parameters are selected, based on physical reasoning and from findings of earlier studies. The parameters that are selected for the final prediction model are presented for a typical section in the figure below.

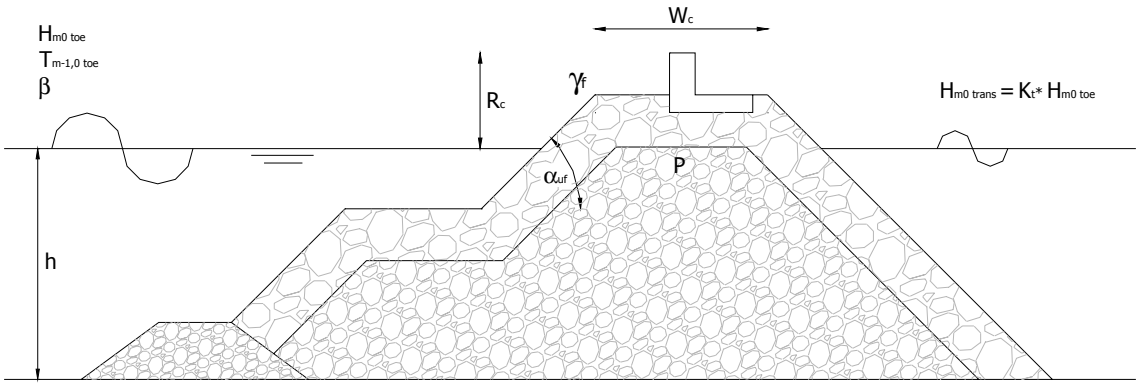

Overview of parameters used within the prediction model for a breakwater section

Different from CLASH is the selection of the total crest width W_c [m] and the notional permeability factor P [-]. Different from the empirical formulae from DELOS are the water depth at the toe of structure h [m], the roughness factor γ_f [-] and the notional permeability factor P [-]. With including the roughness factor and the notional permeability factor it is found possible to handle both mound and smooth structures within one single prediction model, although these structures behave completely different on wave transmission. The advantage of handling both types of structures within one model is that the model is capable of finding common important parameters and parameters that distinguish these different structures, making it possible to handle structures in between as well. Very few datasets with composed structures with a parapet and structures applied with berm were present in the database, which made some parameters from CLASH pre-empt. Note that all used parameters are present at the crest of the low-crested structure, around sea water level.

The CLASH prediction method (Van Gent et al., 2004 and Verhaeghe, 2005) is applied in this study as well. This is a Multilayer Perceptron Neural Network, with the Bayesian Regularization as training algorithm.

The final prediction model of this study is also carried out by means of an ensemble of neural networks. This ensemble is obtained from a certain number of neural networks, which are trained based on a bootstrap resampling technique (Van den Boogaard et al., 2000). The training and testing process are repeated many times to solve the problem of representativeness of the training and testing set. Secondly the ensemble of NN's results in a set of predictions from which an uncertainty assessment is made. Confidence intervals have given insight in the reliability of the prediction.

Prediction model validity and boundaries

The present prediction model shows significantly improved predictions of the wave transmission coefficient compared to the existing empirical formulae. The prediction model has proven to be capable of handling both smooth and mound structures, although their behavior to wave transmission is found completely different.

The following boundaries of input parameters are found to give reliable and valid predictions.

Input Parameter	**Prediction model input boundary**
Incident significant wave height, $H_{m0\ toe}$ [-]	$H_{m0\ toe} > 0.03$m $H_{m0\ toe} / h < 0.50$
Mean wave steepness, $s_{0\ m-1,0\ toe}$ [-]	$0.009 < s_{0\ m-1,0} < 0.060$
Mean angle of wave incidence, β [^{o}]	$0^o < \beta < 70^o$
Relative water depth, $h / H_{m0\ toe}$ [-]	$1.20 < h / H_{m0\ toe} < 9.80$
Relative crest freeboard, $R_c / H_{m0\ toe}$ [-]	$-2.00 < R_c / H_{m0\ toe} < 0.70$
Relative crest width, $W_c / H_{m0\ toe}$ [-]	$0.60 < W_c / H_{m0\ toe} < 6.00$
Upward front slope, cot $\alpha_{u\ f}$ [-]	$1.0 < \cot \alpha_{uf} < 3.8$
Roughness factor, γ_f [-]	1.0
Notional Permeability factor, P [-]	0.10

Prediction model input boundary for smooth structures

Parameter considered	**Prediction model input boundary**
Incident significant wave height, $H_{m0\ toe}$ [-]	$H_{m0\ toe} > 0.03$m $H_{m0\ toe} / h < 0.50$
Mean wave steepness, $s_{0\ m-1,0\ toe}$ [-]	$0.006 < s_{0\ m-1,0} < 0.080$
Mean angle of wave incidence, β [^{o}]	$0^o < \beta < 45^o$, but enter as input value: $\beta = 0^o$
Relative water depth, $h / H_{m0\ toe}$ [-]	$1.55 < h / H_{m0\ toe} < 11.00$
Relative crest freeboard, $R_c / H_{m0\ toe}$ [-]	$-3.50 < R_c / H_{m0\ toe} < 1.80$
Relative crest width, $W_c / H_{m0\ toe}$ [-]	$0.01 < W_c / H_{m0\ toe} < 47.00$
Upward front slope, cot $\alpha_{u\ f}$ [-]	$1.0 < \cot \alpha_{uf} < 5.0$
Roughness factor, γ_f [-]	$0.38 < \gamma_f < 0.90$
Notional Permeability factor, P [-]	$0.10 < P < 0.60$

Prediction model input boundary for mound structures

All parameters that are used in the DELOS formulae and in the present prediction model as well are showing physically tendencies between the given boundaries. The relevant parameters that were introduced in this study new for wave transmission have shown to be important for the prediction of wave transmission. The water depth at the toe of structure h [m] is found important for smooth structures, contrary for mound structures where other parameters are apparently dominating wave transmission resulting in a smaller influence. For an increasing water depth the wave transmission decreases for smooth structures. No explanation is given in this study, but it is expected, the water depth having its influence on wave transmission, affects the shape of the incident waves. The roughness factor γ_f in combination with the notional permeability factor P [-], are found important to distinguish mound from smooth structures and also handling types of structures in between for different permeability's and various types of armour units.

Application of the model for future users

The model is very suitable for predicting the wave transmission coefficient for conventional smooth- and mound breakwater structures by future users, although one should have some knowledge about the physics involved in the field of coastal engineering to interpret the results right. At this moment the model is using the software packages MS Excel and Matlab 7, but some possibilities are proposed to make the prediction model available for future users. Some possibilities are: Linking the Matlab

interface to a PHP-web page, compiling the Matlab interface to a stand-alone downloadable program or to use Excel as interface, instead of Matlab.

The strength of the prediction model is that it not only predicts a K_t, but also gives insight in the reliability of the prediction itself. One has the possibility to perform a sensitivity analysis to all input parameters in order to obtain an optimal design and a reliable predicted K_t. For design purposes the model is therefore very suitable, because in a short period of time one can have a reliable indication of a breakwater structure with a transmission coefficient that fulfils the design criterion on this point.

1 Introduction

1.1 Study background

Wave transmission is often an important criterion in the design of a breakwater structure and influences early decisions on the type of structure and the applied construction material. In design stages classical formulae are used to predict the wave transmission coefficient. The finished European Union funded project DELOS was focusing on wave transmission and an extensive database on low-crested mound structures was generated. During DELOS, a new empirical wave transmission formula was found, but still showed a considerable scatter, probably due to a limited number of parameters included.

Another recently finished EU-project, named CLASH was concentrating on wave overtopping. An extensive homogeneous database was composed. Homogeneous means that every available dataset was screened carefully before the data was included to the database. A new aspect of this database was that the geometry of every type of structure could be described by a limited number of parameters (toe, berm, crest, slopes, etc.). The second part of CLASH involved the development of a prediction tool, using neural networks in combination with resampling techniques. These kind of neural networks are difficult to make, but easy to use for people in this field of interest. The use of the database on its own and the neural network prediction model for wave overtopping have been shown already (Van der Meer et al., 2005).

The study described in this report concentrates on wave transmission and is based on both European Union projects DELOS and CLASH. For wave transmission a simple neural network has already been tested for some DELOS datasets and promising results were obtained (Panizzo et al., 2003). The present study aims to improve the prediction of the wave transmission coefficient with the successful methods of CLASH.

The main objectives of this study are:

- Screening the existing wave transmission database of DELOS in order to make it homogeneous and collecting new datasets to add to the DELOS database.
- Developing an accurate prediction model, based on neural networks according to the existing CLASH prediction method.
- Using the homogeneous database and prediction model to analyze the influence of various parameters in wave transmission and comparing this with existing empirical formulae.
- Making the prediction model available to users in the field of coastal engineering.

Till present, the last two mentioned objectives have not often been applied by developers of a neural network and this is certainly new in this field.

1.2 Problem definition

1.2.1 Main question

The main question of this study can be formulated as follows:

Is it possible to obtain accurate and improved results in predicting the wave transmission behind various types of low-crested structures with use of a predicting model, based on neural networks and a homogeneous database as starting point?

1.2.2 Sub questions

In addition to the main question the following sub questions arise:

- Which suitable parameters, influencing wave transmission, should a homogeneous database contain in order to describe the hydraulic and structural properties of available test data well?
- How reliable are these parameters and do they describe the structure well for each individual test?
- Which parameters of the homogeneous database show influence in the prediction model of the wave transmission coefficient and what parameters could be neglected because of minor influence?
- What is the accuracy and improvement compared to the results of the neural network made by Panizzo et al. (2003) and the DELOS formulae (Van der Meer et al., 2004)?
- Depending on the out comings of the questions mentioned above: Could this prediction model be made available for users in the field of coastal engineering?

1.3 Goal description

1.3.1 Aim of the study

The aim of this study is to find possibilities to make a widely applicable prediction model for wave transmission behind various types of low-crested structures. Accuracy and simplicity are important factors that make this prediction model useful or not. Until now, wave transmission could only be predicted with classical formulae and with help of a simple neural network for only mound type of breakwater structures. This study is mainly focused to improve the use of neural networks as prediction model for wave transmission by:

- Making the prediction of the wave transmission coefficient more accurate with use of a homogeneous database and neural networks in combination with resampling techniques (CLASH method).
- Making it possible to handle a variety of types of low-crested breakwaters, in such a way the prediction model can be used in a wide range (for instance permeable and impermeable structures or rough and smooth structures).
- Making the prediction model available for future users, like classical formulae are used at this moment.

1.3.2 Mission statement

The mission of this study can be summarized in one sentence:

> *"Obtain and apply an accurate and available prediction model for the wave transmission coefficient, for various types of low-crested breakwater structures, with help of neural networks in combination with resampling techniques and a homogeneous database."*

1.4 Methodology

In general the same methodology of CLASH is followed during this study, adjusted to the subject of wave transmission. A homogeneous database is used as starting point to train a neural network in combination with resampling techniques. The obtained prediction model can be used to predict the wave transmission in a better way than existing classical formulae and gives insight in the accuracy and parameter influences.

2 Review on wave transmission

This chapter gives a brief review on wave transmission. A small literature study is performed on this subject in advance of the main study itself. In the second paragraph, different types of low-crested breakwater structures will be defined. Secondly, the governing parameters affecting wave transmission will be discussed, followed by a description of the most relevant studies on this subject.

2.1 The wave transmission phenomenon

Breakwaters are applied worldwide to create sheltered areas for commercial, recreational, environmental or protective reasons. When incident waves are blocked by a high-crested breakwater structure, most of the wave energy will be dissipated and there will appear some reflection. Energy dissipation can be clearly visual in the form of spectacular wave attacks causing severe wave overtopping, expressed in a discharge or in a percentage of the total incident waves.

As the name already implies, low-crested structures have relative small crest freeboards compared to the incident waves, and are frequently or always overtopped. In this case, one speaks of wave transmission instead of wave overtopping, expressed as ratio of the transmitted wave height over the incident wave height. A transmitted wave can often be clearly noticed at the leeside of a low-crested structure.

Figure 2-1 Overtopping or transmission?

One can think of many cases where low-crested are more favorable than high-crested structures. Breakwaters are very costly and a smaller crest height simply gives a considerable cost reduction. In areas where shore erosion is causing problems, submerged structures are often preferred, because of the limited visual impact, while being effective in reducing the height of incident waves before they reach the shore. There are even plans proposed to build an offshore submerged breakwater along the Dutch coast to offer sufficient protection against the onslaught of the waves during notorious westerly storms. This plan is based on experiences in protection isles in Dubai. It is clear, that the main design criterion for low-crested structures is the allowable wave transmission coefficient and therefore very interesting to predict in early design stages.

2.2 Types of low-crested structures

There exist many types of breakwater structures, which can be divided according to their structural characteristics. This study is only including low-crested breakwater structures. Low-crested breakwaters are structures, which are regularly or always overtopped by the incident waves (according to the DELOS project definition). Most artificial structures of this type along European shores are constructed with rubble mound jetties. DELOS was therefore restricted to this type of structures and to natural boulder reef as term of comparison. During this study more type of

structures than within DELOS have been taken into account. All present structures will be defined in the following paragraphs.

2.2.1 Mound type breakwaters

Mound types of breakwaters are actually no more than large heaps of loose elements, such as gravel, quarry stone or for instance concrete units. The stability of the exposed slope of the mound (the armour layer) depends on the ratio between load (waves) and strength (weight of elements). A 'statically stable breakwater' is a structure where the weight of the elements in the armour layer is sufficient to withstand wave forces. These are usually the widely applied conventional rubble mound structures. Reef breakwaters are made of homogenous materials and are dynamically stable. The structure is allowed to deform under severe wave attack. Submerged structures are breakwaters completely present under sea water level. Some cross sections of mound breakwater structures are given in Figure 2-2.

Special types of mound breakwaters are artificial reefs, consisting of special armour units. These units are placed on top of rubble mounds and are usually submerged. These structures behave more or less the same as other mound type breakwaters (found to be very permeable) and will be treated like mound type breakwaters.

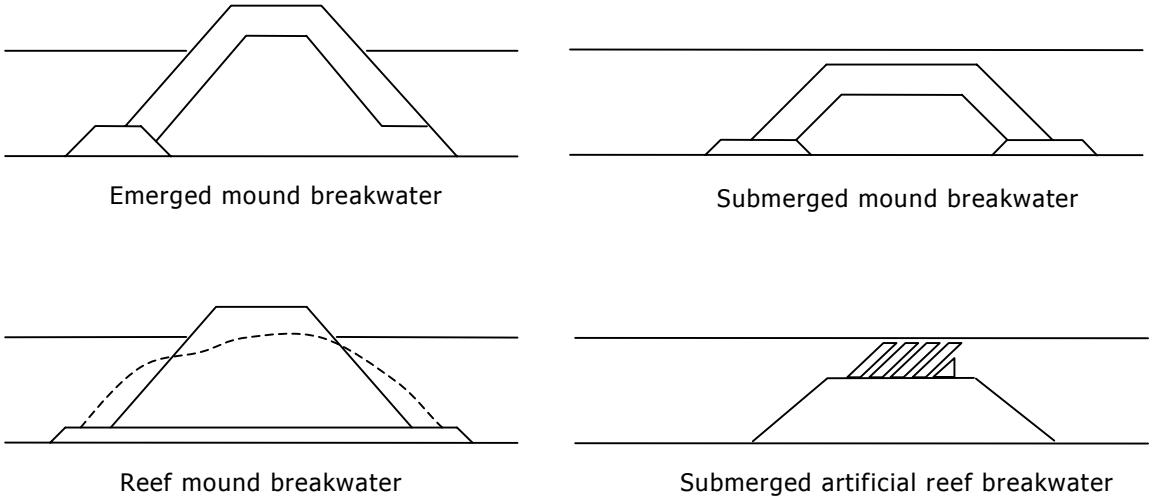

Figure 2-2 Mound type of breakwaters

2.2.2 Smooth type breakwaters

Smooth type breakwater structures are treated separately, although these structures can partly be composed of loose material. Smooth structures always have a smooth and impermeable cover layer. Only wave overtopping causes wave transmission, because transmission through the structure is simply impossible. Logically, these structures are always statically stable under wave attack and can be submerged as well. The structure can be covered with an impermeable material like concrete or with an asphalt layer, but also very densely packed revetments can cause a smooth and impermeable surface. Smooth type breakwaters behave very differently on wave transmission and one of the big challenges of this study is to handle these types of structures within one neural network with other type of structures.

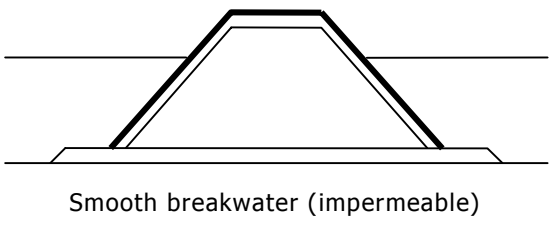

Figure 2-3 Smooth type of breakwater

2.2.3 Composite breakwaters

Composite types of breakwaters combine a monolithic element with a berm composed of loose elements. In fact, there is an abundance of alternatives that combine a rigid element and a flexible structure. The difference with a caisson type breakwater is that there is clearly a separated structure present, placed on top of a rubble mound.

2.3 Parameters influencing wave transmission

To obtain a valid and useful prediction model it is important to have pre-knowledge of the parameters influencing wave transmission. A division is made in hydraulic and structural parameters, influencing wave transmission.

2.3.1 Hydraulic conditions

Incident wave height
The most important hydraulic parameter involved in wave transmission, is the incident wave height. In case of irregular waves, this parameter is commonly expressed like the significant wave height. The incident wave height is directly present in the definition of the wave transmission coefficient K_t:

$$K_t = \frac{H_{m0\ \ transmitted}}{H_{m0\ \ incident}} \ [-] \qquad \textit{Eq. 2.1}$$

Other parameters are always related to the incident wave height. A crest freeboard for instance can only be called high if the incident wave height is relatively small. A stone diameter can only be called small if the incident wave height is relatively large. If the term relative is used in this report, it is in general meant relative to the incident wave height.

Incident wave period
For the incident wave period can be stated, that a longer wave period means lower wave steepness for a constant wave height. For mound structures without overtopping, waves with a longer period can propagate easier through the structure and therefore give a larger K_t. For mound and smooth structures as well that are overtopped, lower wave steepness will increase the wave run-up and from this it results in more wave transmission.

For submerged breakwaters, Van der Meer (1990) found that longer waves could pass unhindered, while the breakwater influenced the shorter waves. The best way to describe the incident wave period is from a spectral analysis. It is found that the spectral mean wave period $T_{m-1,0\ toe}$ is most suitable to be used for coastal structures, because of usually shallow water conditions (TAW, 2002).

Angle of incidence
According to Van der Meer et al. (2004), the influence of the angle of incidence to the normal of the structure is related to the permeability of the structure. The influence is non to marginal for a rubble mound structure, whereas the influence for the smooth structures is quite relevant. For smooth structures the wave transmission coefficient decreases significantly with an increasing angle of incidence. More wave energy is transposed in the lateral direction of the breakwater structure and less wave energy is present to the lee side of the structure if the angle of incidence increases to the normal of the structure.

2.3.2 Geometry of structures

Crest freeboard
The structure crest freeboard, often symbolized as R_c in most reports, is the distance between sea water level and the crest of the breakwater structure. In every study the crest freeboard is found to be one of the most important structural parameters for wave transmission.

For emerged impermeable structures, wave run-up only determines the degree of overtopping and therefore wave transmission. Transmission through the structure itself is for impermeable structures zero. Wave transmission will not occur providing there is no overtopping. A decreasing relative crest freeboard leads to more overtopping. Therefore, the transmission coefficient K_t will increase. For mound structures, although the wave energy transfer through the structure body affects

transmission, the crest freeboard still plays an important role in wave overtopping. In general, a higher relative freeboard gives a lower transmission coefficient.

When a structure (mound or smooth) is submerged and the crest is situated well below the water level, the influence of the crest freeboard will disappear. Nevertheless, the crest freeboard R_c is found to be one of the most important parameters for both rubble mound (rough) and smooth structures and is always taken into account in transmission studies.

Crest width
Previous studies, including the DELOS project, indicated that the influence of the crest width is obvious: A wider crest will reduce wave transmission (Briganti et al., 2003). At low-crested structures, a larger relative crest width will lead to a longer way for the waves to overtop the structure and therefore more wave energy dissipation is present. Van der Meer and Daemen (1994) summarized the influence of the relative crest width for submerged structures. An increasing relative crest width will force the waves to break and therefore more energy is dissipated on the crest, resulting in a lower transmission coefficient. A small relative crest width has no influence on wave transmission at all.

For the case of emerged smooth structures, the crest width has small influence, because all overtopped water discharges will pass over the structure, independently of the width (to a certain level of course).

Structure slopes
For emerged structures, the seaside slope influences wave run-up and therefore wave overtopping, hence wave transmission. On the gentler slope more energy will be dissipated and less transmission occurs. The seaside slope is included in the surf similarity parameter, also known as the Iribarren number (ξ), describing the type of wave breaking on the slope itself, and has its influence on wave transmission. For submerged breakwaters the seaside slope seems to be of minor importance, because wave run-up is not present.

The influence on the leeside (back) slope is not been studied in the past. It is expected to be of minor importance, as the lee side is not influencing the type of breaking. On the other hand, a gentler back slope causes more wave energy dissipation as the waves have to travel a longer distance.

Berm presence
Some breakwaters are applied with a berm, although not often applied for low-crested structures as the crest itself is already present around sea water level. A berm is a horizontal area at the seaward slope of a breakwater structure to affect incident waves by forcing them to break. At sea water level a berm is most effective in dissipating wave energy. To identify a berm it has to fulfill this property of affecting incident waves, hence it has to be positioned in the centre area of the structure because there wave action is concentrated.

Toe presence
A toe looks at first sight the same as a berm, but is usually situated well under the water level. A toe is placed for stabilizing the armour layer and is not intended for dissipating wave energy. Usually a toe is made of a lighter material than the armour layer. However, a toe can be felt by incident waves, especially when the water level is relative low and is present within the area of influence.

2.3.3 Material properties

Surface roughness / permeability
The roughness and the permeability of the surface of a breakwater structure are also affecting the wave energy dissipation. In general can be stated, that the rougher and more permeable a surface, more wave energy will be dissipated. The roughness and permeability are important for emerged breakwaters, because they are strongly influencing wave overtopping and wave run-up and therefore wave transmission. The roughness and permeability of the surface become less important for submerged structures, because in those cases wave run-up is not present and the crest is below sea water level.

Smooth and mound structure behave completely different for wave transmission. At smooth surfaces almost no wave energy is dissipated due to friction and permeability effects. Contrary to mound structures where in case of very rough structures, the surface can dominate the wave transmission

phenomenon. Because of the influence of the roughness, in case of smooth structures other parameters can show more influence on wave transmission than the case for mound structures, like explained in the case for the angle of incidence, crest freeboard, crest width and the slopes.

Core permeability
Breakwater structures with a permeable surface (armour layer) and a permeable core (rubble), allow waves to travel through the structure itself and contribute to wave transmission as well. The core permeability is of importance for breakwater structures with a relative high crest freeboard. Wave overtopping for relative low crest freeboards mainly causes wave transmission.

An impermeable core will block incident waves traveling through an emerged breakwater structure, resulting in a lower transmission. Highly permeable structures (homogeneous) allow waves to travel through the structure, but overtopping waves will experience this same effect and a lot of wave energy is dissipated.

2.4 Relevant studies on wave transmission

Many studies have been performed in the past to get better insight in wave transmission. The recent DELOS project was focusing on wave transmission and improvements have been made. The most relevant studies on wave transmission, close related to this study, are treated in this paragraph.

2.4.1 Van der Meer and Daemen (1994)

Van der Meer (1990) proposed a formula for wave transmission in his report "Data on wave transmission due to overtopping". The analysis on data sets of wave transmission led to a practical formula in Daemen (1994). Where Van der Meer (1990) used the incident wave height H_i to make R_c dimensionless, Daemen introduced the nominal diameter D_{n50} to make R_c and H_i as well dimensionless. The influence of both R_c and H_i could be studied individually.

2.4.2 D'Angremond et al. (1996)

d'Angremond et al., 1996 (often also referred to De Jong) proposed another transmission formula for mound structures. The formula was derived, based on available data on rubble mound breakwaters and breakwaters with an armour layer of Tetrapods. An extensive investigation on the influences of crest width and surf similarity parameter was carried out in this research.

For mound structures:

$$K_t = -0.4\frac{R_c}{H_{si}} + 0.64\left(\frac{B}{H_{si}}\right)^{-0..31}\left(1 - e^{-0.5\xi}\right) \qquad \textit{Eq. 2.2}$$

Having a lower boundary of: $K_{tl} = 0.075$

Having a upper boundary of: $K_{tu} = 0.8$

For smooth structures:

$$K_t = -0.4\frac{R_c}{H_{si}} + 0.80\left(\frac{B}{H_{si}}\right)^{-0..31}\left(1 - e^{-0.5\xi}\right) \qquad \textit{Eq. 2.3}$$

Having a lower boundary of: $K_{tl} = 0.075$

Having a upper boundary of: $K_{tu} = 0.8$

2.4.3 Briganti et al. (2003)

Briganti et al. (2003) analyzed the extensive DELOS database and used the 2D random wave datasets to improve the prediction of the transmission coefficient starting with the formulae of Van der Meer and Daemen (1994) and d'Angremond et al. (1996). The same set of parameters was used

as the governing ones for wave transmission in the aforementioned papers. The outcome of this analysis is the calibration of two design formulae based on the d'Angremond et al. (1996) relationship. The analysis highlighted the need of a supplementary formula allowing a reliable estimate of the transmission coefficient at wide crested breakwater ($B/H_i>10$). Because the formula will be used in this study as comparison for the new prediction model the formula is given:

For mound structures with W_c / H_i > 10:

$$K_t = -0.35\frac{R_c}{H_{si}} + 0.51\left(\frac{B}{H_{si}}\right)^{-0.65}\left(1-e^{-0.41\xi}\right) \qquad \textit{Eq. 2.4}$$

Having a lower boundary of: $K_{tl} = 0.05$

Having a upper boundary of: $K_{tu} = -0.006\frac{W_c}{H_i} + 0.93$

For mound structures with W_c / H_i < 10 the formula of d'Angremond (1996) is still valid:

$$K_t = -0.4\frac{R_c}{H_{si}} + 0.64\left(\frac{B}{H_{si}}\right)^{-0..31}\left(1-e^{-0.5\xi}\right) \qquad \textit{Eq. 2.5}$$

For the range 8 > W_c / H_i > 12 an interpolation should be made between the two different formulae.

Having a lower boundary of: $K_{tl} = 0.075$

Having a upper boundary of: $K_{tu} = 0.8$

For smooth structures the d'Angremond (1996) formula remains the same.

$$K_t = -0.4\frac{R_c}{H_{si}} + 0.80\left(\frac{B}{H_{si}}\right)^{-0..31}\left(1-e^{-0.5\xi}\right) \qquad \textit{Eq. 2.6}$$

Having a lower boundary of: $K_{tl} = 0.075$

Having a upper boundary of: $K_{tu} = 0.8$

Furthermore, a preliminary analysis of the spectral shape changes have been performed on the new tests carried within the DELOS project. This analysis is based on the correlation of the energy shift induced by the low crested structure and the same parameters are used in estimation the wave transmission coefficient. A parameter useful to quantify the shift has been defined and also the spectral decay of the transmitted spectra has been studied.

2.4.4 Van der Meer et al. (2004)

Incident and transmitted wave angles are not always similar: for rubble mound structures, the transmitted wave angle is about 80% of the incident one, whereas for smooth structures the transmitted wave angle is equal to the incident one for incident wave angles less than 45% and is equal to 45% for incident wave angles larger than 45%. The influence of the wave angle on the transmission coefficient is small for rubble mound structures, whereas smooth structures show a clear influence on the wave angle, which can be described by a cosine function.

$(\cos\beta)^{2/3}$ is added to a re-analyzed formula of d'Angremond (1996), valid for smooth structures only:

$$K_t = \left[-0.3\frac{R_c}{H_{si}} + 0.75\left(1-e^{-0.5\xi}\right)\right](\cos\beta)^{2/3} \qquad \textit{Eq. 2.7}$$

Having a lower boundary of: $K_{tl} = 0.075$

Having a upper boundary of: $K_{tu} = 0.80$

The formula is valid to use for the following conditions:

$1 < \xi_{op} < 3$, $0^o \leq \beta \leq 70^o$ and $1 < W_c / H_i < 4$

3 Homogeneous database on wave transmission

3.1 Backgrounds of database

3.1.1 Database objectives

The homogeneous database will be used to train the neural network and it has therefore significant influence on the prediction of the wave transmission coefficient. It is important and necessary to make a database homogeneous in order to obtain useful and accurate results from the prediction model. It can be stated too, that the more test results this database will contain, the more input values there will be available for a neural network to train with, and from this the results will also be more accurate and overfitting of the neural network can be avoided (see Chapter 4). For these reasons a considerable part of the study is spent to compose a reliable homogeneous database.

The database consists of a variety of low-crested structure tests, discussed in Paragraph 2.2. The structures are tested at different test facilities, under different circumstances and with use of different measure techniques. Making a homogeneous database means in principal that the collected datasets are first screened carefully for reliability and secondly added to one database in such a way, that all datasets are described with a fixed number of parameters. The used parameters can be divided in: general, hydraulic and structural parameters. To have insight in these parameters, reports about the individual tests are collected and examined in detail.

It is important to consider carefully which parameters the homogeneous database should contain. One can state that the more information is included in the database, the more valuable the database will be for further research purposes. At the same time one has to try to limit the number of parameters in a certain sense. Preference for simplicity over needless complexity can be mentioned here, having in mind that a neural network can perform better if the number of input parameters is restricted. A homogeneous database has already been made in this way for wave overtopping within the EU-project CLASH, with a number of 31 fixed parameters (see Verhaeghe et al., 2003). The main part of these parameters seems to be import and suitable for wave transmission as well, but there are parameters involved that are found to be pre-empted. In order to have consistency, in a first attempt it is tried to use as many as the same parameters of the CLASH database. In this way, the database becomes also a valuable source of information, although some parameters might not be of use for the prediction model.

3.1.2 DELOS database

A first effort made within the EU-funded project DELOS, has been both to perform new tests on low-crested structures and to gather many existing datasets on wave transmission to build an extensive database. A second effort was to perform a review and an upgrading of the existing formulae by means of this extensive database. More details are given in Briganti et al. (2003) and Van der Meer et al. (2004), see Paragraph 2.4.

A wide database concerning experiments on wave transmission at low-crested structures in wave flumes has finally been collected. Earlier work by Van der Meer and Daemen (1994) and

d'Angremond et al. (1996) has been used as starting point. They began to collect and reanalyze data from different sources, giving a description of the various phenomena, which led to two different formulae. The gathered database, made up of 2,337 tests, includes the data previously described and analyzed by Van der Meer and Daemen (1994) and by d'Angremond et al. (1996), that is referred to as the "old database" in DELOS studies. This database includes rubble mound rock structures as well as Tetrapod and Accropode armour layers.

Within the DELOS project, series of 2D random wave tests have been carried out in 2001 at the University of Cantabria, Spain, (referred as UCA here after) and at the Polytechnic University of Catalonia, Spain, (referred to as UPC), described in Gironella et al. (2002). Both narrow and large crests have been tested, in particular in the UCA tests the parameter B/H_i ranging from 2.6 to 30, allowing a detailed analysis on the influence of this parameter.

Large-scale tests in the Large Wave Channel (GWK), of the Coastal Research Centre (FZK), in Hannover (Germany), have been performed and analyzed by the University of Naples, Italy, Calabrese et al. (2002). The main objective of these tests was to look at low-crested and submerged breakwaters in presence of broken waves on a beach.

Furthermore, tests from Seabrook and Hall (1998) have been included in the database. Structures tested in this study are classical rubble mound submerged breakwaters. Both the relative freeboard and the relative crest width have been varied within a wide range. In particular B/H_i reaches values of 74. Also tests results from Hirose et al. (2000) concerning new type of concrete armour units, called Aquareef, designed for submerged structures, have been added to the DELOS database. Similar to the Seabrook and Hall (1998) tests, the relative crest width has been varied from very small values up to $B/H_i = 102$. Both datasets contain submerged structures only. Finally, experimental data coming from Melito and Melby (2000) investigation on hydraulic response of structures armoured with Coreloc, have been considered. These tests have been performed both on submerged and emerged structures with the relative freeboard varying in a wide range.

3.1.3 CLASH database

The CLASH database (Verhaeghe et al., 2003) forms the starting point for the homogeneous database on wave transmission. For this reason a small review on the CLASH database is given in this paragraph.

Before the EU-funded project CLASH started, no universal prediction method for wave overtopping at coastal structures existed. The CLASH-project intended to fill the deficit of a generally applicable overtopping formula by creating a generic prediction method with the aid of artificial neural networks. As the application of the neural network technique requires a huge amount of existing overtopping information to train the network, one of the main tasks within the CLASH - project was to set up a large homogeneous database, consisting of overtopping test results. Existing datasets on overtopping were gathered from universities and research institutes all over the world. These data were partly originating from partners within CLASH, but also data from elsewhere in Europe and worldwide (e.g. USA, Japan) contributed to the database.

Establishing a reliable database required detailed information on the overtopping tests. It has to be stressed that the reliability of the database was all the more important, as the database was to be used for the development of a neural network as well. Therefore, in a second phase, each particular dataset was screened carefully on consistency. This was done by analyzing the original test reports. Not only information about the wave characteristics, the overtopping structure and corresponding overtopping was gathered, but also information concerning the test facility, the processing of the measurements and the precision of the work is searched for. To account for the effect of reliability in the database, a 'reliability-factor' was defined for each test. Values from 1 to 4 can be assigned to this factor, standing for 'very reliable' up to 'not reliable'. In the third phase, all gathered information was included in the database by means of a fixed number of parameters. The parameters were chosen in such a way that an as complete overview as possible of the overtopping tests was represented. At the same time it was tried to limit the number of parameters, as a neural network only can consist of a restricted number of input parameters depending on the number of tests that were available. Distinction was made between hydraulic information (incident wave characteristics, measured overtopping volume), structural information (test section characteristics) and additional general information (reliability of the test, complexity of the structure). Finally, each test was incorporated in the database by means of 31 parameters of which 11 hydraulic parameters, 17 structural parameters and 3 general parameters.

In the first stage of the CLASH project, little was known about the combined effect of roughness and permeability of structure slopes composed of concrete armour blocks. White spot tests performed in this context, resulted in more precise roughness / permeability factors γ_f for a lot of armour types, replacing the estimated values of γ_f included in the first preliminary database. This γ_f is used in this study as well and the same values will be used as within the CLASH project.

3.2 Origin of transmission datasets

The total amount of data collected during DELOS is extended during this study to a total number of 3,382 tests. All available datasets are summarized (in the same order as present in the homogeneous database) to give insight in the diversity of the tested breakwater structures.

Dataset	Type of structure	Armour unit	Characteristics	Number
Aquareef (2002)	Artificial reef	Aquareef element	Highly permeable / submerged	1,063
UPC (2002)	Mound structure	Rubble stone	Permeable / emerged and submerged	20
Wang (2002)	Mound structure	Rubble stone	Permeable / emerged and submerged	84
Wang (2002)	Smooth structure	Smooth	Impermeable / emerged and submerged	84
Zannutigh (2000)	Mound structure	Rubble stone	Permeable / emerged and submerged	56
UCA (2001)	Mound structure	Rubble stone	Permeable / emerged and submerged	53
Seebrook & Hall (1998)	Mound structure	Rubble stone	Permeable / submerged	633
Melito & Melby (2002)	Mound structure	CoreLocs	Permeable / emerged and submerged	122
Seelig (1980)	Smooth structure	Smooth	Impermeable / emerged	13
Seelig (1980)	Mound structure	Rubble stone	Permeable / emerged	51
Seelig (1980)	Mound structure	Placed rock	Impermeable / emerged	18
Van der Meer (1988)	Reef structure	Rubble stone	Permeable / emerged and submerged	31
Daemrich & Kahle (1985)	Smooth structure	Smooth	Impermeable / submerged	147
Daemrich & Kahle (1985)	Mound structure	Tetrapods	Permeable / submerged	196
Daemen (1991)	Reef structure	Rubble stone	Permeable / emerged and submerged	53
Van der Meer (2000)	Smooth structure	Smooth	Impermeable / emerged and submerged	18
Van der Meer (2000)	Mound structure	Rubble stone	Permeable / emerged and submerged	5
Powell & Allsop (1985)	Mound structure	Rubble stone	Permeable / submerged	42
Calabrese (2002)	Mound structure	Rubble stone	Permeable / emerged and submerged	45
Ahrens (1987)	Reef structure	Rubble stone	Permeable / emerged and submerged	201
DH-M2090 (1985)	Mound structure	Rubble stone	Permeable / emerged	32
DH-H2061 (1994)	Mound structure	Rubble stone	Permeable / emerged and submerged	32
DH-H4087 (2002)	Mound structure	Rubble stone	Permeable / submerged	20
DH-H1872-2D (1994)	Mound structure	Tetrapods	Permeable / emerged	9
DH-H2014 (1994)	Smooth structure	Smooth	Impermeable / emerged and submerged	11
DH-H1974 (1994)	Mound structure	Accropods	Permeable / emerged	10
TU Delft (1997)	Mound structure	Gabions	Permeable / emerged	137
DH-1872-3D (1994)	Mound structure	Tetrapods	Permeable / emerged	30
Allsop (1983)	Mound structure	Rubble stone	Permeable / emerged	21
Padova (2004)	Mound structure	Rubble stone	Permeable / emerged and submerged	11
Daemrich, Mai, Ohle (2001)	Mound structure	Rubble stone	Permeable / submerged	100
DH-4171 (2003)	Smooth	Placed rock	Impermeable / emerged	9
DH-H524 (1990)	Reef structure	Rubble stone	Permeable / emerged and submerged	14
			Total number of tests	**3,370**

Table 3-1 Available transmission tests

Of these tests, 67.1% of the total amount concerns submerged breakwaters, and 9.3% concerns impermeable breakwater structures. As mentioned before, most datasets are gathered during the DELOS project. The datasets are collected worldwide and show diversity in the type of structure and the number of tests performed.

Structure type	Number [n]	Percentage [%]
All tests	3,370	100.0
Mound structures tests	3,117	92.5
Rubble stone (rock)	1,687	50.0
Concrete elements	367	10.8
Artificial reef elements	1,063	31.5
Smooth structures tests	282	7.5
Composite structures tests	9	0.3

Table 3-2 Distribution of type of breakwaters

3.3 Parameters present in database

3.3.1 Description of parameters

As stated before, the database has two goals to fulfill. The database on its own forms a valuable source of information and more parameters included will make the database more valuable. On the

other hand, too much information can make the database difficult to analyze and needlessly complex. The database forms the starting point to train a neural network with and for that reason a limitation of the number of parameters is important as well, having in mind that a neural network performs better with the number of input parameters limited to a minimum (see Chapter 4). In a first attempt, the same parameters as used in the CLASH database are determined for the transmission database as well. CLASH was successful in describing the hydraulic and structural parameters and the parameters used seem to be at first sight important for wave transmission as well. A total number of 33 parameters used in the database are given below. Note that these parameters are described in the database and only a selection of these parameters is used for the prediction model.

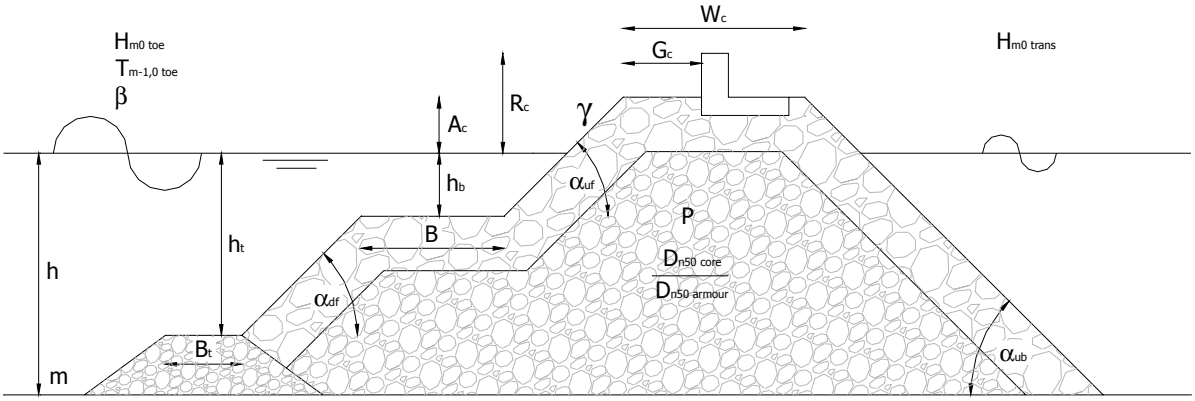

Figure 3-1 Overview of governing parameters present in homogeneous database

General parameters (3)

	Name	Definition
1	Name	This parameter assigns a unique name to each test
2	RF [-]	The 'Reliability Factor', (RF) gives an indication of the reliability of the test. It can adopt values 1,2,3 or 4
3	CF [-]	The 'Complexity Factor', (CF) gives an indication of the complexity of the section. It can adopt values 1,2,3 or 4

Table 3-3 Definition of general parameters

Hydraulic parameters (10)

	Name	Definition
4	$H_{m0\ deep}$ [m]	Significant wave height from spectral analysis determined at deep water
5	$T_{p\ deep}$ [s]	Peak period from spectral analysis determined at deep water
6	$T_{m\ deep}$ [s]	Mean period from spectral analysis or from time domain analysis determined at deep water
7	$T_{m-1,0\ deep}$ [s]	Mean period from spectral analysis in deep water
8	β [^{o}]	Angle of wave attack relative to the normal on the structure
9	$H_{m0\ toe}$ [m]	Significant wave height from spectral analysis at the toe of the structure

10	$T_{p\ toe}$ [s]	Peak period from spectral analysis determined at the toe of the structure
11	$T_{m\ toe}$ [s]	Mean period from spectral analysis or from time domain analysis at the toe of the structure
12	$T_{m-1,0\ toe}$ [s]	Mean period from spectral analysis at the toe of the structure
13*	$H_{mo\ trans}$ [m]	Significant wave height from spectral analysis behind the structure determined at one wave length distance from the structure

Table 3-4 Definition of hydraulic parameters

Structural parameters (19)

	Name	Definition
14	h_{deep} [m]	Water depth at deep water
15	m [-]	Slope of foreshore
16	h [m]	Water depth just seaward of the toe of the structure
17	h_t [m]	Water depth on the toe of the structure
18	B_t [m]	Width of the toe of the structure
19	B_h [m]	Width of the horizontally schematized berm
20	γ_f [-]	Roughness / permeability factor for the structure
21*	p_f [-]	Permeability factor of the core of the structure: $\frac{D_{n50\ \ core}}{D_{n50\ \ armour}}$
22*	P [-]	Notional permeability factor (Van der Meer, 1988a)
23	cot $\alpha_{d\ f}$ [-]	Cotangent of the structure slope downward of the berm at the seaward side of the structure
24	cot $\alpha_{u\ f}$ [-]	Cotangent of the structure slope upward of the berm at the seaward side of the structure
25	cot $\alpha_{excl\ f}$ [-]	Mean cotangent of the structure slope, without contribution of the berm at seaward side of the structure
26	cot $\alpha_{incl\ f}$ [-]	Mean cotangent of the structure slope, with contribution of the berm at seaward side of the structure
27*	cot $\alpha_{u\ b}$ [-]	Cotangent of the structure slope upward at the leeside of the structure
28	R_c [m]	Crest freeboard of the structure
29	B [m]	Width of the berm
30	h_b [m]	Water depth on the berm

31	A_c [m]	Armour crest freeboard of the structure
32	G_c [m]	Width of the armour crest of the structure
33*	W_c [m]	Total width of the crest of the structure

Table 3-5 Definition of structural parameters

The parameters marked in the tables above (marked with *), are introduced new in this study and are not present in the CLASH database (Verhaeghe et a., 2003). The marked parameters are supposed to be important in the case of wave transmission. Four parameters from the CLASH database have not been selected: q [m^3/s], the overtopping discharge per meter width and P_{ow} [-], percentage of the waves resulting in overtopping, because these parameters concern wave overtopping. B_h [m], the width of the horizontally schematized berm and tan α_B [-], the tangent of the slope of the berm are not of use for this database, because no structures have appeared with sloping berms. Therefore, $B = B_h$ is applied in this study.

3.3.2 Parameter calculations

For a major part of the homogeneous database all data was known on forehand, but missing parameters were calculated to complete the database.

Calculations	Dataset	Number of tests
Wave characteristics at the toe of structure from deep-water wave characteristics using the SWAN model	Aquareef (2000)	1,063
$H_{m0\ toe}$ from $H_{s\ toe}$ using the model of Battjes and Groenendijk (2000)	Powell and Allsop (1985)	42
	H2061 (1994)	70
	H4087	20
	H1872-2D (1994)	9
	H1974	10
	H1872-3D (1994)	30
	Allsop (1983)	21
	Padova (2004)	11
	Total number of calculated tests	1,276 (37.9%)

Table 3-6 Calculations for missing parameters in database

3.3.3 Parameter estimations

If some hydraulic characteristics where missing, they are estimated with the given wave relations

Estimations	Dataset	Number of tests
$T_{m-1,0\ toe}$ is calculation with deep-water wave period relations from other spectral wave periods	All tests except Aquareef (2000)	2,307
The roughness factor is estimated (not given by Verhaeghe et al., 2003)	Aquareef (2000)	1,063
	Total number of estimated tests	3,370

Table 3-7 Estimations for missing parameters in database

3.4 Deep and shallow water wave relations

Different relations exist for waves in relative deep or relative shallow water conditions. These relations become important in case missing hydraulic parameters have to be estimated. The relations used do not deviate from the CLASH project; still a summary of relations is given in this paragraph.

3.4.1 Regular and irregular waves

Wind is a turbulent flow with irregular velocity variations. So, when wind blows over a water surface, the resulting waves will be irregular too. An irregular wave field is best described with a so-called variance- or energy density spectrum. A variance-density spectrum can be used for the statistical description of any fluctuating signal. The unit of frequency is H_z and for variance m^2, hence the unit for variance density is m^2/H_z. The physical meaning of a spectrum is clear when one realizes that the variance is identical to the energy in waves (= $^1/_2\rho g a^2$) reduced by a factor ρg. The physical meaning is thus the distribution of energy over the various wave frequencies, hence the name energy-density spectrum. Most of the available tests are performed with irregular waves from which the spectrum is known (mainly Jonswap or Pierson-Moskowitz).

3.4.2 Deep water relations

In relative deep water, the approximately linear behavior of waves allows for a theoretically statistical description of the wave characteristics, based on a Gaussian distribution of instantaneous values of the surface elevation. This results in a Rayleigh distribution of wave heights that is fully determined by the local wave energy.

For deep-water conditions (depth / wave length > 0.5), with a narrow spectrum (the appearance of the sea surface elevation is quite regular), the height of the wave is practically twice the height of the crest: $H \approx 2\eta_{crest}$

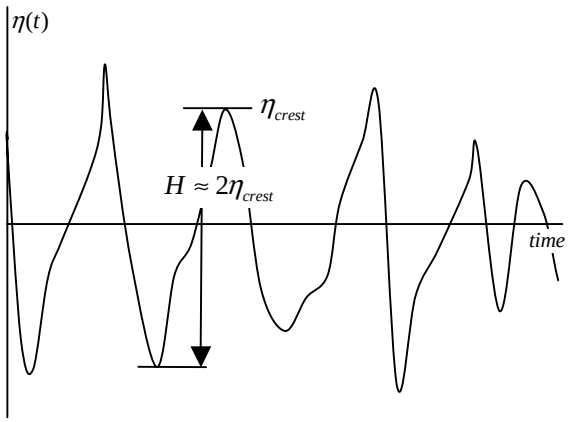

Figure 3-2 The wave height H for wave conditions with a narrow spectrum

The probability density function of H can be determined from the probability density function of η_{crest} with a simple transformation:

$$p(H) = p_{\eta_{crest}}(\eta)\frac{d\eta_{crest}}{dH} \qquad \textit{Eq. 3.1}$$

The probability density function of η_{crest} is a Rayleigh-type function, which has only one parameter, the zero-th moment order moment (m_0) of the variance density spectrum:

$$p_{\eta_{crest}}(\eta) = \frac{\eta}{m_0}\exp\left(-\frac{\eta^2}{2m_o}\right) \qquad \textit{Eq. 3.2}$$

So transforming this function gives the Raleigh distributed wave height:

$$p(H) = \frac{H}{4m_0} \exp\left(-\frac{H^2}{8m_0} \right)$$ *Eq. 3.3*

The significant wave height is defined as the mean value of the 1/3-highest wave heights. This fraction of the waves can be identified in the Rayleigh distribution, so that the significant wave height can be determined from this distribution. Substituting leads to following expression:

$$H_{m_o} \approx 4\sqrt{m_o}$$ *Eq. 3.4*

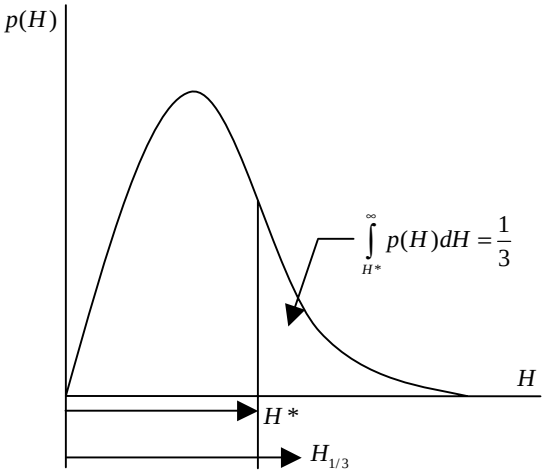

Figure 3-3 The significant wave height in the Rayleigh probability density function

When the significant wave height is estimated with use of total wave energy, m_0, the notation H_{m0} is proposed to use instead of $H_{1/3}$. In actual sea conditions, the spectrum has a finite width and consecutive wave heights are correlated, so the significant wave height estimated from a zero-crossing analysis differs from the significant wave height as estimated from the spectrum. Goda found the empirical relation $H_{1/3} = 0.95 H_{mo}$. For simplicity, the following will be used from now on for deep-water conditions:

$$H_{1/3} = H_{mo}$$ *Eq. 3.5*

Contrary to the wave height, the wave period of deep-water waves does not exhibit a universal law such as the Rayleigh distribution. Nevertheless, it has been empirically found that characteristic period parameters are interrelated at deep water.

Spectral periods can be related with significant wave period parameters. The following relationship is mentioned: $T_p \approx 1.05 T_{1/3}$ (Goda, 1985), in which T_p is the peak period and $T_{1/3}$ the significant wave period. Rice (1944) found that the mean period of zero-upcrossing waves T_m can be expressed as:

$$T_{m0,2} = \sqrt{\frac{m_0}{m_2}}$$ *Eq. 3.6*

T_m is not always the most reliable estimated characteristic wave period, because the value of m_2 is sensitive to small errors or variations in the measurement technique or in the analysis technique. Another mean period is therefore sometimes used, which is less dependent on high-frequency noise. This period gives more influence to the lower frequencies in the spectrum, independent of the shape of the spectrum. In this way it is simple to determine for double peaked and 'flat' spectra the wave run-up, -overtopping and -transmission.

It can be defined as:

$$T_{m-1,0} = \sqrt{\frac{m_{-1}}{m_0}} \qquad \textit{Eq. 3.7}$$

For single peaked spectra, a fixed relationship between T_p and $T_{m-1,0}$ is accepted (TAW, 2002):

$$T_p \approx 1.1 T_{m-1,0} \qquad \textit{Eq. 3.8}$$

3.4.3 Shallow water relations

Wave height distributions in relatively shallow water deviate from those in deep water due to the effects of the restricted depth-to-height ratio so that the Rayleigh distribution is no longer valid. Battjes and Groenendijk (2000) proposed a model that predicts the local wave height distribution on shallow foreshores for a given local water depth, bottom slope and total wave energy.

In shallow water, shoaling, triad interactions and depth-induced breaking become relevant. Shoaling enhances the triad interactions, which cause profile distortion with an excess of crest height and shallow troughs, in contrast to the Gaussian waves in deep water. The change in the shape of the wave height distribution has led to a new model. A Composite Weibull-distribution is proposed to describe the wave height distributions on shallow foreshores. Below a transitional value of the wave height (H_{tr}), the Rayleigh distribution remains valid. Above this value the exponent in the distribution has a different value.

$$F(H) = \Pr\{\underline{H} \le H\} = \begin{Bmatrix} F_1(H) = 1 - \exp\left[-\left(\frac{H}{H_1}\right)^2\right] \rightarrow H \le H_{tr} \\ F_2(H) = 1 - \exp\left[-\left(\frac{H}{H_2}\right)^{3.6}\right] \rightarrow H \ge H_{tr} \end{Bmatrix} \qquad \textit{Eq. 3.9}$$

H_{tr} at a certain water depth is found from the spectral parameter m_0, the foreshore slope angle α and the water depth d:

$$H_{tr} = (0.35 + 5.8\tan\alpha)d \qquad \textit{Eq. 3.10}$$

The parameterization of H_{rms} by m_0 and d:

$$H_{rms} = \left(2.69 + 3.24\sqrt{\frac{m_0}{d}}\right)\sqrt{m_0} \qquad \textit{Eq. 3.11}$$

With a normalized transitional wave height, $\tilde{H}_{tr} = H_{tr} / H_{rms}$, a given table can be used in order to find desired statistical properties. It is possible in this way to find $\tilde{H}_{1/3}$ which can be used to determine the wanted $H_{1/3}$ by:

$$H_{1/3} = \tilde{H}_{1/3} H_{rms} \qquad \textit{Eq. 3.12}$$

The deep-water relations for the periods also deviate. In some cases the spectrum was measured at the toe of structure in shallow water and in that case the spectral periods can be calculated. The proposed deep-water relationships could also be used as a best guess in these shallow water conditions but this will affect the reliability of the values.

3.5 Determination of hydraulic parameters

The hydraulic parameters describe the wave characteristics that were present during the tests. In most cases wave characteristics were determined at the toe of the structure with use of a spectral analysis during the tests. However, in some cases the wave conditions were not measured at the toe of the structure but in deeper water: the foreshore. In order to obtain homogeneity, these wave conditions can be used to calculate the wave characteristics at the toe of the structure: inshore. In those cases, numerical simulations with the SWAN model have been made: starting from deeper water wave characteristics and the present foreshore, the wave characteristics at the toe of the structure are calculated.

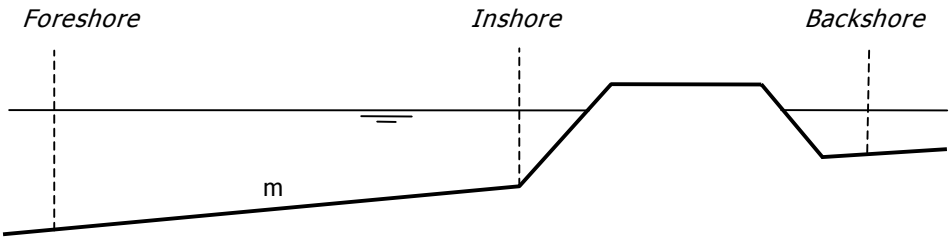

Figure 3-4 Definition of foreshore, inshore and backshore

3.5.1 Foreshore wave characteristics

Wave conditions that are measured at the foreshore (deep water) are included in the database. For some tests this information is used to calculate the missing wave characteristics at the toe of the structure. When no measurements are available in the foreshore, the values in the database are left blank.

Significant wave height from spectral analysis in deep water $H_{m0\ deep}$ [m]
The mean value of the 1/3-highest wave heights is, by definition, defined as the significant wave height. In relatively deep water the following relation exist:

$$H_{m_0\ \ deep} = 4\sqrt{m_{0\ \ deep}} \qquad \textit{Eq. 3.13}$$

For relative deep-water conditions the following relation is used:

$$H_{m_0\ \ deep} = H_{1/3\ \ deep} \qquad \textit{Eq. 3.14}$$

Periods from spectral analysis determined in deep water $T_{p\ deep}$, $T_{m0,2\ deep}$, $T_{m-1,0\ deep}$ [s]
The deep-water relations from Section 3.4.2 are used to determine all wave periods, although relative deep-water conditions are not always present. The treated deep-water period relations are the best approximation to determine missing wave periods. The following relations are used:

$$T_{1/3} \approx 1.20 T_{m0,2} \qquad \textit{Eq. 3.15}$$

$$T_p \approx 1.05 T_{1/3} \qquad \textit{Eq. 3.16}$$

$$T_p \approx 1.1 T_{m-1,0} \qquad \textit{Eq.3.17}$$

3.5.2 Inshore wave characteristics

Important wave characteristics are present at the toe of the structure. In most tests the wave characteristics are measured at this specific point, where usually also shallow water conditions are present. The inshore wave characteristics will be used in the prediction model.

Significant wave height from spectral analysis at the toe of the structure $H_{m0\ toe}$ [m]
In case of tests with rather shallow water depths at the toe of the structure, the proposed point model by Battjes and Groenendijk (2000) can be used to determine the wanted wave height $H_{mo\ toe}$ in case only the wave height $H_{1/3}$ as derived from time domain analysis, is given. The input parameters for the point are in these cases the given value $H_{1/3}$, the slope of the foreshore m and the water depth h at the toe of the structure, leading to the corresponding m_0 at the toe of the structure. The Battjes and Groenendijk method (2000) leads then to the wanted parameter $H_{mo\ toe}$. This method allows to determine a good approximation of the significant wave height at the toe of the structure in shallow water depths.

When no measurements are carried out at the toe of the structure the wave characteristics will be calculated with the SWAN model with use of the wave conditions at the foreshore, depth and slope of the bottom.

Periods from spectral analysis determined at toe of the structure $T_{p\ toe}$, $T_{m\ toe}$, $T_{m-1,0\ toe}$ [s]
The deep-water relations (Equation 3.15, 3.16, 3.17) for wave periods in deep-water will also be used as best approximation of the wave periods at the toe of the structure.

3.5.3 Backshore wave characteristics

Because this study is only focusing on the transmitted wave height no wave periods will be included in the database.

Significant wave height from spectral analysis behind the structure $H_{m0\ trans}$
The same relations are used to determine the significant wave height behind the structure. If more wave heights were measured behind a structure, the wave gauge as close to one wavelength distance from the structure is assigned as $H_{m0\ trans}$.

3.6 Determination of structural parameters

In this paragraph the selected parameters that will be used as structural parameters of the homogeneous database are described. The definitions are directly used from Verhaeghe et al. (2003)

3.6.1 General schematization of structures

An important area, named in CLASH: 'the area of influence' or 'centre area', is between the lines up and down $1.5H_{mo\ toe}$ referred to sea water level. It is found that within this area the structure has most influence on the wave transmission, because it is in this area where the wave action is concentrated (Van der Meer et. al., 1998). Structural parameters are related to the area of influence, which means that one structure can have different values for the fixed structural parameters depending on the water level and incident wave height. According to the wave height, this area will be larger or smaller. According to the water level the total area will be positioned more downwards or upwards.

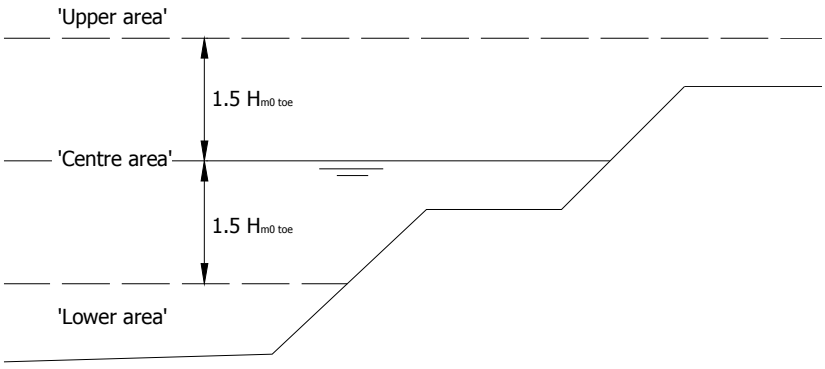

Figure 3-5 Definition of structure areas

The part of the structure within the area of influence will be called the centre area of the structure. The area below will be called the lower area; the area above will be called the upper area. The structural parameters are related to the boundaries of these areas.

Berm definition
To identify a berm it has to fulfill the property of affecting incoming waves, hence it has to be positioned in the centre area of the structure because here the wave action is concentrated. In other words: A berm can be identified as a berm in the homogeneous database when incoming waves actually 'feel' this horizontal part of the structure. When a berm is positioned in the upper or lower area it is not considered as a berm anymore. In these cases a berm can be identified as one of the two other possible horizontal areas: a crest or a toe.

Crest definition
The crest forms the top of the structure and is usually horizontal. It is possible that on top of the crest a parapet is placed to reduce overtopping, so there is a clear separation between the armour crest and the structure crest. A crest is not always present in the upper area, because there are submerged structures present as well.

Toe definition
The armour layer is not necessary extended over the full water depth down to the seabed. The armour layer should than be supported by a toe. A toe is positioned at the seabed at the front side of the structure and consists of a horizontal area, like a berm, for stability reasons. A toe has minor influence on the incoming waves, contrary to a berm, because it is positioned well below sea water level. A toe can be identified as a toe when the horizontal area is positioned in the lower area of the structure.

It is possible a breakwater consists of a berm, but that it is identified as a toe in the homogeneous database because it is positioned in the lower area. Otherwise a toe can be identified as a berm when it is positioned in the centre area.

Note: *The above-described positions relative to the area of influence of the toe, berm and crest <u>are not binding</u>. Tests with very small wave heights at the structure's toe, leads to a very restricted centre area, where the berm is situated in the lower part of the structure. It is quite obvious in this case that is concerns a berm and not a toe, and consequently; it will be identified as a berm. Below, the same structure is considered with different identifications of the horizontal area of the structure, depending on the position, size of the central area and structural properties.*

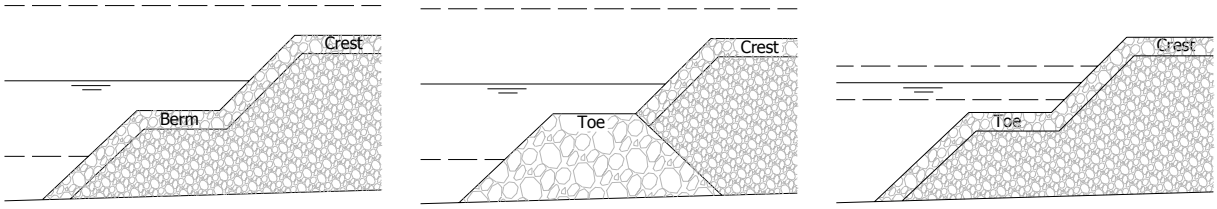

Figure 3-6 Identifying toe, berm and crest based on their position and structural characteristics

3.6.2 Structural parameters

The definitions of the structural parameters are directly used from Verhaeghe et al. (2003)

Water depth at deep-water h_{deep} [m]
h_{deep} is the water depth at deep-water in meters. At this water depth the deep-water wave characteristics $H_{mo\ deep}$, $T_{p\ deep}$, $T_{m\ deep}$, and $T_{m-1,0\ deep}$ are present. It is not always the case that relative deep water is present. It depends on the position of the wave gauges during the tests.

Slope of foreshore m [-]
The slope of the foreshore is described by the parameter m, by means of 1 (vertical): m (horizontal). If no uniform sloping foreshore exists, m has to be approximated. A relevant approximation consists of the mean value of m over a horizontal distance of about 2 wavelengths L_{0p} (deep-water wave length based on T_p).

Water depth just seaward of the toe of structure h [m]
The value of h refers to the water depth just in front of the entire structure. It is often called the water depth "at the toe of the structure" in reports. In case of a horizontal flume bottom, the value of h is equal to the value of h_{deep}.

Water depth on toe of the structure h_t [m]
In case a toe is present, the toe water depth is defined as the depth on the toe, measured from the middle of the toe. When no toe is present h_t = h, because a toe is always placed on top of the seabed with the water depth h.

Width of the toe of the structure B_t [m]
The value of B_t is measured on top of the toe. In case no toe is present, B_t will be equal to zero.

<u>Example 1</u>

Figure 3-7 shows the toe of the structure of the dataset of Zannutigh (2000). Only a few tests in this dataset have the toe positioned in the centre area. It is clear in this case that the horizontal part of the structure should be treated like a toe and therefore the width is included in the database with parameter B_t.

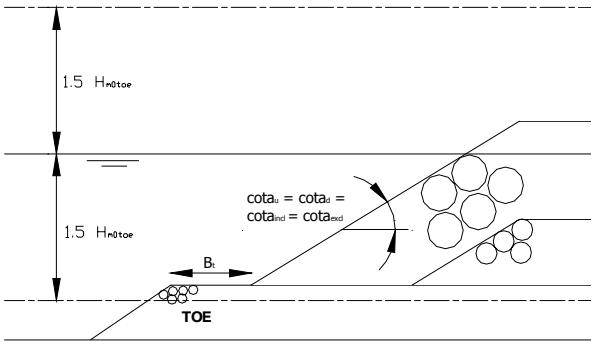

Figure 3-7 Toe presence Zannutigh (2000) dataset

Example 2

For dataset M2090 (1985), the lower part of the structure consists of a composite toe as can be seen in Figure 3-8. According to the CLASH method, the two parts of the toe are incorporated into an average toe. It is assumed that the slope of a structure toe is around 1:2. By starting at the beginning of the toe, assuming a slope of 1:2, and taking an average toe width, the value of B_t is determined.

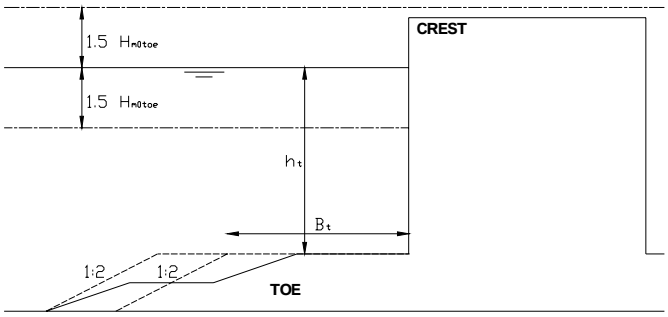

Figure 3-8 Toe presence M2090 (1985) dataset

Example 3

The same case is present for the dataset of H1872 (1993). The toe of this structure is composed of three parts and the same methodology is applied to determine an average width of the toe. The toe width of datasets H1974 and Allsop (1983) are determined in the same manner like this example.

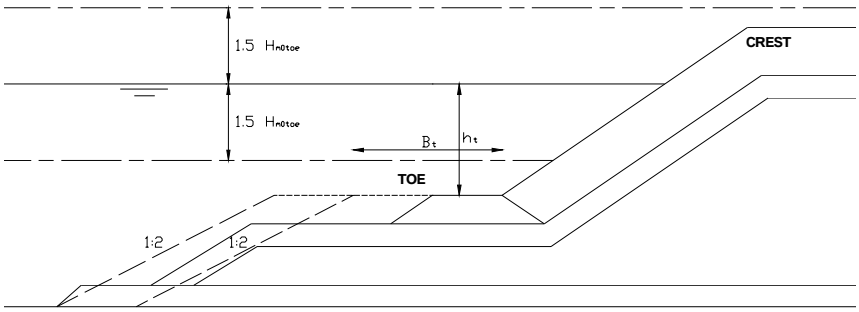

Figure 3-9 Toe presence H1872 (1993) dataset

Water depth on the berm h_b [m]
The water depth on the berm is defined as h_b, measured in the middle of the berm. If the berm is situated above sea water level, the value of h_b will be negative. If no berm is present h_b = 0, because a berm is mostly situated round sea water level.

Width of the berm B [m]
The value of B is measured on top of the berm. In case no berm is present, B equals to zero. Because all berms present in the database are completely horizontal, no use made of the CLASH parameters B_h.

Crest freeboard of the structure R_c [m]
R_c is the crest freeboard of the structure. It is the distance, measured vertically, from sea water level to the highest point of the structure.

Armour crest freeboard of the structure A_c [m]
A_c is the armour crest freeboard of the structure. It is the distance, measured vertically from sea water level to the upper limit of the armour layer. When the armour layer is the highest point of the structure $R_c = A_c$.

Width of the armour crest of the structure G_c [m]
G_c represents the armour crest width. In this way G_c only includes the permeable horizontal part of the crest, as it is assumed that overtopping water passes unhindered an impermeable surface if it reaches it.

Total width of the crest of the structure W_c [m]
The structure crest width W_c includes the total width of the structure. If no vertical structure (parapet or capping wall) is present at the crest: $W_c = G_c$.

Cotangent downward front slope cot $\alpha_{d\ f}$ [-]
Cot $\alpha_{d\ f}$ is the cotangent of the mean slope in the centre area of the structure below the berm. It is determined by taking the point of the structure at a level of $1.5H_{mo\ toe}$ below sea water level and

connecting it with the seaside endpoint of the berm. If the toe of the structure is situated in centre area then the starting point of the toe has to be used instead of the point at level $1.5H_{mo\ toe}$ below sea water level to determine $\alpha_{d\ f}$.

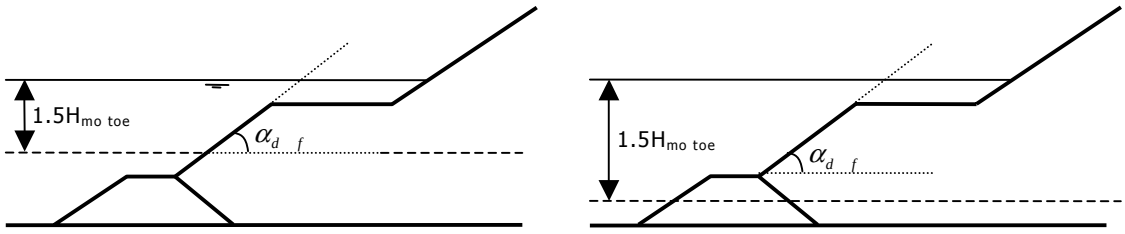

Figure 3-10 Defining $\alpha_{d\ f}$

Cotangent upward front slope cot $\alpha_{u\ f}$ [-]
Cot $\alpha_{u\ f}$ is the cotangent of the mean slope in the centre area of the structure above the berm. It is determined by taking the point of the structure at a level of $1.5H_{mo\ toe}$ above sea water level and connecting it with the leeside endpoint of the berm. If the crest of the structure is situated in the centre area of the structure then the starting point of the crest has to be used instead of the point at level $1.5H_{mo\ toe}$ above sea water level to determine $\alpha_{u\ f}$.

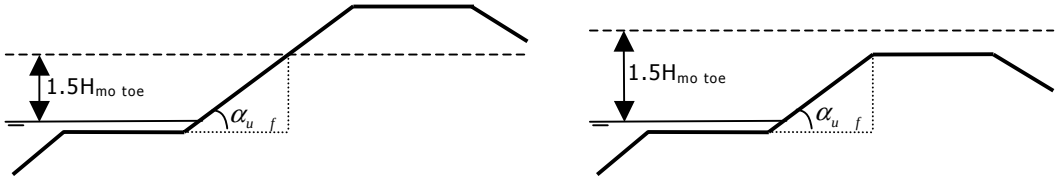

Figure 3-11 Defining $\alpha_{u\ f}$

Mean front slope (berm included) cot $\alpha_{incl\ f}$ [-]
Cot $\alpha_{incl\ f}$ is the cotangent average slope where the berm is included in this average value. It is determined by taking the point on the upper slope at a level of $1.5H_{mo\ toe}$ above sea water level and connecting it with the point on the lower slope at a level of $1.5H_{mo\ toe}$ below sea water level. Also here applies that if the toe or crest is situated in the centre area, the lowest and/or the highest point, which determines cot α_{incl} is determined by the nearest point.

Mean front slope (berm excluded) cot $\alpha_{excl\ f}$ [-]
Cot $\alpha_{excl\ f}$ is the cotangent average slope where the present berm is not taken into account. If the structure has no berm, cot α_{incl} = cotα_{excl}.

Example 3

The structure of the Aquareef (2002) dataset is in this example to show the determination of cot $\alpha_{incl\ f}$ and cot $\alpha_{excl\ f}$. In this dataset the use of the area of influence can be seen clearly. In Figure 3-12 the lower area is present below the berm and this forms the starting point of the dashed line. In Figure 3-13, the same structure is treated with a lower incoming wave height, resulting in a lower area positioned above the berm. The starting point of the dashed line is now from the beginning of the berm. So depending on the position of the area of influence the values of cot $\alpha_{incl\ f}$ and cot α_{excl} are varying.

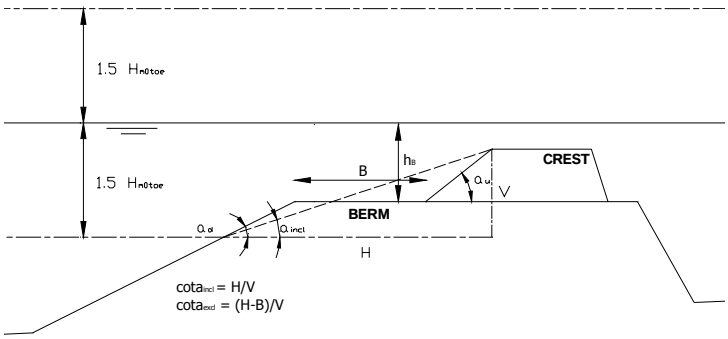

Figure 3-12 Defining front slopes of Aquareef (2002) dataset with berm in centre area

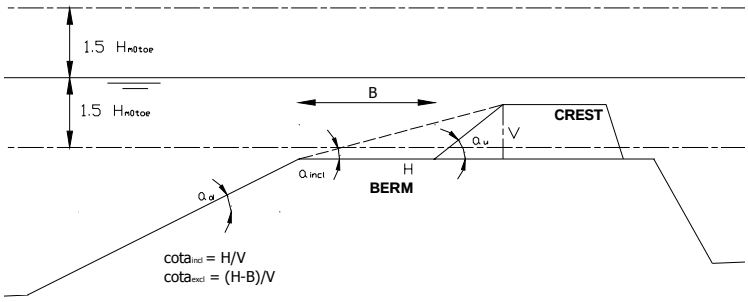

Figure 3-13 Defining front slopes of Aquareef (2002) dataset with berm in lower area

Cotangent upward back slope cot $\alpha_{u\ b}$ [-]
This parameter can be determined in the same way as cot $\alpha_{u\ f}$ but in this case at the back of the structure.

Roughness / permeability factor for structure γ_f [-]
An indication of the roughness and the permeability of structure is given by the parameter γ_f.

Type of armour layer	Roughness / Permeability factor γ_f
Smooth impermeable surface	1.00
Placed rock	0.90
Rocks (1 layer, impermeable core)	0.60
Rocks (1 layer, permeable core)	0.45
Rocks (2 layers, impermeable core)	0.55
Rocks (2 layers, permeable core)	0.40
Cubes (1 layer, random positioning)	0.50
Cubes (2 layers, random positioning)	0.47
Antifers	0.47
HARO's	0.47
Accropods	0.46
X-blocks	0.45
Core-locs	0.44
Tetrapods	0.38

Table 3-8 Defining roughness factor

The roughness has influence for emerged structures because the roughness affects the run-up (so overtopping as well), but the effect on submerged breakwaters is questionable.

Notional permeability factor P [-]
Van der Meer (1988a) used the notional permeability P in his stability formula to describe the permeability for waves underneath the armour layer. P is roughly defined as:

P = 0.1 Impermeable breakwater (core)
P = 0.4 Breakwater with core, filter and armour layer
P = 0.5 Breakwater with only core and armour layer

P = 0.6 Homogeneous structure, which consists only of armour rocks

The notional permeability can be used for wave transmission as well in combination with the roughness factor.

Ratio of nominal core diameter over nominal armour diameter p_f [-]
To express the permeability of the core relatively to the armour layer, the ratio of the nominal core diameter over the nominal armour diameter (referred to p_f from now on) can be used as indication. In general, the size of armour units is related to the incident wave height for stability reasons and for mound structures the armour layer is quite permeable. If p_f is close to zero it means the core material diameter is very small compared to the armour units, hence the core is found to be impermeable: this is the lower boundary of p_f. A homogeneous structure is found to be the most permeable structure and p obtains a value of 1: this is the upper boundary. P_f only described the permeability of the core and it is range is $0 < p_f < 1$. A smooth structure has no armour units so p_f can no be calculated. Having in mind that 0 means an impermeable core, the value of 1 is appropriate to use. p_f can always be estimated if diameters are missing by comparing a structure with structures from which the p_f is known.

3.7 Determination of general parameters

The general parameters of the homogeneous database are the 'complexity-' and 'reliability factor'. To each test both factors are awarded to give information about the complexity of the determination of the structural parameters and the reliability of the hydraulic parameters. These two factors will be used to calculate a final weight factor. The weight factor will finally be used to compose the input database for the neural network. Depending on the value of the weight factor (ranging from 1 to 9), a single test will occur with the same frequency in the input database. Hence, the most reliable data is given more influence in the prediction of the transmission coefficient.

Complexity factor
The complexity factor is related to the structural parameters ranging from 1 (a simple section) to 4 (a very complicated section) according to Verhaeghe et al. (2003). The factor is estimated during the process of homogenizing the database. It is based on the experience obtained during the determination of the structural parameters of a certain tested section.

An example of a simple section is a conventional homogeneous type breakwater structure with a trapezoidal shape. A more complex section for instance is a reef type breakwater which is not dynamically stable. In the latter case it is hard to define the crest width of the structure, because the transition between slopes and crest are not clear due to the deformation of the initial structure. The definitions of the complexity factors are given in the table below:

Complexity factor CF (-)	Definition (Verhaeghe et al., 2003)
1	Simple section: The structural parameters describe the section exactly or as good as exactly.
2	Quite a simple section: The parameters describe the section very well, although not exactly.
3	Quite complicated section: The parameters describe the section appropriate, but some difficulties and uncertainties appear.
4	Very complicated section: The section is too complicated to describe with the chosen parameters, the representation of the section by them is unreliable.

Reliability factor
The reliability factor is related to the hydraulic parameters. The factor depends on the used measurement instruments, testing circumstances and the determination of the hydraulic parameters.

Reliability factor RF (-)	Definition (Verhaeghe et al., 2003)
1	Very reliable test: All needed information is available; measurements and analysis were performed in a reliable way.
2	Reliable test: Some estimations / calculations have be made and / or some uncertainties about measurements / analysis exist, but the overall test can be classified as 'reliable'.

3	Less reliable test: Some estimations / calculations had to be made and / or some uncertainties about measurements / analysis, leading to a classification of the test as 'less reliable'.
4	Unreliable test: No acceptable estimations could be made; calculations and / or measurements / analysis include faults, leading to an unreliable test.

The determination of the reliability factor is depending on more factors than the complexity factor. The same criteria of Verhaeghe et al. (2003) have been used to qualify the factors of RF and the corresponding values assigned to it.

3.8 Pre-selection of parameters for NN configuration

A pre-selection of parameters is made to perform a further analysis on, before using them in the prediction model. Because the total number of tests is 3,370, the total number of input parameters for the neural network has to be limited to obtain a good performance. Additionally, a neural network is only a mathematical tool and it is therefore important to have parameters present from which the influence on wave transmission is expected to be of interest. It has to be avoided to train a neural network with useless parameters, because the total number of input parameters has to be minimized and furthermore the neural network can find relations, which are not right.

As stated before, most parameters in the database are used in CLASH as well. There is a major difference with structures from the wave overtopping database and the wave transmission database. In case of wave overtopping, structures are designed to be as effective as possible to minimize wave overtopping, resulting in high relative crest heights, steep slopes (cause more reflection), presence of parapets, high positioned berms, etc. In case of wave transmission the structures are low-crested (otherwise there is no transmission at all) and these characteristics are clearly present, the structures have simpler sections. Because of this big difference, some parameters in the transmission database, which are used in CLASH as well, could be determined but were not really used to specify the characteristics of a certain test section.

3.8.1 Selected parameters

The following parameters are selected for further analysis. Although more parameters have been determined in the homogeneous database, these parameters are expected to be of influence on wave transmission. The influences of these parameters are known from earlier findings and are expected to give the neural network information to find relations with.

	Hydraulic parameters	**Symbol**
1	Incident significant wave height at toe of the structure	$H_{m0\ toe}$ [m]
2	Incident mean wave period at toe of the structure	$T_{m-1,0\ toe}$ [s]
3	Mean angle of incidence	β [^{o}]
4	Transmission coefficient	K_t [-]
	Structural parameters	
4	Water depth in front of the structure	h [m]
5	Crest freeboard	R_c [m]
6	Total crest width	W_c [m]
7	Berm width	B [m]
8	Berm depth	h_B [m]
9	Cotangent downward front slope	cot $\alpha_{d\ f}$ [-]
10	Cotangent upward front slope	cot $\alpha_{u\ f}$ [-]
11	Cotangent upward back slope	cot $\alpha_{u\ b}$ [-]
12	Mean front slope (berm included)	cot $\alpha_{incl\ f}$ [-]
13	Mean front slope (berm excluded)	cot $\alpha_{excl\ f}$ [-]
14	Roughness factor	γ_f [-]
15	Notional permeability	P [-]
16	Ratio nominal core diameter over armour diameter	p_f [-]

Table 3-9 Selected parameters for further analysis

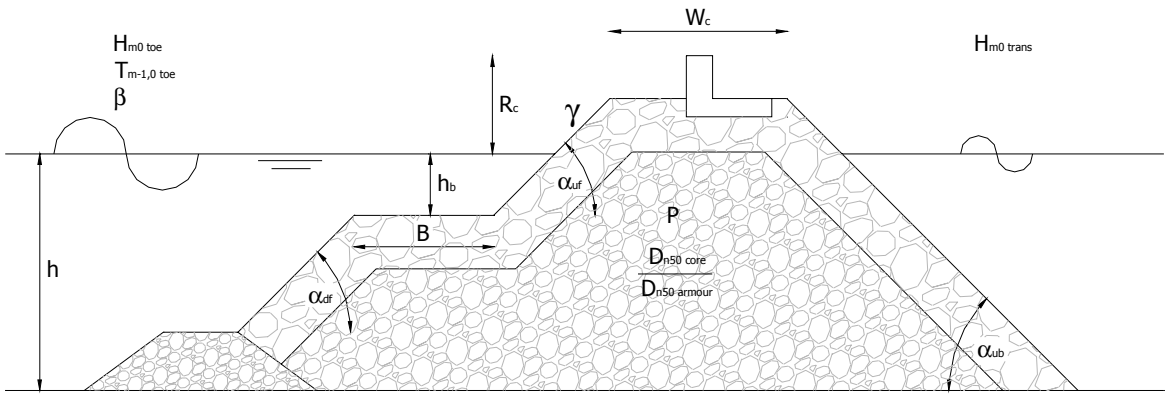

Figure 3-14 Selected parameters given for a general breakwater section

3.8.2 Discarded parameters

Some parameters can be discarded on forehand for the prediction model. A brief motivation is given in this section these specific individual parameters.

Deep-water hydraulic parameters $H_{m0\ deep}$ [m], $T_{p\ deep}$ [s], $T_{m0,2\ deep}$ [s], $T_{m-1,0\ deep}$ [s]
Verhaeghe et al. (2003) found that including deep-water hydraulic parameters in the prediction model did not improve the prediction of wave overtopping. It is assumed the same conclusion is true for this study. Deep-water hydraulic parameters will be neglected. Of course the deep-water hydraulic parameters are used to calculate missing parameters at the toe of the breakwater structure. Hydraulic parameters at the toe of the structure are selected for further analysis before included in the prediction model.

Armour crest freeboard A_c [m]
Because only 9 tests are present of a composed structure (see Paragraph 3.2), the armour crest freeboard is excluded from further use. The specific tests concern a structure with a small parapet on top of the crest. The number of tests present in the database, concerning composed structures, is too small to give the neural network new information to find relations with. Besides, the value of the relative crest freeboard R_c will be present to take into account the total height of the structure.

Armour crest width G_c [m]
Like the armour crest freeboard, also for the armour crest width the same is true. Only 9 tests are present of a composed structure. Moreover, the considered tests have found to be smooth, so an armour crest width parameter would certainly give no extra information to the neural network.

Slope of foreshore m [-]
Because waves are measured at the toe of the structure, it is assumed that the influence of the foreshore slope is already included in the values of the hydraulic parameters at the toe of the structure. The slope of the foreshore is excluded from further use.

Water depth on toe of the structure h_t [m] and Width of the toe of the structure B_t [m]
The influence of the toe of the structure is assumed to be very low. There are some structures present with a toe, but in order to reduce the number of input parameters the toe parameters are neglected. Additionally, it is found that all toes in the database are positioned well below sea water level and outside the area of influence. In case of the Aquareef dataset the horizontal section is treated like a berm, although it can be argued to treat this section as a toe. To include the effect of this horizontal section it is treated like a berm. In this way (in case of doubt) a toe presence, expected to be of influence on wave transmission is taken into account as a berm.

3.8.3 Discarded datasets

After the determination of the reliability- and complexity factor (RF and CF) some test data is excluded from further use for the prediction model. The excluded tests are found to be unreliable and / or have a very complex section.

Part of Ahrens (1987) dataset
A part of Ahrens (1987) dataset is given a CF = 4, as these sections heavily deformed during the tests. A selection is made for tests at which the crest height, during the test, lowered less than ten percent of the initial height. These tests are used within the prediction model.

Roeleveld (1997) dataset
The Roeleveld (1997) dataset is not taken into account, because this specific dataset was tested with regular waves. This dataset is given a RF = 4, which means it is not taken into account within the prediction model.

3.9 Analysis of data

The distribution of data points is important for a neural network, because it will determine the range of the predictions accuracy. In regions with many data points the neural network is able to find more relations and this will result in a better accuracy in these regions. An analysis on the distribution of data in the homogeneous database is made in order to find the following information:

- Determining regions where data points are concentrated. In these regions the neural network is supposed to be most accurate and this could be validated in a later stadium.
- Detecting white spots. White spots are regions where no data points are present. In those regions the neural network will interpolate results and the prediction model performance must be analyzed carefully in these regions in a later stadium if expected tendencies are right.
- Detecting parameters which are such likely distributed, that the neural network would find no extra relations to learn with. These parameters can be discarded before the prediction model will be trained.

Because the distribution of wave steepness, relative crest freeboard and relative crest width are expected to be of most influence for the wave transmission phenomenon, separate paragraphs are included for the distribution of those parameters. Less important parameters are treated within one paragraph.

3.9.1 Distribution of wave steepness

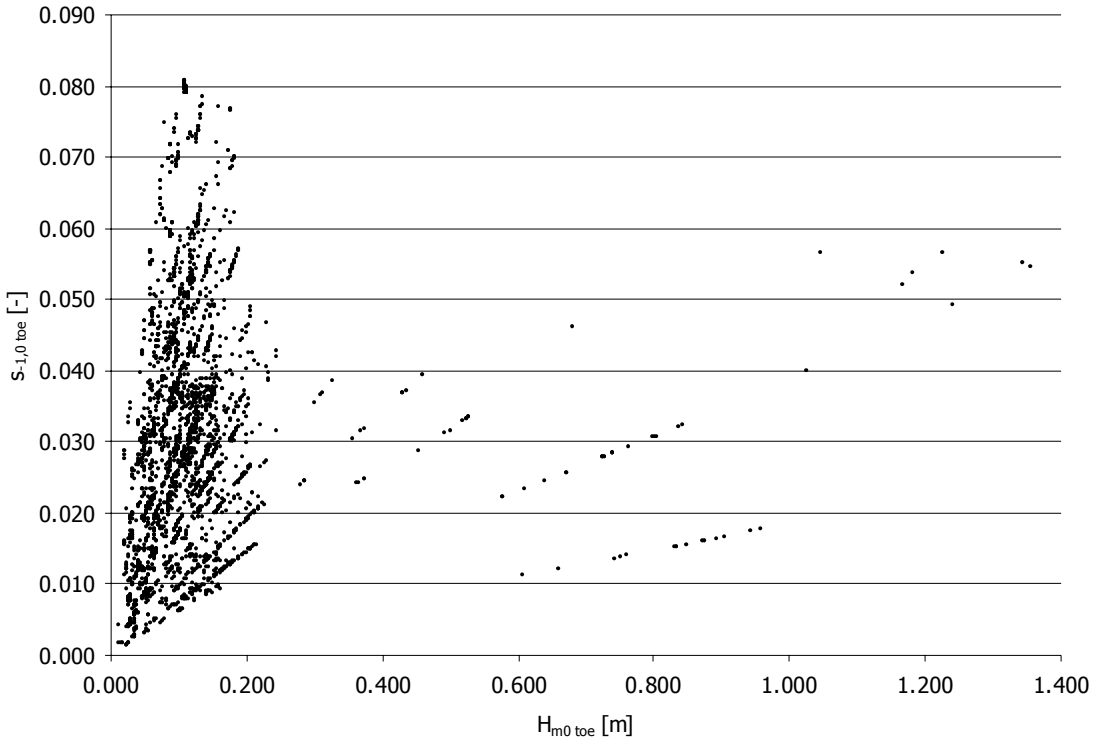

Figure 3-15 Wave height at toe vs. wave steepness

No prototype measurements are present in the database. The database consists of small- and large scale tests as shown in Figure 3-15. The figure shows the wave steepness as a function of the wave height for all available tests. A wave steepness over 0.07 is physically not possible, as the waves should break beyond this point. A wave steepness lower than 0.005 is difficult to generate in a wave flume or wave basin. Very small waves, lower than 0.03m are difficult to generate as well. These data will be considered as less reliable and therefore a reliability factor of at least 3 ('less reliable test') is assigned to those individual tests.

Note: *The data points in Figure 3-15 are distributed along straight lines. These straight lines consist of tests from the data set, in which the water level was varied, resulting in different incident wave heights and wave steepness.*

3.9.2 Distribution of relative crest freeboard

Figure 3-16 shows for small positive and negative values of the relative crest freeboard a dense distribution of data points. It is to be expected that a neural network will be more accurate in these regions, contrary to large positive or negative values of the relative crest freeboard. Regions where nearly no data points are present, will eventually determine the boundaries of the prediction capacity of the model.

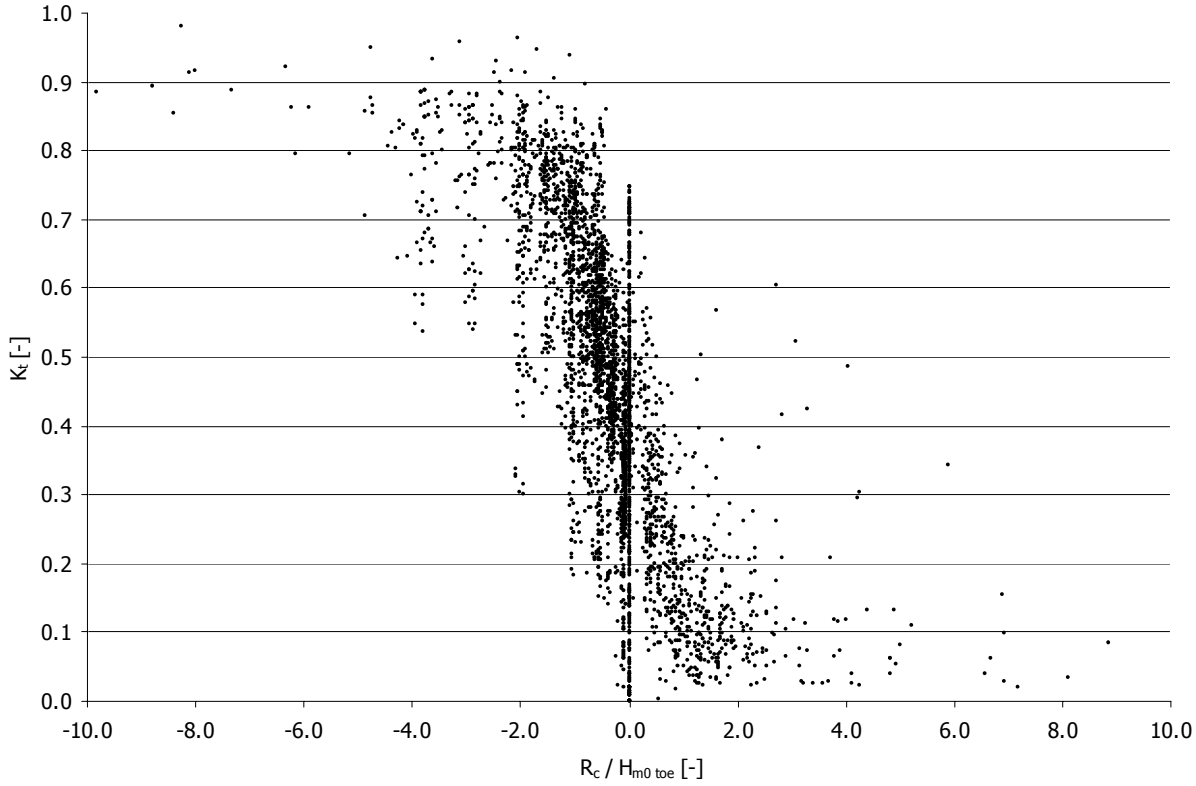

Figure 3-16 Relative crest height versus wave transmission coefficient

From Figure 3-16 can be concluded that the concentration of data points is between relative crest freeboards of –4.0 till 4.0. Beyond those boundaries, the distribution of data points is sparse and the accuracy of the prediction model is expected to be considerably lower. Distribution plots of the relative crest freeboard of individual datasets are shown in Paragraph 3.9.3. There are no data points present with a K_t=0 or a K_t=1. Hence, the neural network will be less accurate in areas close to these values of K_t.

3.9.3 Distribution of relative crest width

Figure 3-17 shows the distribution of the relative crest width. 80% of all tests have a W_c / $H_{mo\ toe}$ < 10. The concentration of data points is ranged between relative crest widths of 0 till 35.

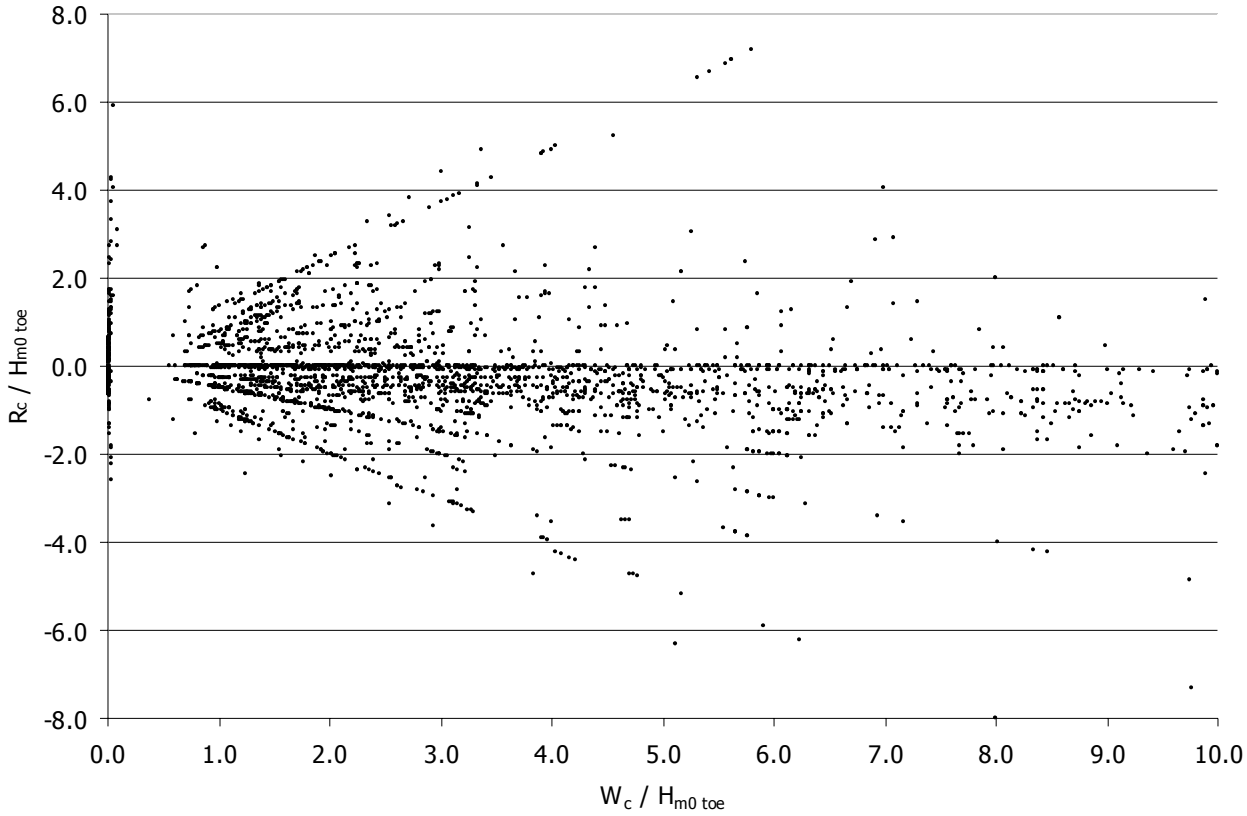

Figure 3-17 Relative crest width versus relative crest height

Note: *Large crest widths do not automatically result in a low K_t, because a structure can be submerged (negative crest freeboard) and there can still be a considerable wave transmission. A so-called white spot is present for large crest freeboards in combination with large crest widths (see Figure 3-17. This white spot is not affecting the prediction model, because in this region the wave transmission is very limited and not of interest to predict.*

3.9.4 Distribution of individual parameters

Roughness factor

As mentioned before, the range of values that a structure can adapt to γ_f, is between 0.35 (an Icelandic berm breakwater) and 1.00 (a smooth structure).

In the database most values are distributed between 0.40 and 0.50. There is clearly a gap present between these values and a value of 1.00. (Rubble) mound structures are specified rough and porous, which always results in an γ_f round 0.5. Smooth structures are always given a value of 1.00. Hence, the gap simply forms the difference between smooth and rubble mound structures.

In order to make a distinction between different types of armour units (this is investigated in Clash) a lot of values between 0.40 and 0.50 are found, describing very well the difference in behavior. Because most structures concern rubble mound, the value of 0.45 is frequently present.

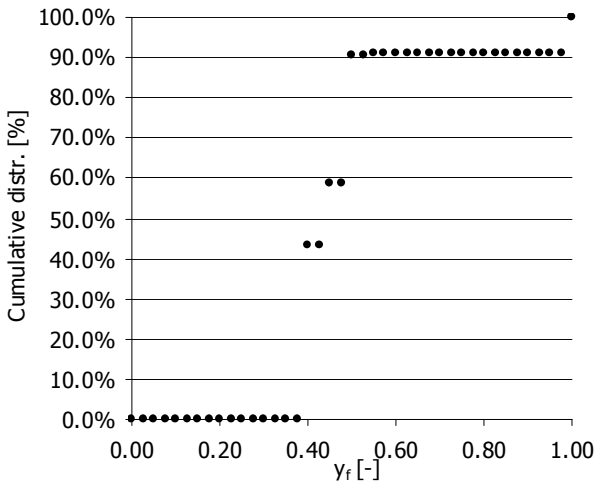

Figure 3-18 Distribution of γ_f [-]

Ratio nominal core- over armour diameter
The ratio of nominal core- over armour diameter (p_f) can vary between 0 (impermeable) to 1 (homogeneous). Like the roughness factor, there is a concentration of a ratio of core- over armour diameter between 0.35 and 0.60; due to the fact mound structures have often a medium permeability. Around 10% of the tests are given a value of 0.00, corresponding to the number of tests with a roughness factor of 1. Most structures, which are impermeable, are smooth as well, but there are exceptions present.

Notional permeability factor
The notional permeability factor (P) is another possibility to include permeability and is known from the widely applied stability formula of Van der Meer (1988a). The notional permeability factor P gives the permeability for waves underneath the armour layer. P can adopt values of: 0.10, 0.40, 0.50 and 0.60 (see Paragraph 3.6.2). Like the ratio of nominal core- over armour diameter, for P as well around 10% of the tests imply impermeable structures (P=0.10). Homogeneous structures are given a value of 0.60.

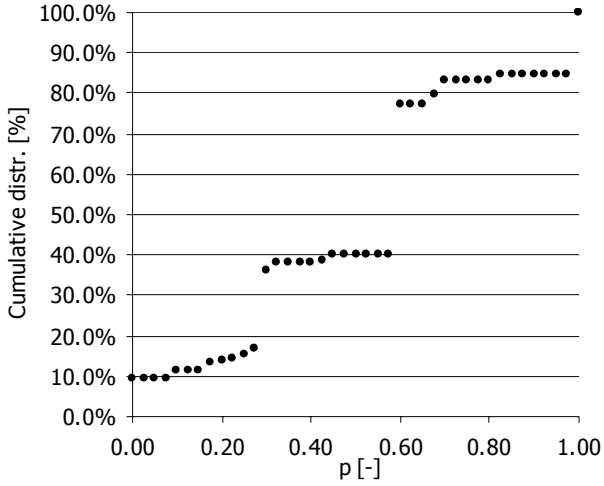

Figure 3-19 Distribution of p_f [-]

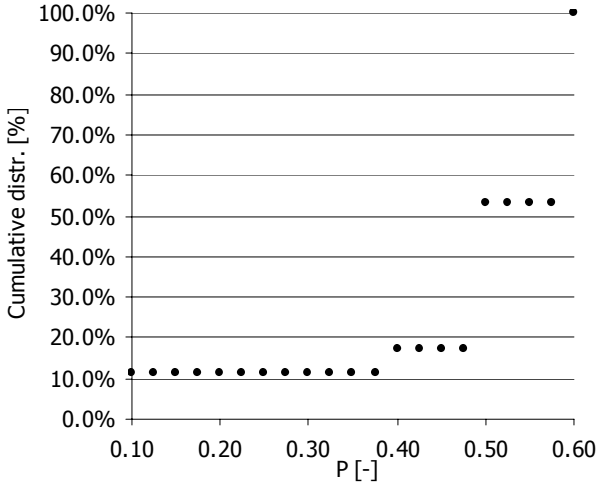

Figure 3-20 Distribution of P [-]

Based on the distribution of the figures of the ratio of core- over armour diameter and the notional permeability no conclusions can be drawn for the prediction model. Because P only can adopt four different values it looks less useful, but also the distribution of the ratio core- over armour diameter is showing four levels. Both parameters clearly distinguish permeable from impermeable structures and this is the main goal of using a permeability parameter. There could be a difference for structures with a medium permeability, but using the permeability parameters in combination with the roughness factor, a specific structure can be characterized well. Because it is difficult to choose a parameter for permeability in this stadium it is preferred to select a parameters after analyzing performances with a neural network.

Angle of incidence
A governing part of the database concerns tests with an angle of incidence to the normal of the structure. Only a minor part (see Figure 3-22) is tested under a certain angle of incidence. Especially for smooth structures the angle of incidence is expected to be of importance and will therefore be included in the prediction model, despite the distribution of the parameter. However, questions can be put to the limited number of available tests. It is not clear if this will cause problems for the prediction model, but because the angle of incidence is expected to be important it is selected in a first attempt.

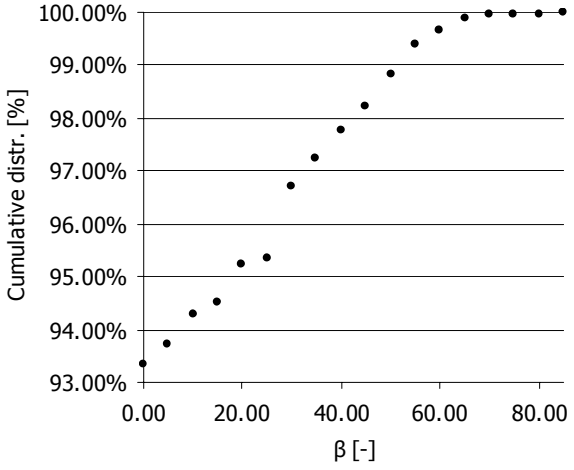

Figure 3-21 Distribution of β [-]

Structure slopes
From Figure 3.24 can be concluded that most structures have a uniform front slope (also structures applied with berm), ranging from a cotangent α of 0 (vertical) to 5 (very gentle). Most front slopes are distributed between cotangents of 1.5 and 2.0, as can be seen from figure 3-24. The back slope (no figure included) has more or the less the same distribution as the cotangents upward front slope and its influence in the prediction model is therefore questionable. It is expected the neural network will not be given extra information, if for most tests the front- and back slope have the same values. Only for tests with deviating slopes, improvements can be expected.

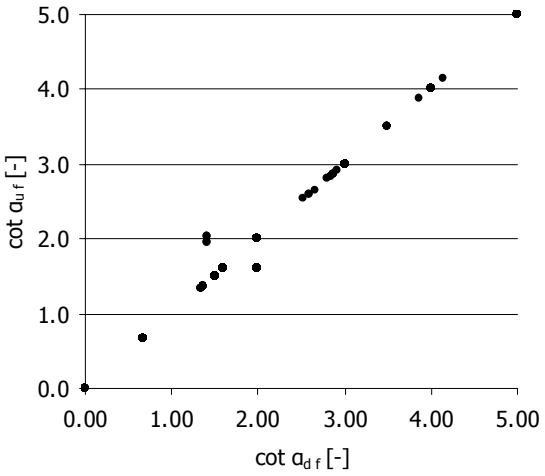

Figure 3-22 Distribution of cot $\alpha_{d\,f}$ vs, cot $\alpha_{u\,f}$

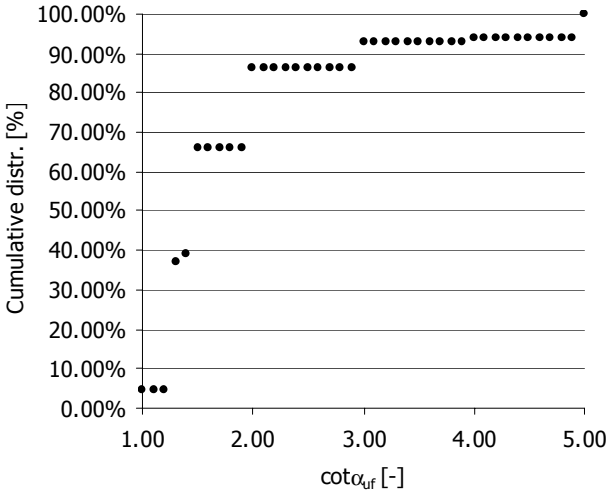

Figure 3-23 Distribution of cot $\alpha_{u\,f}$ [-]

Water depth in front of structure
The relative water depth in front of the structure is uniform distributed between 0 and 5. Also there are a lot of tests present from 5 till 10 and only few tests with very large relative water depths up to 34.5 are present. It is expected the water depth will have influence on wave transmission, but based on Figure 3-25 no conclusions can be drawn yet.

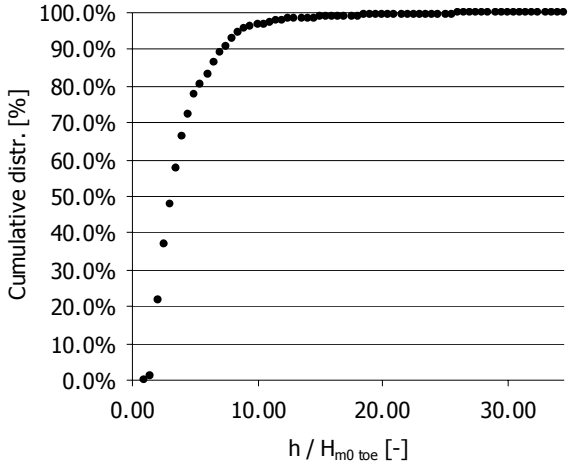

Figure 3-24 Distribution of h / $H_{m0\ toe}$ [-]

Berm parameters
There are two possibilities to include berms in the prediction model. The first option is by using the berm width in combination with the berm depth. The second option is by using the two mean front slopes: the mean front slope including berm (cot $\alpha_{incl\ f}$) and the mean front slope excluding berm (cot $\alpha_{excl\ f}$). It is difficult to bind conclusions on the distribution of the two options. It is preferred to investigate the performance of both options in a neural network in a later stadium to make a final decision.

Figure 3-27 shows that relative berm depths close to sea water level result in very low wave transmission coefficients. This agrees with the statement, that berms are most effective round sea water level. Relative deep berm depths give higher transmission coefficients, because the berm is not felt by the waves.

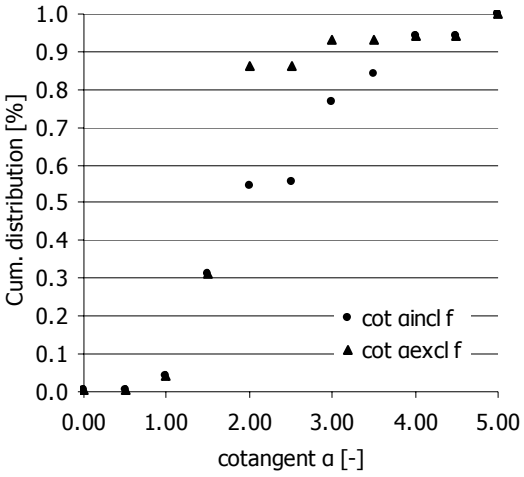

Figure 3-25 Distribution of cot α [-]

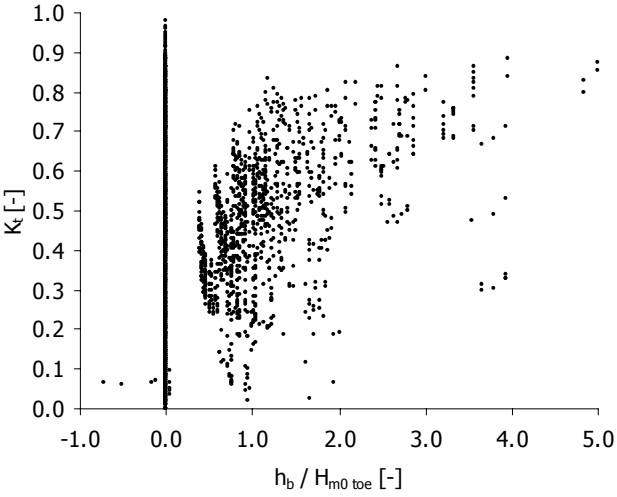

Figure 3-26 Distribution of h_b / $H_{m0\ toe}$ vs. K_t

3.10 Dataset testing to the DELOS formulae

All datasets are analyzed in detail to obtain the following information:

- Detecting wrong data points (wrong measurements). Wrong data points have a high probability to be detected if distribution plots are made. Wrong data points can be exposed from the prediction model.
- Detecting input mistakes. The composure of the database is done by hand and input mistakes cannot be excluded. Analyzing the data on forehand can result in finding input mistakes before the prediction model will be trained.

For individual datasets, distribution figures are made for the relative crest freeboard vs. K_t, because it known from previous studies that the relative crest freeboard is dominating the behavior of wave transmission. Outliers from the data clouds can indicate a measurement mistake or special conditions within one test serie. In any case the data point can show a deviation in the prediction model as well, and should therefore be noticed on forehand. Additionally, all individual datasets have been compared with the DELOS formulae. If the DELOS formulae show a good prediction but some points rather deviate from this, there is an indication as well of possible wrong data points.

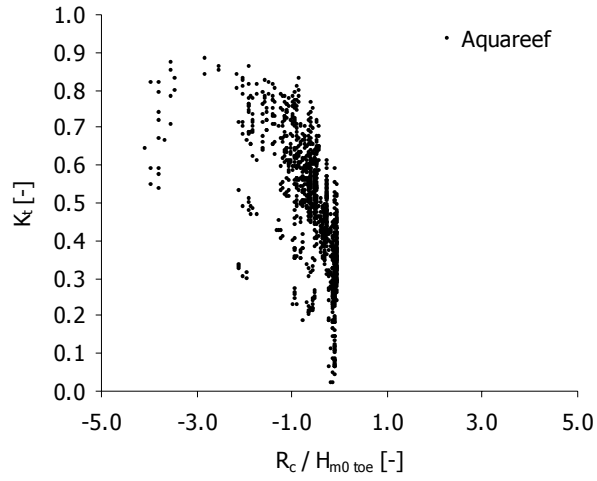
Aquareef
K_t [-]
R_c / $H_{m0\ toe}$ [-]

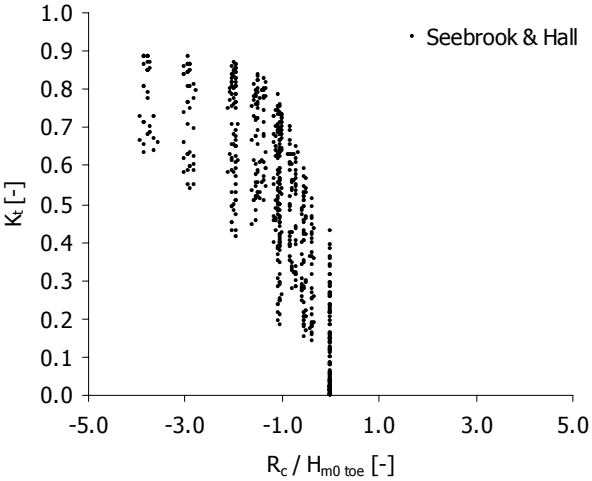
Seebrook & Hall
K_t [-]
R_c / $H_{m0\ toe}$ [-]

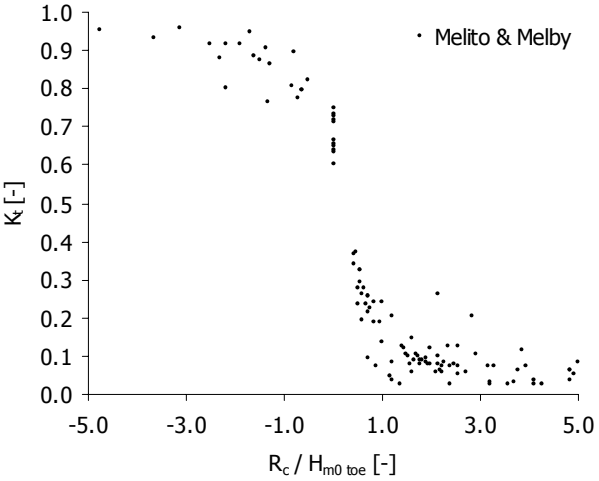
Melito & Melby
K_t [-]
R_c / $H_{m0\ toe}$ [-]

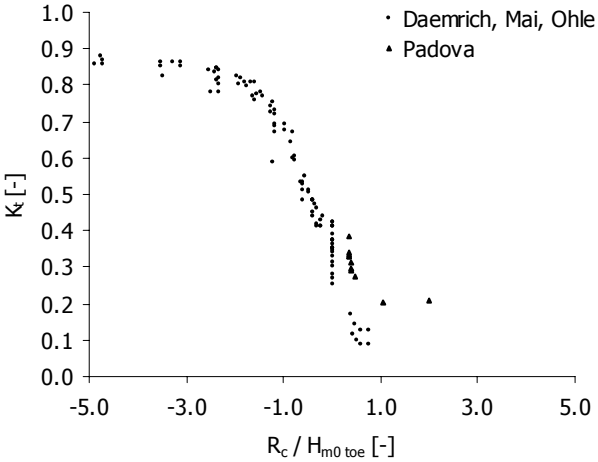
Daemrich, Mai, Ohle
Padova
K_t [-]
R_c / $H_{m0\ toe}$ [-]

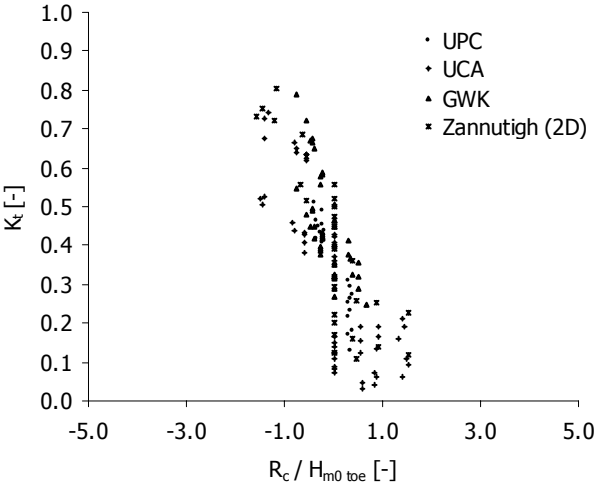
UPC
UCA
GWK
Zannutigh (2D)
K_t [-]
R_c / $H_{m0\ toe}$ [-]

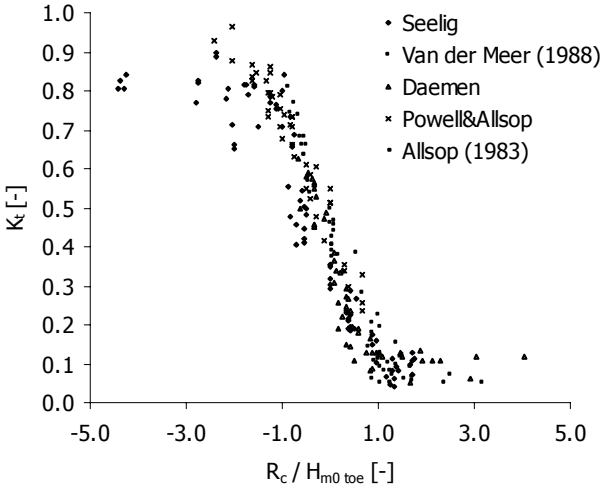
Seelig
Van der Meer (1988)
Daemen
Powell&Allsop
Allsop (1983)
K_t [-]
R_c / $H_{m0\ toe}$ [-]

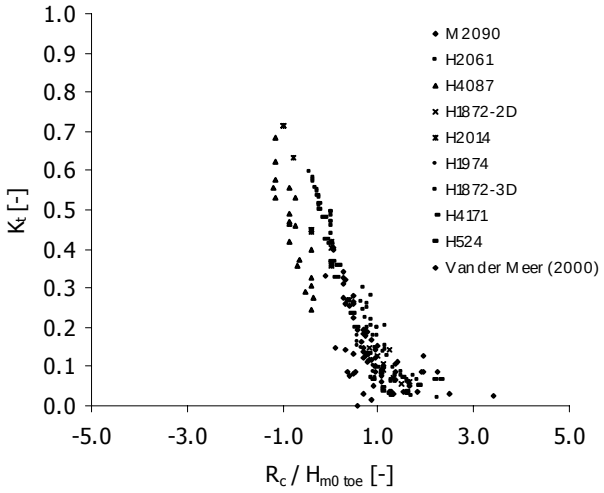

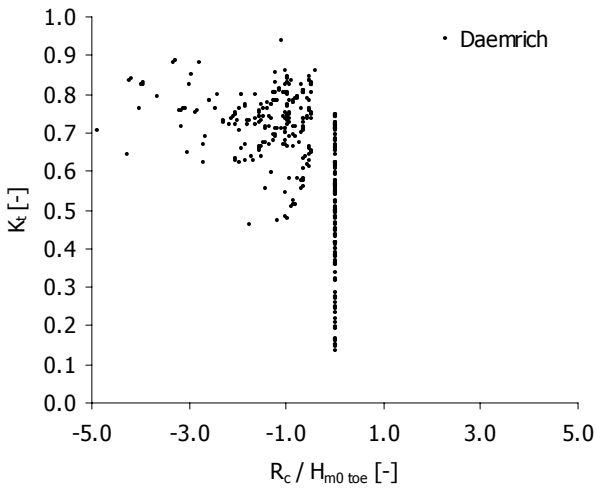

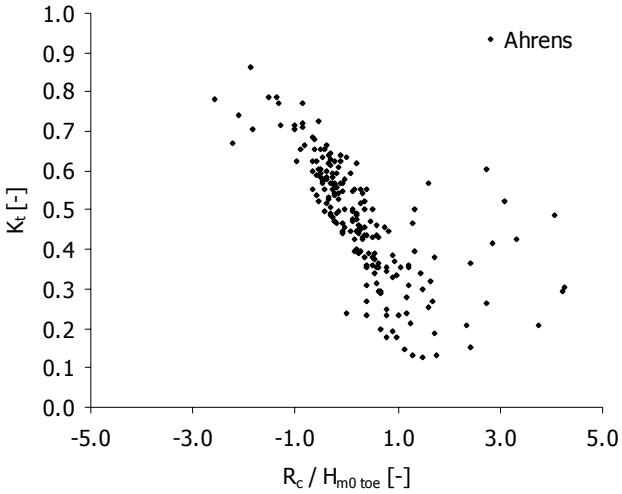

The following data points are found to be outliers. The specific points are examined in detail and a second check with the DELOS formula will give a final answer.

Dataset	Data point	Possible cause
Melito & Melby	(2.126 ; 0.261)	Low wave steepness compared to other test. Longer waves result in a higher Kt. No input mistake or wrong measurement.
Melito & Melby	(2.848 ; 0.207)	The same case as the previous outlier
Daemrich	(-1.090 ; 0.939)	Transmitted wave height seems too high. Probably a wrong measurement.
Daemrich	(-4.257 ; 0.644)	Low wave steepness. No input mistake or wrong measurement.
Daemrich	(-1.745 ; 0.462)	Low wave steepness
Daemrich	(-4.867 ; 0.705)	Low wave steepness / very small incident wave height. Assumed a wrong measurement
Daemrich, Mai	(-1.220 ; 0.588)	Low incident wave height, and a low Kt. Test is already given a RF = 3.

Table 3-10 Overview outliers

The DELOS formulae, Briganti et al. (2003) and Van der Meer et al. (2004), have been applied to the same datasets. For the Ahrens dataset the reef formula proposed by Van der Meer et al. (1994) is applied. The figures are showed below:

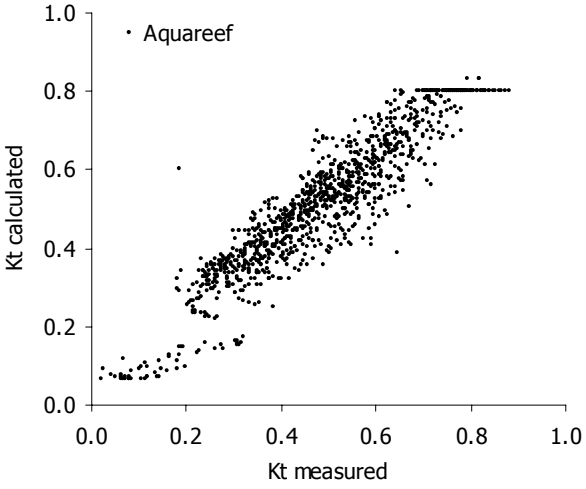
Aquareef
Kt calculated
Kt measured
0.0
0.2
0.4
0.6
0.8
1.0

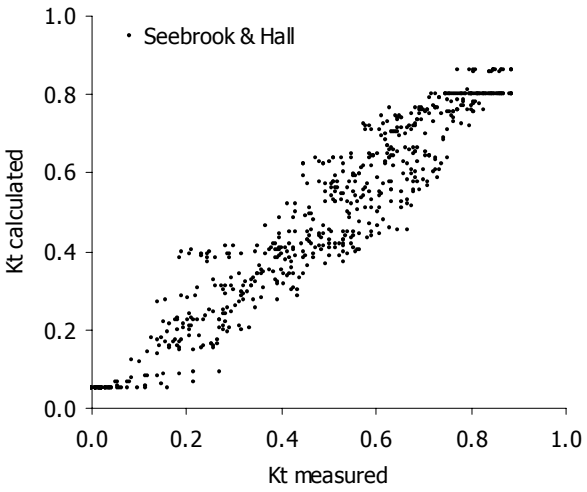
Seebrook & Hall
Kt calculated
Kt measured
0.0
0.2
0.4
0.6
0.8
1.0

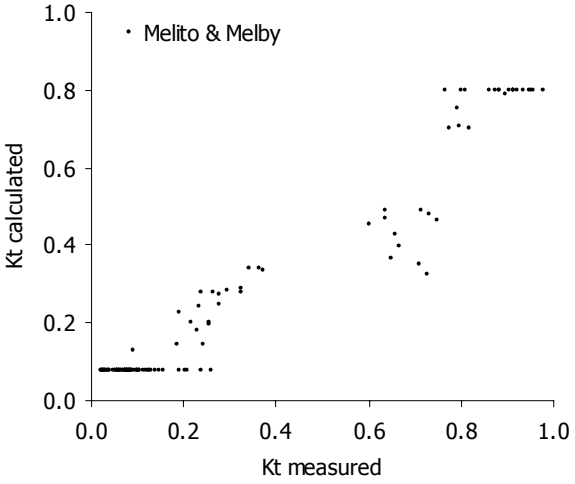
Melito & Melby
Kt calculated
Kt measured
0.0
0.2
0.4
0.6
0.8
1.0

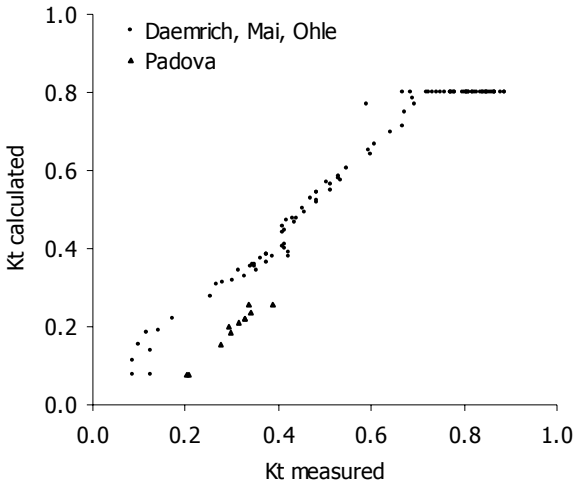
Daemrich, Mai, Ohle
Padova
Kt calculated
Kt measured
0.0
0.2
0.4
0.6
0.8
1.0

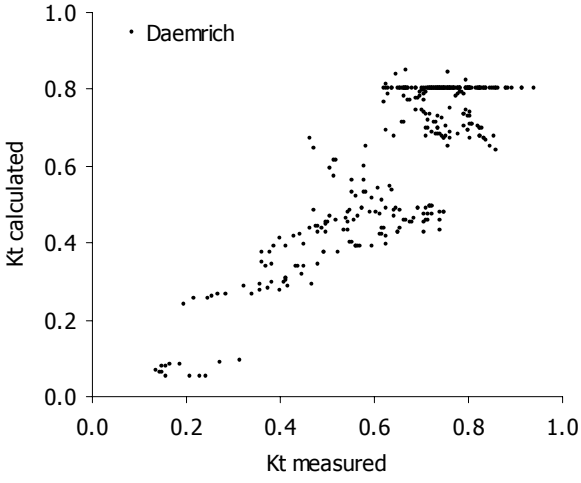
Daemrich
Kt calculated
Kt measured
0.0
0.2
0.4
0.6
0.8
1.0

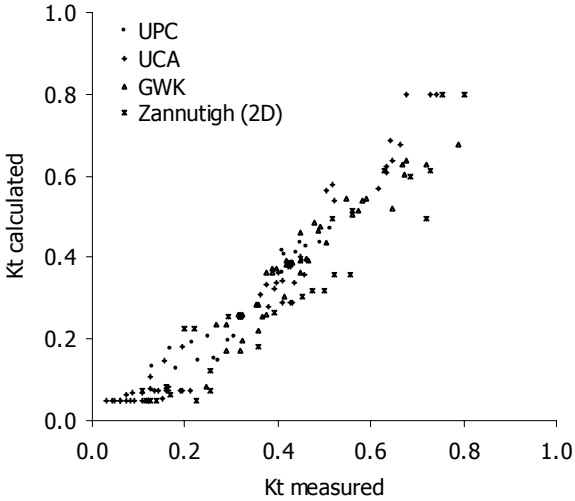
UPC
UCA
GWK
Zannutigh (2D)
Kt calculated
Kt measured
0.0
0.2
0.4
0.6
0.8
1.0

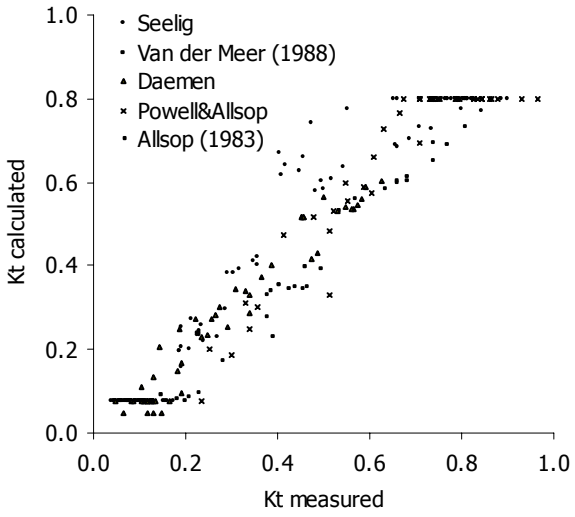

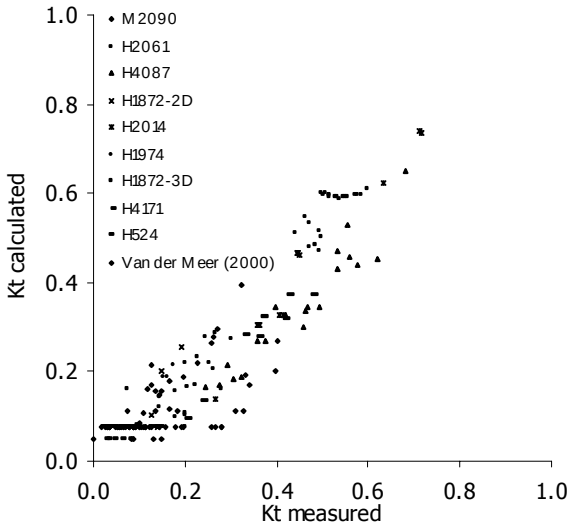

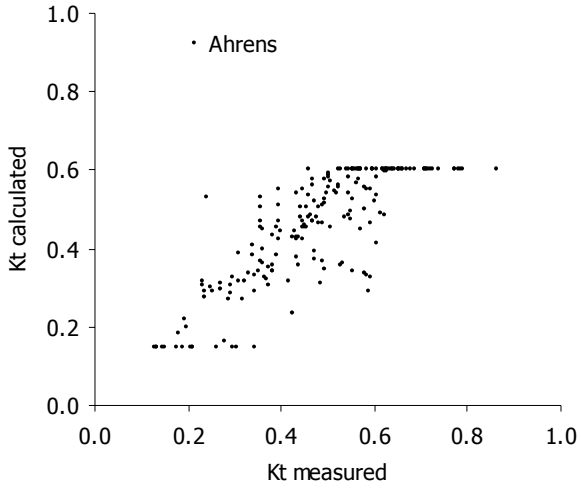

It is quite difficult to determine outliers, because the data points are present in a cloud for which it is difficult to see the boundaries. For the tests the data points are considered to be outliers, because the position of these data points deviate clearly from the data could.

Dataset	Data point	
Aquareef	(0.186 ; 0.600)	Overprediction of the transmission coefficient. Kt measured is too low. Test is very unreliable.
Daemrich, Mai	(0.588 ; 0.767)	Point is obvious deviating from other data. Measured K_t is too low.

Table 3-11 Outliers overview in DELOS prediction formulae

Because it is very difficult to tell on forehand if the data points named in Table 3-10 and Table 3-11 are really wrongly measured tests, they will be included to train the prediction model. Except for the Aquareef test (which seems to be an outlier too in the neural network of Panizzo et al. (2003)) named in Table 3-11 (test number 747 in database). If the prediction model shows to have difficulties too in the prediction of these points they will be exposed from training the neural network.

4 Prediction model

This chapter concerns the prediction model that is made during this study to improve the prediction of wave transmission. A brief introduction on prediction models is written in Paragraph 4.1. An explanation about what neural networks are and insight in the DELOS and CLASH prediction models is given.

A large amount of data is needed to train a useful aNN. With too less data the aNN will not be able to predict accurate results for a wide range of values and for a variety of structures. Therefore, the database is treated in order to make it usable for the network and solve the following questions:

- Are input parameters made dimensionless or scaled? (Section 4.2.1)
- How does the aNN take into account the quality of the tests, which is assigned with the general parameters? (Section 4.2.2)
- What will be the total size of the input to train the network? (Section 4.2.3)

On the other hand, the creation of the aNN is done following the prediction methods of CLASH and Verhaeghe (2005). According to these methods, the main steps to build up the aNN are:

- Build a single aNN, define its proper architecture like the number of neurons, number of hidden layers, neurons per layer, transfer functions and training algorithms (Paragraph 4.3).
- Build a consistent aNN by means of committee of networks with the use of resampling techniques (Paragraph 4.5).

However, there is one intermediate step in between. It entails choosing the final input parameters, which show relevant influence on wave transmission and leave out those parameters, which have no (or very little) influence (Paragraph 4.4). This intermediate step can be done provided that the architecture of the network is well defined. On the other hand it has to be stated that if any parameter is left out; it is important and necessary to define again the proper architecture for the aNN with the new set of input parameters. Clearly, there is a loop present in the process in order to find the optimum model.

Summarized, after the right architecture of the neural network is found with all relevant parameters, a committee of neural networks is made using resampling techniques to obtain the final model. With this committee of neural networks analyzing techniques can be performed (Paragraph 4.6) in order to check the validity of the model. With these analyses it will be possible to obtain insight in the accuracy and reliability of the model. If the model shows any wrong result, adjustments will be needed in the model (mainly leaving out or changing some parameters). As a result, a new architecture will have to be determined again because of the new set of parameters, appearing another feedback. The definitive prediction model will be obtained with this last set of input parameters, the new architecture and the new committee of networks (Paragraph 4.7).

All aforementioned steps are explained in detail in the following chapters. It is important to realize that reliable and accurate results can only be obtained with a good architecture of the aNN, hence a correct and well validated programming is needed. In the following figure the process is schematized:

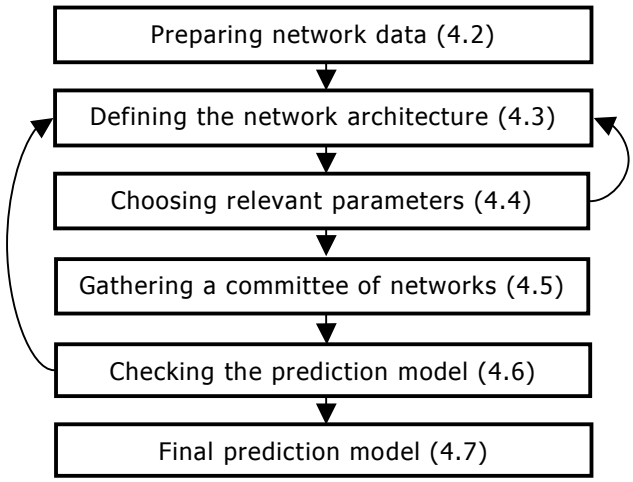

Figure 4-1 Process schematization

Note: *Matlab® 7.0 release 14 and its Neural Network Toolbox 4.0 have been used to develop the prediction model for the wave transmission prediction model of this study.*

4.1 Background on prediction models

There are several empirical formulas available from which wave transmission can be predicted. These formulations have their limitations such as the range of applicability and additionally the reliability of the predicted transmission coefficient is still relatively low.

Computational prediction models, called 'artificial neural networks' (hereafter aNN's), have proven to be useful in many fields of technology. Thanks to these tools it is possible to solve complicated problems where many relations are involved. These kinds of models have already been applied in some researches related to coastal engineering. Some previous studies are: "Study of the stability of rubble mound breakwaters" by Mase et al. (1995), "Prediction of wave forces on vertical structures" by Van Gent and Van den Boogaard (1998), "Study of wave run-up and overtopping" by Medina (1999) and Medina et al. (2002), "Analysis of wave transmission behind low-crested structures using neural networks" by Panizzo et al. (2003), "Neural network modeling of wave overtopping at coastal structures" by Van Gent et al. (2004), "Wave overtopping at coastal structures" by Verhaeghe (2005). Especially the work of the European projects CLASH and DELOS (last two mentioned studies) show many familiarities with the prediction model described in this report.

As stated before, one of the main goals of this study is to use an aNN to solve the wave transmission phenomenon, trying to improve the results compared to previous prediction formulae. This paragraph will explain briefly what aNN's are, as well as the relations of this study to the CLASH and DELOS projects.

4.1.1 Neural networks in general

An artificial neural network is a numerical tool that is very useful for solving classification and regression problems. The intrinsic idea of the method is to imitate the behavior of an animal brain. Input information arrives to so-called neurons after processing this information between all the interconnected neurons, and a final result is given as output.

Neural network structure
An aNN obtains information from I_i *input parameters (placed in the so-called input layer) and this information is managed by* H_n *neurons (placed in the so-called hidden layer) to finally deliver* O_j *output parameters (output layer). An aNN is therefore represented by means of a* $I_iH_nO_j$ *- structure, where* i *is the number of inputs parameters,* n *the number of hidden neurons and* j *is the number of output parameters. Although there is always one input layer and one output layer present, it is possible to have more than one hidden layer. It is clear that in this study the output is restricted to*

only one parameter: the wave transmission coefficient, K_t. The number of neurons in the hidden layer is determined in the Section 4.3.5. Graphically the neural network is schematized in Figure 4-2:

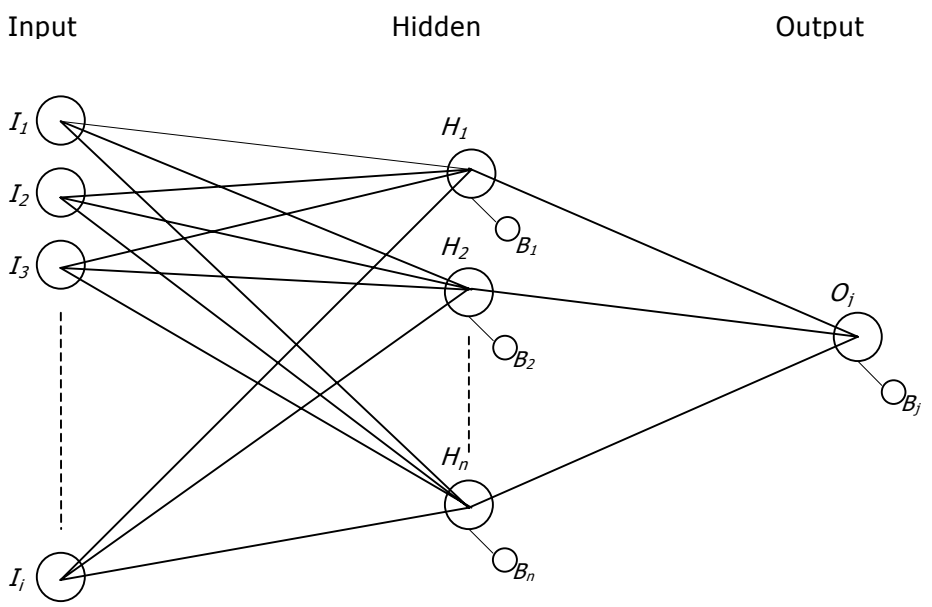

Figure 4-2 Neural network schematization

All input parameters are connected to every neuron in the hidden layer. The strength of the relationship between an input parameter and a certain neuron in the hidden layer is represented by a set weight (W_{ni}). On the other hand, every neuron (in the hidden layer as well in the output layer) also has a bias ($B_{n,}$) connected to adjust the calculation work of the neuron itself.

Neurons apply a kind of processing to the information that they receive. Received information is the total value of all different input parameter values connected to a neuron, times their weight plus the bias of the neuron. The process applied by the neuron to this information is carried out by a transfer function: TF, which transforms all the information to just one value. This process is done in the hidden layer, but also in the output layer where the output neurons receive the results of the hidden neurons and repeat the same process, applying also a transfer function to the summation of all values times their weight, plus the bias of the output neuron itself.

Mathematically, for a neuron of the hidden layer this can presented like:

$$a_n = f(\sum_i W_{ni} \cdot I_i + B_n) \qquad \textit{Eq. 4.1}$$

For a neuron in the output layer:

$$a_j = g\left(\sum_n W_{jn} \cdot f(\sum_i W_{ni} \cdot I_i + B_n) + B_j\right) \qquad \textit{Eq. 4.2}$$

Both regression and classification problems can typically be solved by feed-forward neural networks ('feed-forward' refers to the fact that these networks consist of several layers in which the information moves in forward direction). This kind of networks can be used as a general function approximator, because it can approximate any function with a finite number of discontinuities, arbitrarily well, given that sufficient neurons are present in the hidden layer. There exist two types of feed-forward neural networks: Multilayer Perceptrons (MLP's) and Radial Basis Functions (RBF's). For the specific kind of problem in this study (regression), the MLP's are frequently used neural networks (besides, RBF's may require more neurons).

Neural network learning

A basic aspect of aNN's is the learning process. Learning is basically the process that determines the value of weights and biases. Starting with small random initialization values of weights and biases, the network processes the inputs. The resulting output of a network generally deviates from the desired output. The goal of the learning process is to adapt the weights and biases in such a way, that the difference between the desired and calculated output becomes smaller. If learning is repeated iteratively (one learning process is called an epoch) then the overall process is called training. During training, the proper values of weights and biases are approached. In the prediction model of this study, a supervised training is present, because inputs and their respective outputs from the database are provided to the aNN. In particular a kind of batch training is used; this means that the weights are only updated after calculating the entire training set. Therefore, the aNN adjusts its weights and biases, minimizing the error between the predicted value and the desired value.

There are different types of training methods available. The choice of an appropriate training method depends on the problem that is faced. The best type of algorithm will change depending if classification or regression problems are handled.

An associated problem appears during training. This is known as the generalization problem. This occurs if an aNN fits very well the data points used to train the network, but predicting with new data results in a large error. This large error is caused by overfitting and can occur if there are too many neurons present in the hidden layer. Underfitting (see Figure 4-4) is also possible of course, but in that case the aNN is not able to give a good result for both cases. To solve the problem of overfitting, a generalization method has to be used. Actually, it is possible to train the aNN and solve the problem of generalization at the same time. A Bayesian regularization algorithm can be used in this case (this will be explained further on).

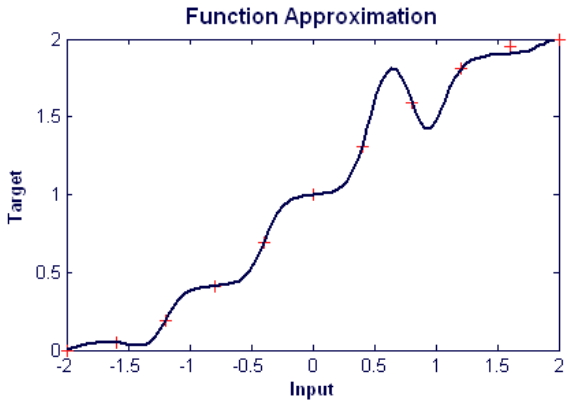

Figure 4-3 Example of overfitting

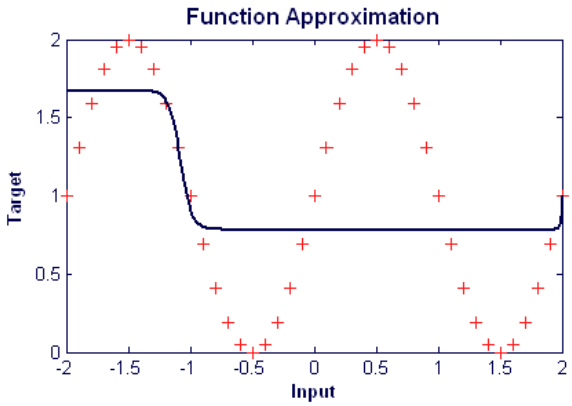

Figure 4-4 Example of underfitting

Neural network performance

The prediction performance of an aNN is measured by two different statistical values: the correlation coefficient (R) and the root mean square error (RMSE).

The correlation coefficient is a normalized measure of linear relationship strength between variables. The square of the correlation coefficient is used to express the correlation between the predicted and the measured values. Values close to $R^2 = 1$, mean a very high correlation (the predicted values are very close to the measured values) and values of R^2 close to zero represents the opposite. Therefore, a good performing aNN will show high values of R^2 close to 1.

The correlation coefficient is defined as:

$$R(i,j)) = \frac{C(i,j)}{\sqrt{C(i,i)C(j,j)}} \qquad \textit{Eq. 4.3}$$

Where C is the covariance defined as:

$$C = \mathrm{cov}(x_1, x_2) = E[(x_1 - \mu_1)(x_2 - \mu_2)] \qquad \textit{Eq. 4.4}$$

Being E = expectation and $\mu_i = E(x_i)$ (mean)

The RMSE, it is defined as:

$$RMSE = \sqrt{\frac{1}{N}\sum_{n=1}^{N}\left(K_{t_{measured}} - K_{t_{preicted}}\right)^2} \qquad \textit{Eq. 4.5}$$

Where N is the size of the test set (the number will be different, depending on the set: training or test set). Low values of the RMSE mean that the predicted values are close to the measured values and vice versa. In this study one is interested in obtaining low values of RMSE and a R^2 as close to a value of 1. The value of R^2 can always be used to compare the performance of the aNN with other prediction methods, for instance the DELOS formulae. The RMSE can be used as comparison, provided the sizes of output sets are similar.

4.1.2 DELOS prediction model

During the DELOS project two prediction models have been made: empirical formulae after an extensive analysis of available data and a neural network prediction to show the capacity of those kinds of prediction models.

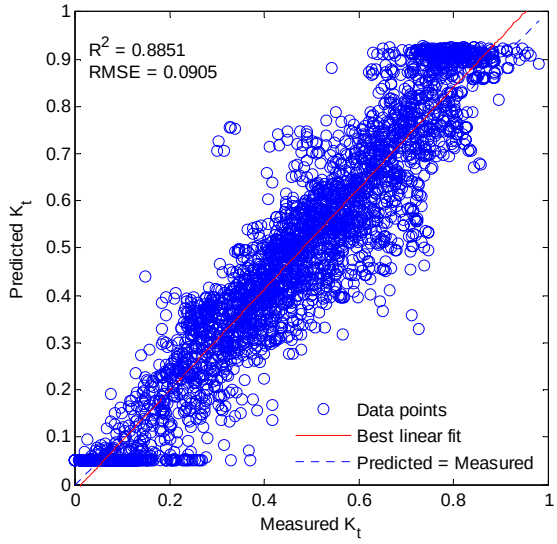

Figure 4-5 DELOS prediction

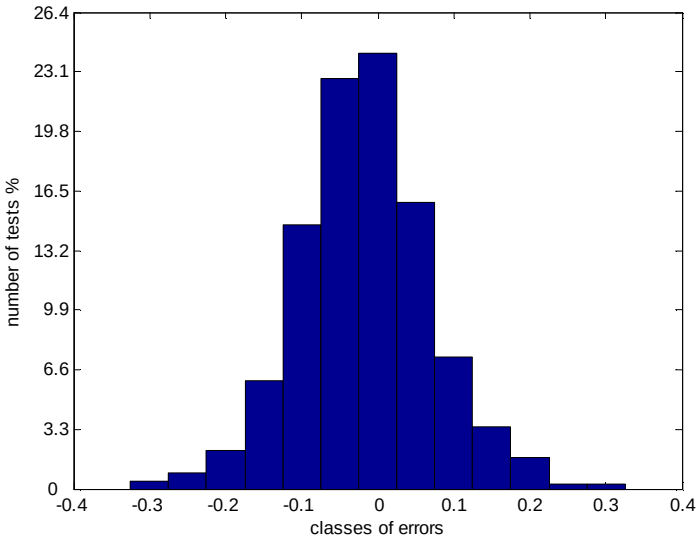

Figure 4-6 Distribution of DELOS error

The results after applying the homogeneous database (without Ahrens dataset and caisson structures) to the DELOS formulae are quite accurate, although the width of the band of predicted values is rather wide. Despite this, more than 80% of the tests are predicted with an error lower than 0.1 (absolute value).

With some datasets of the DELOS database a simple neural network has been used to investigate the possibility of predicting wave transmission (Panizzo et. al., 2004). In total 2,337 tests were used, described with 6 dimensionless parameters:

$$R_c/H_i,\ H_i/D_{n50},\ W_c/H_i,\ W_c/L_{op},\ I_r,\ H_i/h$$

Promising results were obtained. The aNN consisted of 6 neurons in the hidden layer and a RMSE of 0.0381 with R^2 = 0.973 was reached without any model testing (no test set was used to validate the neural network, (see Figure 4-7)). Comparing with the DELOS formula, the prediction of the aNN showed a considerable improvement. However, this aNN was only trained with mound structures (no smooth structures were included) and it is not available to use it for new datasets.

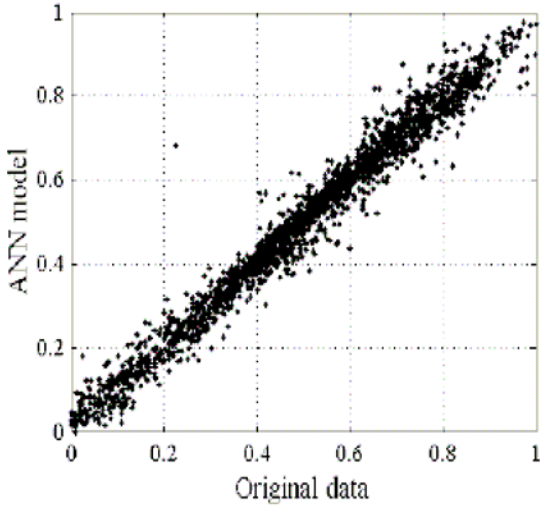

Figure 4-7 Panizzo et al. (2004) prediction

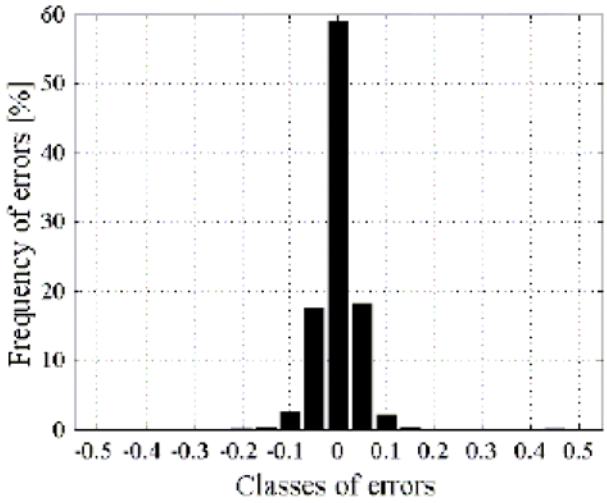

Figure 4-8 Distribution of error Panizzo et al. (2004)

The result above are obtained without model testing. So the values are referred to the training set (100% of the total). In case of a test set consisting of a 10% of the available tests, the results obtained are R^2 = 0.970 and RMSE = 0.0396 with a dataset of 2,337 tests.

4.1.3 CLASH prediction model

Within the European project CLASH a huge database of tests of wave overtopping was collected (more than 10,000 tests) and a generic predictive method of overtopping was applied.

Within this project one model was made by Van Gent et al. (2004) from Delft Hydraulics but another model outside the CLASH project, was carried out by Verhaeghe (2005) from Ghent University (called from now the Verhaeghe model); both models were based on neural networks. The first model is a quantifier that determines the mean overtopping discharge whereas the second model consists of two subsequent neural networks: a classifier that detects whether overtopping occurs or not and a quantifier that only is run in case that the classifier is detecting overtopping.

In any case, both studies revealed that aNN's were capable to model the relationship between the input parameters involved in wave overtopping and the mean overtopping discharge at coastal structures. The accuracy between the predicted overtopping discharge and the measured overtopping discharge was significantly improved. The predictions were rather accurate compared to the observed overtopping discharges (Pozueta et al., 2004). Taking into account these interesting results this current study is based on the methods used in these two prediction models. The main important methods of the CLASH and Verhaeghe's prediction models are:

- A Multilayer Perceptrons neural network was used.
- A weight factor matrix was applied to enhance the importance of reliable tests and well-described structures (Pozueta et al., 2004).
- Division of available data to 85% training set and 15% test set in order to detect overfitting and the initial aNN performance.
- Use of a so-called bootstrap resampling technique, which enables to use all the available data and solves the problem of representativeness (explained below).
- Use of an ensemble of aNN's to improve the prediction and to make an uncertainty assessment and a sensitivity analysis.

One of the most important problems to face was the problem of representativeness. A great amount of data is needed to train and check an aNN, if one wants to make an accurate and reliable prediction model. Applying weight factors and resampling techniques makes it possible to increase the total number of tests (weight factors) and also to use the entire database for training and testing the neural network (bootstrap method).

Summarized, the EU-funded project CLASH and Verhaeghe showed that an aNN is a good tool to prepare a prediction model and is very suitable to be used as an example for the prediction model of wave transmission in this study. Hence, the wave transmission aNN that will programmed in this study will show many similarities with the aNN's of CLASH and Verhaeghe, although there are some

relevant differences to take into account. The CLASH database is about three times bigger than the wave transmission database, making it possible to use more input parameters and handling a larger variety of structures. Additionally, the parameters involved in the overtopping prediction model are not completely the same as for wave transmission (due to different phenomena).

4.2 Preparing network data

The used database consists of 3,382 tests, from different origins and from different types of breakwater structures as shown in Table 3-1. The database has been homogenized with the aim of consequently describing all tests in the same manner. The homogenized data is applied with a scaling process in order to solve the problem of handling tests of different test scales (small scale-, large scale- and prototype tests). This step is found to be very important for the neural network, because scaled data allows to be compared with each other.

The more data is available, the better aNN model will be obtained because in this way the model will "learn" better and more cases can be handled. An artificial way to increase the number of tests of the original database is by means of using weight factor.

The network has to be trained with the available data in order to make it able to predict new cases thanks to the "experience" acquired in the training. A division in the available data is done in order to train the network but also check it with new cases using the same database.

All these matters are explained in the following paragraphs.

4.2.1 Scaling process

The entire database is scaled according to Froude's law, by converting the incident wave height at the toe of the structure to a reference value of 1m. This converting is necessary in order to make it possible to compare results of different test scales. Tests for instance, with wave heights of a few centimeters can be compared with tests of wave heights up to a few meters, which would give very different results. Furthermore the neural network is always fixed on an incident wave height of 1m, which is favorable for the prediction capacity.

Another possibility to solve the problem of different test scales is to make all input parameters dimensionless. However, when using this method the problem of choosing which parameter should be used in order to make a certain parameter dimensionless arises. Besides that, if a certain parameter has a value of zero information is lost. In that case it is unknown if the parameter in the denominator is big or small. Because of the problems mentioned above it is preferred to use the method of scaling by Froude's law. This procedure was also applied in the CLASH project, but not in DELOS where the parameters were made dimensionless.

The initial number of input parameters which have been used to train the aNN is 13 (incl. incident wave height as scale factor). For a first attempt these parameters are used to set the initial architecture of the neural network. The selection of parameters differs from the final prediction model, because an extensive analysis is carried on the performance of different parameters. Two of these parameters are hydraulic parameters (spectral wave period and angle of wave attack) and others are structural parameters.

A statistical analysis of the selected parameters after applying the Froude's law is shown in the next table:

Parameter	Mean	Standard deviation	Maximum	Minimum	Unit
Hmo toe	1	0	1	1	m
Tm-1,0 toe	5.24	2.03	21.70	2.82	s
h	3.99	3.03	6.01	-0.72	m
hb	0.40	0.78	30.81	0.35	m
B	0.49	0.86	4.99	0.00	m
Rc	-0.41	1.29	8.87	-9.84	m
Wc	7.38	11.36	90.48	0.01	m
Cot α df	2.04	0.90	5.00	0.00	-
Cot α uf	1.94	0.92	5.00	0.00	-
Cot α ub	1.51	1.16	5.00	0.00	-

γ f	0.49	0.16	1.00	0.38	-
P	0.50	0.15	0.60	0.10	-
β	2.21	9.36	83.00	0.00	-

Table 4-1 Input parameter distribution after Froude scaling

4.2.2 Weights factors

According to Pozueta et al. (2004), from the reliability of a specific test and the complexity of a structure test section a weight factor is assigned to a test between 0 and 9. In general can be said, the more reliable the test is found to be, the higher this weight factor is set. The value of the weight factor (hereafter WF) is easy to determine from the combination of the values of the reliability- and complexity factor (RF and CF had been treated in Paragraph 3.7):

Weight Factor		***CF***			
		1	*2*	*3*	*4*
	1	9	6	3	0
RF	*2*	6	4	2	0
	3	3	2	1	0
	4	0	0	0	0

Table 4-2 Determination Weight Factor

The value of WF is used to give more weight to tests, which have been well measured and were the specific section was easy to describe within the homogeneous database. The value of WF represents the number of times an individual test will be repeated in the aNN training set. For example, a value of 0 means that a certain test has a very low reliability or a large complexity (or both of course) and the test will not appear in the training set, a value of 9 means for instance that this test will appears 9 times. Before applying the WF, tests have already been homogenized and scaled.

The network needs a considerable quantity of tests to learn well and to be able to make a general and accurate prediction. By applying the WF, the amount of data to train the network increases and additionally, reliable and more representative tests have a higher presence in the training set than those tests that are less reliable and more difficult to describe. In this way the aNN learns a greater amount of data than present in the original database.

The WF is applied only to the training set in the first stage (determining the architecture of the network) and in the second stage as well (creating an ensemble of aNN's).

4.2.3 Training- and test set composure

In the phase of determining the neural network architecture, the original dataset is divided to create two subsets: the training set and test set. The training set contains data that will be used to train the aNN, whereas the test set contains data that will be used to verify and validate the prediction model and detecting generalization problems because this set is recognized as new data by the network. The first step to create these subsets entails applying a modified WF with only ones and zeros (zero if CF or RF is equal to 4 and one for the remaining tests) to the original dataset. In this way a reduced original dataset is obtained (hereafter ROD) with only tests with a WF > 0 (to be precise 3,118 tests). After this first selection, a second division of the dataset is made: 85% is selected for the training set and the remaining 15% is selected for the test set. The selection of these tests from the ROD is done randomly to avoid the fact of taking only tests of one type of breakwater structure. A test set remains without any changes (exactly 468 tests), but the training set is submitted to the WF, increasing the training set with a total number of test 11,700 tests.

It has to be mentioned that the size of the test set is relatively small, and the prediction performance of the aNN is highly depending on its data selection (one test set may contain many rubble mound tests, whereas another test set may have a lot of smooth structures selected).

4.3 Defining the architecture

Once an adequate training set is obtained (homogenized, scaled and applied with WF), it is possible to start with the first of the main steps to create the aNN itself.

In this first step the basic architecture of the network is determined. The order to define the different elements of the network is given below:

1) *Type of neural network.* There are several types of neural networks available, but a choice is much depending on the kind of problem that is faced (Section 4.3.1)
2) *Number of hidden layers.* An aNN becomes more powerful if an extra hidden layer is added, but the computational costs have to be taken into account. The improvement of adding more hidden layers is not always a guaranty for a better prediction (Section 4.3.2).
3) *Type of transfer functions (TF)*. There are several types of TF, but one or another can be more appropriate, depending on the layer where it is applied and the kind of result that is desired (Section 4.3.3).
4) *Training method and generalization problem*. Several kinds of training algorithms are available. However, one could perform better than others, depending on the problem again. Besides, a method to solve the generalization problem has to be applied if one is interested in predicting the wave transmission of new introduced breakwaters (Section 4.3.4).
5) *Number of neurons in the hidden layer*. The greater the number of neurons used, the better results will be obtained, but the computational cost increases as well as the chance of having overfitting problems (a further explanation is given below). A balance has to be found (Section 4.3.5).

Once the architecture is defined, the second main step can be taken to build the definitive prediction model. In advance, the results of the aforementioned steps have determined the following set-up for the aNN (these values will be explained and justified in the next sections):

aNN structure	Transfer Functions	Training method
I_{12} - H_{17} - O_1	Log-sigmoid (hidden layer) Saturated linear (output layer)	Bayesian Regularization

Table 4-3 Final architecture of neural networks in the prediction model

It is important to remark that slightly different values of RMSE for the training and test set will be obtained in every new run of the network, unless the initial set of weight and biases was fixed as well as the training set and test set. In general these small differences in the performances are not very important, unless one was interested in a comparison between different performances (see Section 4.3.5 and Paragraph 4.4).

4.3.1 Type of neural network

The type of problem that is faced in this study is regression. The most commonly kind of aNN used for that kind of problem is the Multilayer Perceptron (MLP).

4.3.2 Number of hidden layers

According to Hornik (1989), one single hidden layer is sufficient to have a universal approximator, able to approximate any continuous nonlinear function arbitrary well on a compact interval. Moreover, this is a frequently used MLP-configuration: input layer, hidden layer and output layer.

Therefore, the number of hidden layers is one. Besides the time-cost with two layers would be too high (adding an extra-hidden layer with the same s neurons as the previous hidden layer would increase the computational cost in order of s^2 operations) and the improvement in results insufficient.

4.3.3 Type of transfer functions

The total input to a neuron includes its own bias and the summation of all weighted inputs. The output of a neuron depends on the neuron's inputs and on its transfer function. Hence, the choice of the TF will decide the value of the output.

In case of feed forward neural networks, the log-sigmoid transfer function is commonly applied between input and hidden layer, because this is a differentiable function. For the transfer between hidden layer and output layer, the most usual transfer function is a linear function, because it can adapt any value. It is preferred to obtain only results in the interval of $0 < K_t < 1$, because this is the range of physical right values of the wave transmission coefficient. To obtain this criterion, the linear saturated-linear function is applied.

The log-sigmoid TF (see Figure 4-9) works in the following way: it takes an input, which may have any value between plus and minus infinity, and squashes the output into the range 0 to 1.

The saturated linear TF (see Figure 4-10) works in the following way: it takes an input, which may have any value between plus and minus infinity, and gives an output value in the range 0 to 1. If the input value is below 0, then the TF truncates the value into 0. The same for inputs with values above 1, but the TF truncates the value into 1.

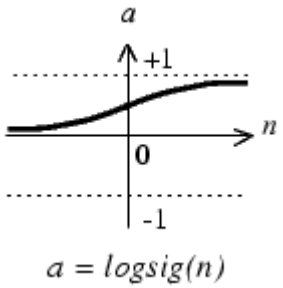

Figure 4-9 Log-sigmoid TF

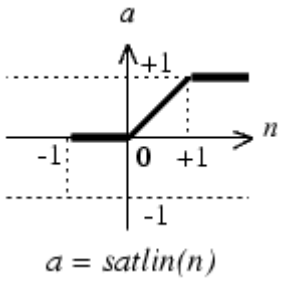

Figure 4-10 Saturated Linear TF

To sum up, the types of transfer functions in this aNN are log-sigmoid function for the hidden layer and a saturated linear function for the output layer.

4.3.4 Training method and the generalization problem

As it has been explained in the Section 4.1.1, training is one of the most important elements of an aNN. The quality of the prediction depends directly on the quality of the training.

One of the main demands to a training method is a high speed of convergence. This matter is closely related to the kind of problem that is faced and the size of the aNN. In this study, it is facing a regression problem with an aNN size around 15-25 neurons present in the hidden layer (it means several hundreds weights). According to Hagan (1994 and 1996), the Levenberg-Marquardt algorithm appears to be the fastest method for training moderate-sized feed forward neural networks (up to several hundred weights) and for function approximation problems. Moreover, this advantage is especially noticeable if very accurate training is required. Therefore, the algorithm that fits best to this study is the Levenberg-Marquardt algorithm.

The Levenberg-Marquardt algorithm was designed to approach second-order training speed, without having to compute the Hessian matrix (like the quasi-Newton methods). When the performance function has the form of a sum of squares (as is typical in training feed forward networks), then the Hessian matrix can be approximated as $H = J^T J$ and the gradient can be computed as $g = J^T e$ where J is the Jacobian matrix that contains first derivatives of the network errors with respect to the weights and biases, and e is a vector of network errors. The Jacobian matrix can be computed through a standard back propagation technique (Hagan, 1994) that is much less complex than computing the Hessian matrix. The Levenberg-Marquardt algorithm uses this approximation to the Hessian matrix in the following Newton-like update:

$$x_{k+1} = x_k - \left[J^T J + \mu I\right]^{-1} J^T e \qquad \textit{Eq. 4.6}$$

When the scalar μ is zero, this is just Newton's method, using the approximate Hessian matrix. When μ is large, this becomes gradient descent with a small step size. Newton's method is faster and more accurate near an error minimum, so the aim is to shift towards Newton's method as quickly as possible. Thus, μ is decreased after each successful step (reduction in performance function) and is increased only when a tentative step would increase the performance function. In

this way, the performance function will always be reduced at each iteration of the algorithm (Marquardt, 1963).

On the other hand, the problem of generalization has to be taken into account. As it has said in the Section 4.1.1, the problem of overfitting can appear during training: the error on the training set is driven to a very small value, but when new data is presented to the network the error can be large. In other words, the network has memorized the training inputs-outputs, but it has not learned to generalize to new situations. There are several measures to solve this problem: implementing a generalization method, increasing the size of the training set or choosing the proper number of neurons (too many could generate complex relationships producing overfitting). In this study all possible measures have been applied.

Within the generalization matter, there are two different algorithms available: regularization or early stopping. Regularization is based on modifying the performance function, which is normally chosen to be the sum of squares of the network errors on the training set; whereas early stopping divides the dataset into three subsets (training set, validation set and test set) and it is based on when the error of the validation test begins to rise (due to overfitting) then the training stops. According to the Neural Network toolbox of Matlab®, regularization generally provides better generalization performance than early stopping, when training function approximation networks. This is because regularization does not require that a validation data set is separated from the training data set; it uses all data for training.

Hence, a regularization algorithm is implemented in the aNN. The algorithm used is the Bayesian regularization based on the Bayesian framework (McKay, 1992). Bayesian regularization updates the weight and bias values according to the Levenberg-Marquardt optimization: minimizing a combination of squared errors and weights, and determining the correct combination in order to produce a network that generalizes well (Foresee, 1997). Additionally, a pre-process is applied to the dataset to normalize all inputs and outputs to the range [-1, +1]. The algorithm works better in this way because values of data points are placed in the same range and therefore easier to approximate.

When using Bayesian regularization, it is important to train the network until it reaches convergence. There are possibilities to detect convergence: the sum squared error, the sum squared weights and the effective number of architecture parameters reaching constant values after the network has converged.

Like the size of the test set, since the total number of architecture parameters in the network (±260 architecture parameters with ±20 neurons in the hidden layer) is much smaller than the total number of tests of the training set (around 11,800), the chance of having overfitting is minor. Also the number of neurons in the hidden layer is studied to avoid overfitting.

4.3.5 Number of neurons in the hidden layer

Networks are sensitive to the number of neurons in the hidden layers. In general, the more neurons a hidden layer contains, the more powerful the network will be: more complicated relationships can be established between different input parameters and the better results can be obtained. However, increasing the number of neurons can cause problems. Too many neurons can contribute to overfitting in which all training points are well fit, but the fitting curve takes noisy oscillations between these points, causing a bad prediction for new points, which do not belong to the training set. But with too few neurons there are problems as well, like underfitting (see Figure 4-4), In this case the network is not flexible enough to match reality properly.

One is always interested in a powerful network, so a maximum number of neurons possible is preferred. As it has stated in the last chapter, a generalization method like Bayesian regularization, is used to solve the problem of overfitting. Moreover in this case, due to the relative large number of data, it is very difficult to experience overfitting, because it would not be easy to join all points with a single function. However, the possibility of encountering the problem of overfitting cannot be neglected. It is important to realize, that a high number of neurons does not always means that the prediction will be much better. It could be that some of the neurons become idle, increasing the computational cost without a significant improvement of the results. A fair balance has to be found between quality of results and computational cost.

A method to determine the proper number of neurons is based on the comparison of the RMSE of an equal aNN, but trained with a different number of neurons. The trend line of the development of

RMSE can be used to determine a first indication for the proper number of neurons. For this approach, the aNN defined in the previous chapters is trained and checked with a number of neurons varying within the interval [10, 30]. It is assumed that the proper number of neurons falls is present in this range. All cases use the same training and test sets, but initial weights and biases are different.

For every case the RMSE of the training set as well as the test set are calculated, and checked with the condition of the overfitting principle. According to this principle a higher number of neurons means more complicated relationships are possible between different parameters and then the fitting is enhancing until all the points are matched with one line (total overfitting). Therefore, increasing the number of neurons the network becomes more powerful, hence better performance should be always obtained in the training set. For the test set this is true as well, until the moment overfitting start to show influence (the network is becoming unable to predict new data). To use this statement, the aNN's are trained up to their RMSE of the training set are lower than the RMSE of the training set of the previous aNN, which have one neuron less. At the same time the RMSE of its test set is calculated. Having done this, it's possible to plot the results and analyze the trends of the RMSE of training and test sets for the different aNN's. Furthermore, with this method, the effect of the random values of the initial weights and biases on the results is eliminated, so possible fluctuations in the training line due to a bad run are not present and like this it is easier to analyze the trends. On the other hand, the same training set and test set is used for all aNN's to make the results comparable.

The training of each aNN will last 1000 epochs at most, it means that the training will stop after 1000 epochs at the most. An epoch is one iteration, where the training function proceeds through the specified sequence of inputs, calculating the output, error and network adjustment (weights and biases) for each input vector in the sequence as the inputs are presented. Although a fast training method is used, the training process is quite time-consuming; the network is still learning along the last epochs. One can think of decrease the number of epochs because the rate of learning is very small in this last part, but a network needs more epochs to learn if number of neurons is relative high (there are more and more architecture parameters involved).

It is possible that more than one training had to be carried out before the RMSE of the previous aNN was reached or improved. Each aNN has random initial values for the initial weights and biases and, because of this, it is possible that components were closer or further from definitive values, additionally taking into account the limit set in the number of epochs, it may happen that the final weights and biases were close or far from those definitive values, giving a smaller or bigger RMSE according to the case.

On the other hand, taking as references other studies, it is found:

Research	Daemen et al., 1994 (with Delos database)	Delos formulae (with this database)	Panizzo et al., 2004 (with Delos database)
RMSE	0.112	0.0905	0.0396 (10% model testing)

Table 4-4 Comparison of RMSE of existing prediction models to homogeneous database

Since a better prediction model is desired, the RMSE of Panizzo et al. (2003) is taken as a minimum goal because it has the lowest RMSE. Two things are important to remark: the RMSE given for Panizzo et al. (2003) is the RMSE of the training set, not of the test set and the dataset used is smaller than this database and, moreover, it only consists of rubble mound structures.

Summarizing, aNN's are trained from 13 to 30 neurons in the hidden layer and both training and test set RMSE are calculated, according to the overfitting principle. A summary of the conditions is given in the next table:

Range of neurons	**Epochs**	**Training algorithm**	**Size of training set**	**Size of test set**
From 13 to 30	1000	Bayesian regularization	11,762 (85%)	468 (15%)

Table 4-5 Settings for the determination of number of neurons

Furthermore, in order to obtain the proper number of neurons, two criteria are applied:

- *Quantitative criterion*. Find the number of neurons where the trend of the RMSE of the test set starts to increase after having been decreasing before (general minima), showing the overfitting symptom.
- *Qualitative criterion*. Find the number of neurons where the RMSE of the test set is quite low with a relatively low value of number of neurons and the general trend is almost horizontal (increasing the number of neurons doesn't obtain great reductions of the RMSE but it gives much higher computational costs).

A thorough analysis is done resulting in Figure 4-11:

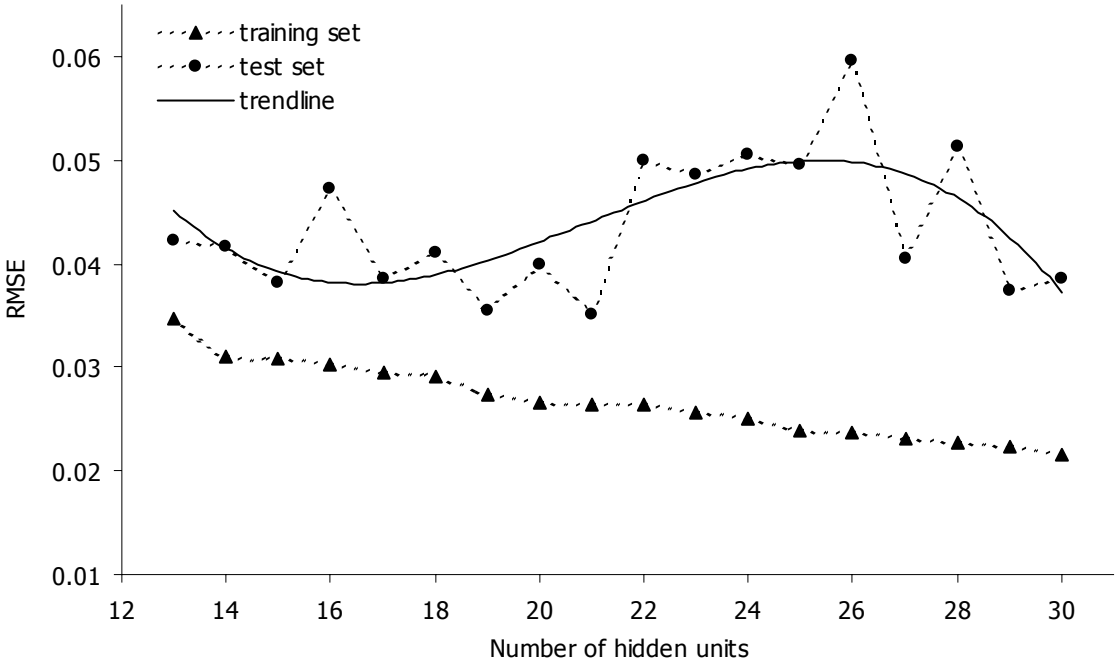

Figure 4-11 Number of neurons versus the RMSE

The general trend in both cases (training set and test set) is downward up to 21 neurons, after this point the RMSE increases suddenly for the test set. On the other hand the test line is always above the training line, completely logical because the network is "designed" (trained) with the training set whereas the test set is recognized as a new data by the aNN, making its prediction a bit more difficult and, consequently, showing an increasing RMSE.

In the first stage (until 21 neurons), the slope of both trends is constant, thus the reduction of the error is proportional to the number of neurons for both training and test sets. Some oscillations appear in this range, they are not very big and they may be caused by the composition of the test set and the training of the aNN, in other words, according to the training the prediction of the test set will be slightly better or worst. If this study was repeated and another plot drew, the points in this stage will appear shift downwards or upwards but in the same range of values of RMSE [0.035, 0.045].

However, the big oscillation in the 22^{nd} neuron can not be understood as a simple fluctuation. This gap measures around 0.015 units of RMSE and breaks the general trend of the test set and creates a big difference between the training set and the test set (around 0.025 units of RMSE). Besides, the trend seems to be horizontal after the gap, but after the 25^{th} neuron big fluctuations appear, showing no improvement as the more neurons are used; clearly, the behavior is unstable in this region of the plot. The reason is probably overfitting, although the training trend is going downwards, the test set worsens its results, revealing the overfitting problem.

Conclusion
Having the two possible criteria (qualitative and quantitative criteria), the neuron plot (Figure 4-11) in mind and the goal of this study (to produce a good predictive model), a reasonable criterion to apply would be the qualitative one for this case because, although a relative global minima is found for 21 neurons, if one wants to combine good results, low RMSE without overfitting risk and relative

low computational cost, the suitable number of neurons seems to be 17; moreover, according to the trend line, this value seems to be the relative lowest value of the test set. Another possibility could be 21 neurons, but it is located next to the big gap indicating there is a risk of overfitting. Of course the computational cost of 17 neurons is relatively high (although low compared with the cost of 21 neurons), but in this case the computational cost problem is secondary because the training process and the bootstrap process will be carried out only one time to produce the definitive aNN and it is worth sacrificing to save time in return for obtaining a good prediction method.

4.4 Choosing relevant parameters

A method to distinguish relevant input parameters from superfluous ones is to simulate a network with all parameters selected and determine the RMSE. After this, the network can be trained with skipping a single parameter each round. Knowing that the RMSE of a simulation with all input parameters would theoretically result the lowest value of the RMSE given that all parameters are containing relevant information. Those simulations with a RMSE equal or with nearly the same value as the simulation with all the parameters have found to be superfluous parameters. On the other hand, those simulations resulting in a high RMSE mean that specific parameters are important, because leaving the parameter out, the RMSE increase considerable. Parameters of minor importance could be left out of the final prediction model. The network architecture (proper number of layers and neurons) should again be checked for the final number of input parameters.

However, this method may detect that some parameters have no influence, however in reality they could have influence. The reason is that for some parameters (for instance β) there is only a reduced number of tests available where this parameter shows a truly influence although this method is unable to notice it. Therefore it is important to take this into account when analyzing the results.

It is relevant to remark since some parameters are closely related, that some simulations have been trained with excluding two parameters instead of a single one. This is the case for the berm width and berm depth as well for the upward slope and downward slope at the seaside of the structure. The relationship between berm width and berm depth is clear; No berm depth can be present if no berm width is given. Regarding the slopes, as their values are often equal (uniform front slope), the effect of leaving out one front slope is not representative for studying the influence, because the network contains in that case still the other slope to train with. It is important to realize that an aNN does not understand the physics of the problem because it is only a mathematical tool. It cannot find intrinsic relationships between parameters (for instance berm width and berm depth).

All simulations share the same conditions: same training- and test set, same number of epochs (1000), same number of neurons in hidden layer (17), etc. The following plots (Figure 4-12 and Figure 4-13) have been produced according to these settings.

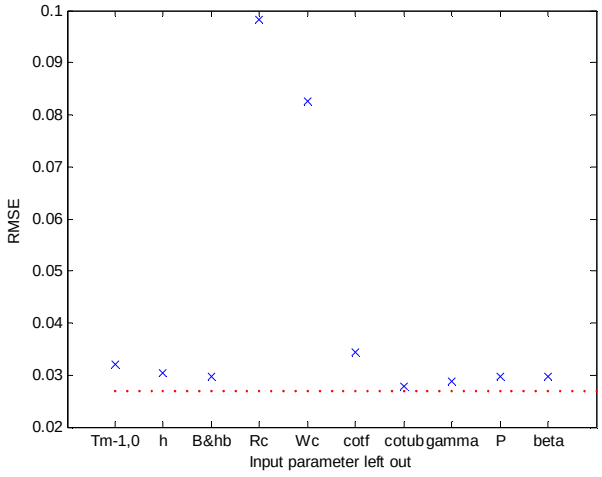

Figure 4-12 Parameter influence for training set

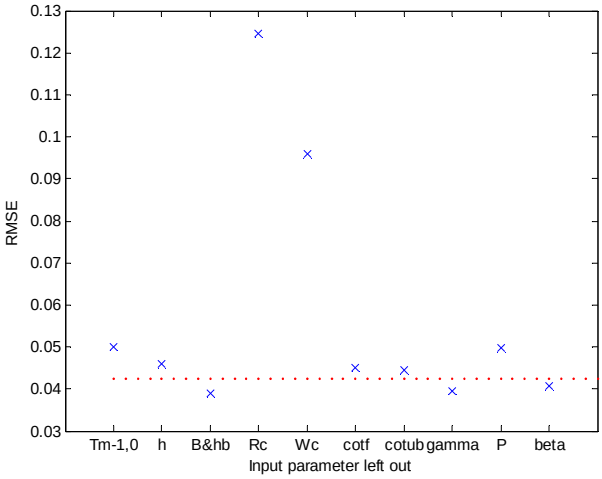

Figure 4-13 Parameter influence for test set

The figures show the influence of single parameters by on turn leaving them out of the neural network and determining the corresponding RMSE. As reference, the RMSE using all parameters is marked with a dotted horizontal line. Specific values of the figures above are summarized in the following table:

Input parameter	RMSE of training set	RMSE of test set
$T_{m-1,0\ toe}$	0.0321	0.0499
h	0.0303	0.0460
B&h_b	0.0296	0.0388
R_c	0.0983	0.1246
W_c	0.0825	0.0960
$\cot\alpha_f$	0.0343	0.0450
$\cot\alpha_{ub}$	0.0279	0.0446
γ_f	0.0287	0.0394
P	0.0298	0.0498
β	0.0298	0.0407
all	0.0268	0.0423

Table 4-6 Overview of specific values when individual parameters are left out

It is possible to distinguish important input parameters from the unimportant ones analyzing Figure 4-12, Figure 4-13 and the Table 4-6 (Sections 4.4.1 and 4.4.2). On the other hand, in order to improve the relevance of some parameters (P and berm parameters) an analysis of alternatives is carried out in Section 4.4.3. After this, a study about a possible uncertain relation between the different slopes is carried out in Section 4.4.4. Finally, a conclusion about the selected input parameters for the final model is written in Section 4.4.5.

4.4.1 Important parameters in the prediction

As physically expected, both crest freeboard and crest width have a large influence on the prediction of wave transmission for both training- and test set. Excluding these parameters from the neural network results in a significant increase of the RMSE. There are other parameters too which certainly show to be of importance although not as clear as crest freeboard, crest width, wave period, depth at the toe of the structure, front slopes of the structure and P. Some of these parameters have already been used in empirical formulae (wave period and slopes combined in the Iribarren number), but other parameters like the depth at the toe of the structure have not been used and according to this analysis, they seem to be important for the prediction capacity.

Concluding, the obvious relevant parameters for the prediction model are:
$T_{m-1,0\ toe}$, h, R_c, W_c, $\cot\alpha_{df}$, $\cot\alpha_{uf}$ (front slope in general) and P.

4.4.2 Unimportant parameters in the prediction

There are some parameters present, which seem to have a low influence on the prediction performance. In fact it seems that without these parameters the prediction even improves, when concerning the test set. These parameters are: the entire berm presence (berm width and berm depth), roughness factor and angle of wave incidence. The values are summarized in Table 4-7.

Parameter	B and h_b	γ_f	β	all
RMSE training set	0.0296	0.0287	0.0298	0.0268
RMSE test set	0.0388	0.0394	0.0407	0.0423

Table 4-7 Performance of neural network excluding individual parameters

A wrong conclusion would be to exclude those parameters from the neural network by thinking that all these parameters are not of importance. The difference between the RMSE of training- and test

sets gives more important information: Showing which parameters become important according to the type of breakwater structure. The predictions of training set give information about how important certain parameters are in general; the training set consists of 11,700 tests so the network has enough data to evaluate the importance of the different parameters. Having this in mind and also Figure 4-13, it can be stated that all parameters are important in the learning phase (all of them are positioned above the red line). However, the test set only consists of 468 tests, hence it is likely that only a few structures with berm or with a certain angle of wave attack or impermeable were present in this test set. Because of minor presence, the overall prediction capacity of this test set underestimates the influence of these parameters. These parameters only reveal their importance when a characteristic structure with one of these properties is asked to predict. These input parameters, B + h_b, γ_f and β, are analyzed in more detail.

Berm influence

An aNN is trained and tested with a ROD without including a berm width (B) and berm depth (h_b) as input parameters (in total 10 input parameters). In this way it is possible to gain insight in the importance of berm parameters (width berm and depth berm) for the prediction model. Additionally, the aNN will be also checked with only those tests of the test set with structures having a berm (around 150 of the total test set of 468).

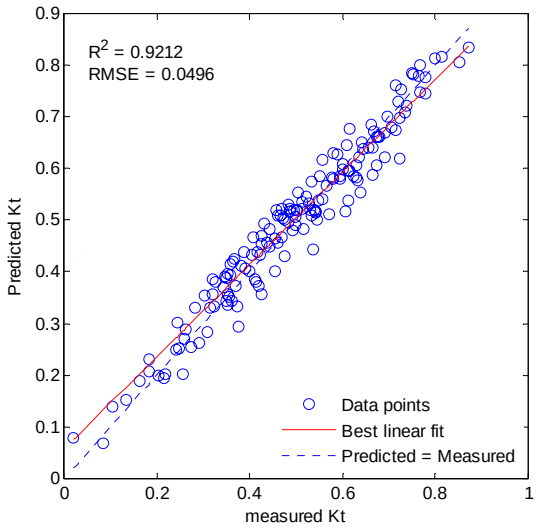

Figure 4-14 Test set B ≠ 0 and training set B and h_b excluded

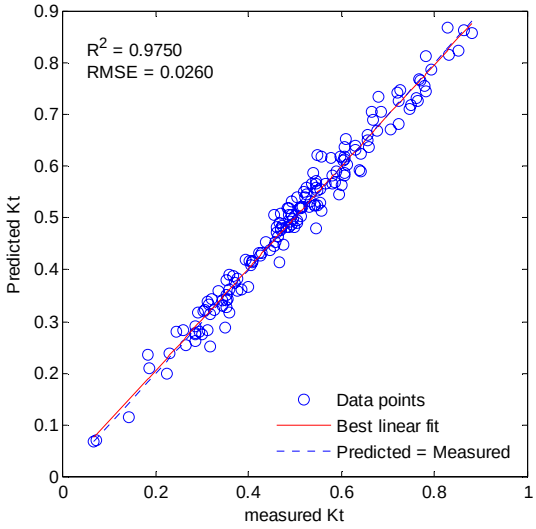

Figure 4-15 Test set B ≠ 0 and training set B and h_b included

Sets with B and h_b excluded	**Correlation R^2**	**RMSE**
Training set (85% of total tests)	0.9825	0.0316
Test set (15% of total tests)	0.9628	0.0453
Test set only containing tests with $B \neq 0$	0.9212	0.0496

Table 4-8 Results of the prediction with B and h_b excluded as input parameters

Sets with B and h_b included	**Correlation R^2**	**RMSE**
Training set (85% of total tests)	0.9860	0.0283
Test set (15% of total tests)	0.9745	0.0371
Test set only containing tests with $B \neq 0$	0.9750	0.0260

Table 4-9 Results of the prediction with B and h_b included as input parameters

The overall predictions are very similar although it is clear that the prediction of breakwaters with a berm worsens without a berm included to the input parameters. This kind of structures is better predicted if the berm parameters are used because in this way the breakwater is better defined.

Furthermore, a third of the total tests are breakwaters applied with a berm (although only Aquareef structures) hence, the utilization of parameters, which represent the berm is advisable to predict properly structures with berm.

Roughness factor influence
The roughness factor is able to separate the database in mainly two types of structures: smooth structures (with $\gamma_f = 1$) and rough structures (with $\gamma_f \neq 1$). However, this differentiation is also done with the P and because of that the network seems to have enough information about the permeability using only this parameter. Nevertheless, the roughness factor is introducing relevant information about the type of armour unit that the permeability parameter can not. The γ_f can notice for rough structures small differences depending on the kind of armour unit used, especially in the interval [0.40, 0.50]. In addition to this, it is possible that for a impermeable mound structure (P=0.1) the γ_f takes different values (from 0.38 to 0.9) because of the type of armour unit

Therefore, the roughness factor will be included as input parameter in order to define properly the surface of the breakwater.

Angle of wave incidence influence
Just like the roughness factor, β is a parameter with the same problem. Most of the tests have a β=0 and from this the network may show that this parameter is not relevant due to the limited number of tests having a β > 0. However, taking the physics into account, this parameter has influence on wave transmission, especially for smooth structures (Van der Meer et al., 2004): the K_t decreases for increasing the angle of wave attack. Therefore this parameter has to be included to the set of inputs of the model in order to predict this physical effect.

4.4.3 Alternative parameters for improvement

The notional permeability P (Van der Meer, 1988a) is used to include the permeability of the structure. But also the ratio $p_f = D_{n50core} / D_{n50armour}$ is found to be a possible way to describe the permeability of the structure in a more quantitative manner. During the analysis of the homogeneous database these two parameters were found to be equally suitable for describing the permeability.

Like the case of permeability, there is another possibility to include a berm to the prediction model. This can be done by means of the use of the determined $\cot\alpha_{incl}$. In this way three less parameters are used in the performance; hence fewer neurons would be needed to carry out the training (saving time).

The influence on the prediction of these alternatives is studied in the following sections.

Permeability parameter selection
Till so far P has been used as parameter to include the permeability of the structure to the prediction model. However, the ratio p_f is also found possible. To distinguish which parameter is better to describe the permeability in case of wave transmission a network is trained with the P and another one with the ratio of the D_{n50}'s, both as permeability factor. The found RMSE's are:

Parameter taken into account	RMSE of training set	RMSE of test set
Notional permeability	0.0303	0.0549
Ratio of D_{n50}'s	0.0305	0.0466

Table 4-10 Performance of neural network including different permeability parameters

The results are very similar using one or the other. The improvement with the ratio of D_{n50}'s is only noticeable for the test set. Next a box plot is shown to analyze this case in detail.

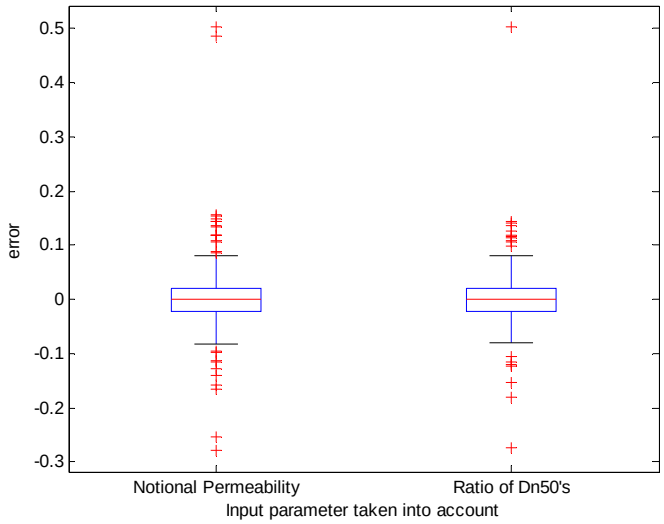

Figure 4-16 Box plots for two different permeability factors

Parameter	Upper whisker	Lower whisker	75 percentile	25 percentile	Median
P	0.081	-0.083	0.019	-0.023	-0.00077
Ratio of D_{n50}	0.082	-0.080	0.020	-0.021	-0.0009

Table 4-11 Specific data of box plots

Note:
A box plot is a very useful statistical tool to interpret data samples. The box plot is a box and whisker plot. The lower and upper lines of the box are the 25th and 75th percentiles of the sample thus the distance between the top and bottom is the interquartile range. The red line in the middle of the box is the sample median; there is skewness if the median is not centered in the box. The whiskers are lines extending above and below the box and they show the extent of the rest of the sample (minimum and maximum values of the sample), assuming no outliers. An outlier (signed with a plus sign) is a value more than 1.5 times the interquartile range away from the top or bottom of the box. These points represent a bad prediction.

Both box plots of Figure 4-16 have the same aspect; they have approximately the same sizes. Both predictions give the same accurate results, although the mean of the P is closer to zero. Concluding: the difference between parameters is marginal. There are more outliers present with P. These outliers make the prediction worse and are difficult to correct. The reasons of these outliers may be because a wrong value of the parameter is assigned to those tests or simply the network cannot predict properly those tests.

Concluding, there is a marginal difference on the prediction performance between the two possible permeability parameters. It seems that the use of the ratio might improve a little bit the prediction of new data (test set). Nevertheless, the P will be the parameter to describe the permeability in the final model because this parameter is well known in the field of coastal engineering. Introducing a new parameter does not improve the results.

One can think of including both permeability parameters too as inputs. The ratio gives a relationship between the size of the armour and core units and the notional permeability would give information about the composition of the structure. The number of inputs parameters increases with one and the overall results are not improving, as can be seen in Table 4-12.

Performance	R^2 (training set)	RMSE (training set)	R^2 (test set)	RMSE (test set)
With 2 permeability's	0.9848	0.0295	0.9686	0.0412
Only with 1 permeability	0.9860	0.0283	0.9745	0.0371

Table 4-12 Performance of neural network combining two permeability factors

Therefore, only one input parameter is used to describe the permeability of the breakwater and it will be the notional permeability P.

Berm parameter selection
To find the best option, a same analysis as the last section is followed. The results obtained are:

Parameters taken into account	RMSE of training set	RMSE of test set
$\cot\alpha_{incl}$	0.0346	0.0385
B, h_b, $\cot\alpha_{df}$ and $\cot\alpha_{uf}$	0.0321	0.0412

Table 4-13 Performance of neural network including different berm parameters

The $\cot\alpha_{incl}$ gives better results in the test set, but not in the training set. The difference in RMSE between the two possibilities is not very large (around 0.025). A box plot is drawn to receive more information:

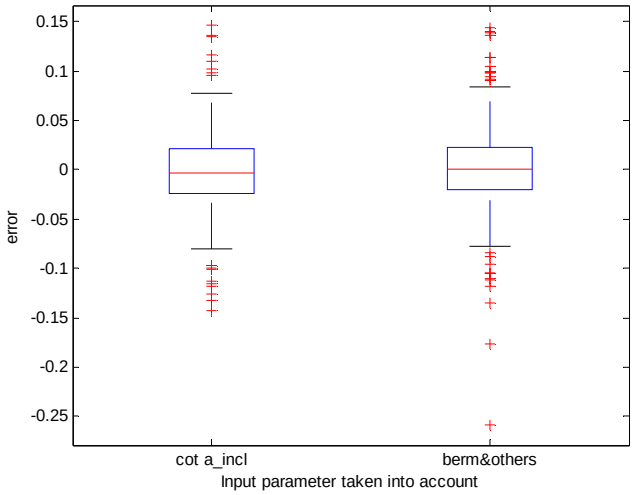

Figure 4-17 Box plots for two different berm parameters

Parameter	Upper whisker	Lower whisker	75 percentile	25 percentile	Median
$\cot\alpha_{incl}$	0.077	-0.080	0.022	-0.025	-0.0034
Berm&others	0.084	-0.078	0.022	-0.020	-0.00014

Table 4-14 Specific data of box plots

Both box plots have approximately the same sizes and statistics, although the outliers are more spread in the case of Berm & others. Both results are very similar, but a relevant better prediction was expected with the utilization of the $\cot\alpha_{incl}$ because 3 less parameters were used and the same number of neurons was kept, so the network was more powerful in order to improve the results (without taking into account overfitting).

The similarity between the results can be explained as follows: a better description of the structure is written using the berm parameters, which compensates the advantage of using less relative neurons. Actually, when using all berm parameters one is using real breakwater dimensions and, furthermore, these parameters are easier to determine for a future user than the invented including berm slopes. There is still one more drawback for the case of $\cot\alpha_{incl}$; it is unable to differentiate between the case of a shallow berm and a deep berm if they have the same upwards and downwards slopes (see Figure 4-18).

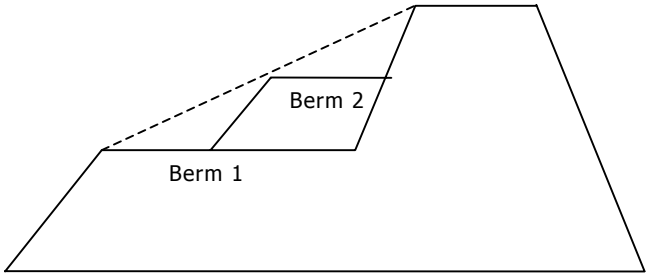

Figure 4-18 Deep berm (berm 1) and shallow berm (berm 2)

Therefore, the chosen parameters to describe the front part of the structure are the berm width, its berm depth and the downward and upward slopes. With these, real parameters are used and the prediction of breakwaters with berm is covered. However, since all the structures applied with berm belong to the same dataset (Aquareef) the network may not predict properly new structures with berm. For this reason a thorough study of the berm will be done in Section 4.6.2.

4.4.4 Investigating uncertain relation

According to the Table 4-6, the back slope has a RMSE very similar although always above the case of using all the input parameters, showing a moderate importance.

The possible conflict may exist between this parameter and the front slopes because the values of $\cot\alpha_{ub}$ are very comparable to the values of $\cot\alpha_{uf}$ (as it has been explained in Section 3.9.4) and maybe the network detect it as a superfluous parameter because it was not introducing new information. Despite this, the RMSE of the back slope is always above the overall prediction (Figure 4-12 and Figure 4-13) and this parameter might give information about what it is happening with the wave, which overcomes the structure.

Therefore, the prediction with the back slope is sufficiently better than the prediction with all the parameters to keep it as an input parameter. Nevertheless, a detailed analysis of this parameter will be carried out in Section 4.6.2 to ensure that there is no disturbance with the other slopes.

4.4.5 Conclusion about input parameters

It can be concluded that all the parameters selected on forehand are important for the overall performance of the prediction model. It has been proven that using real berm parameters (berm width, berm depth and the two front slopes) is more practical and gives better results than the use of a mean slope. As for the permeability, the P is kept because no relevant improvement is obtained with p_f and for practical reasons.

Therefore, the final 12 input parameters till this moment are (the wave height is implicitly in all of them because of the scaling process):

$T_{m-1,0\ toe}$, h, h_b, B, R_c, W_c, $\cot\alpha_{df}$, $\cot\alpha_{uf}$, $\cot\alpha_{ub}$, γ_f, P, β.

However, the back slope as well as the berm parameters will be studied in detail in Section 4.6.2 in order to ensure their relevance in the final prediction.

4.5 Gathering a committee of networks

Now the aNN is properly configured, a consistent aNN is possible to be carried out. For this task, like in the CLASH project, a bootstrap resampling technique is used. Resampling techniques are tools used for uncertainty analysis of the predictions and for skipping the problem of splitting the data in two sets (training and test sets). The use of these techniques involves the generation of different training resamples for every aNN's based on the ROD. The resample is generated by randomly picking data from the ROD with replacement. It means that every individual draw within a resample is independent but with replacement, thus the probability of a certain test to be chosen is $1/N$ for every single draw, being N the total number of tests of the ROD (3,118 tests). In this way several

tests results from the ROD will be selected more often than others and of course, some test will completely not appear. Tests, which are not selected for the training set, will be used as test set.

Therefore, the probability that a test is not present in a resample is $\left(1-1/N\right)^N$ and for a large value of N this becomes close to $1/e$. In other words, the probability of a test to be selected for the training set of a resample is 63% and then the probability that a test belonged to the test set was 37%. Therefore, the size of the test set will be around 1,150 tests whereas the size of the training set should be around 1,960 tests, but the WF is applied another time to the training set, so this set exceeds the amount of tests of 13,000 tests. Therefore, with this technique, more tests are being used for the testing and training; moreover, repeating this operation all the tests will be used for training and for testing.

The following scheme summarizes the resampling process:

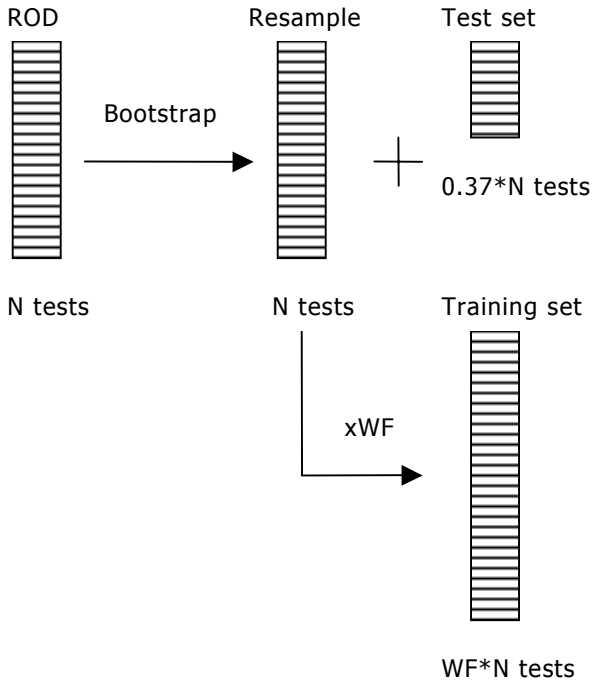

Figure 4-19 Schematization of resampling process

The bootstrap resampling technique is highly time-consuming (taking almost 40 minutes to train one resample), so only a total of 100 aNN's are generated in this way. According to Efron (1982), an amount of 500 or 1000 resamples is preferable in a final stage.

After the resampling phase, it is possible to ensemble all the aNN's and make an analysis of the accuracy of this ensemble. A so-called sensitivity analysis of input parameters used for different types of breakwaters can be performed. With the committee of networks (ensemble) it is possible to make a better prediction of wave transmission than could have been done with only one aNN. At the same time information can be obtained concerning the reliability and accuracy of the prediction itself. Another advantage to mention, it is that the entire database is used for training of aNN. In case of a single aNN, a part of the database (test set) has to be left for validation. If one is interested in knowing the wave transmission coefficient of a certain breakwater (given as an input vector), it is enough with determining its wave transmission for L aNN's, being L the number of aNN's which have been generated by means of bootstrap resampling. The final result is calculated with the mean of L predictions:

$$\overline{K_t} = \frac{\sum_{i=1}^{L} K_{ti}}{L} \quad \textit{(L = 100 in the current study)} \qquad \textit{Eq. 4.7}$$

Before ensemble the aNN's, a statistical study about the set of networks is carried out with the help of a box plot of the RMSE of the test set. Those networks which appear as outliers (a RMSE greater than 1.5 times the interquartile range) will be rejected. The reason of the existence of these networks is simply because of a bad run. Therefore, the global prediction is improved proceeding in this way.

The result of this analysis is the next one:

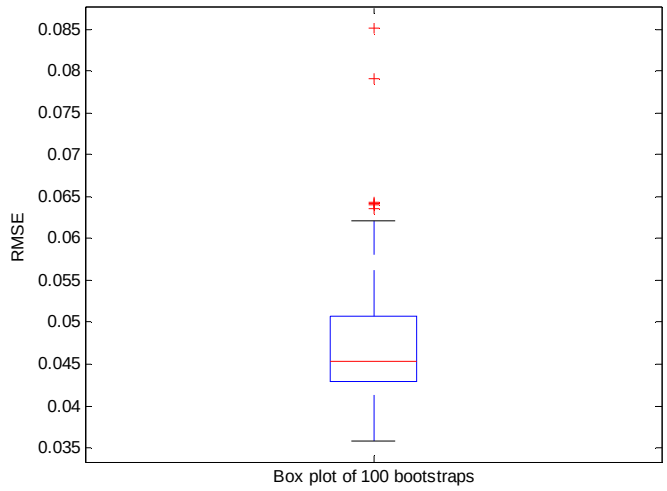

Figure 4-20 Box plot of RMS error distribution

Parameter	Upper whisker	Lower whisker	75 percentile	25 percentile	Median
RMSE	0.062	0.036	0.051	0.043	0.045

Table 4-15 Specific data of box plots

Six outliers are detected during resampling and training. These aNN's give a RMSE for the test set higher than the 1.5*interquartile range above the 75 percentile (RMSE = 0.063). Therefore the total number of aNN's in the set is revised (L = 94).

Summarizing, the configuration of the aNN prediction model is:

Architecture	Transfer Function	Training algorithm	Number of epochs	Number of bootstraps	Time to calculate
$I_{12} - H_{17} - O_1$	Log sigmoid Saturated linear	Bayesian-regularization	1000	94 (100)	65 hours (Pentium 4)

Table 4-16 Final configuration of the prediction model

4.6 Checking the prediction model

Once the prediction model is finished with a final set of 94 aNN's, its results can be studied and checked by analyzing techniques (accuracy and sensitivity analysis) which are described in Section 4.6.1 and are carried out in Section 4.6.2.

These studies can show the more reliable ranges and structures for the model are as well as the behavior of the input parameters to wave transmission.

4.6.1 Analyzing Techniques

Accuracy analysis

The accuracy of the model is checked with the ROD, the same database used for the creation of resamples. The method is to predict the tests of the ROD and analyze its results by means of the values of the RMSE and the R^2 correlation as well as the histogram of the error between the predicted and the measured value in order to detect if under- overprediction is present.

Sensitivity analysis
One of the relevant options that the ensemble of aNN's allows is to study the uncertainty of the prediction model. With a total set of 94 aNN's, it is possible to measure this uncertainty by means of the standard deviation, variance, mean and confidence interval.

The mean is already used to obtain the final value of the predicted K_t. To quantify how good this prediction is confidence intervals are used. To be precise, the 95%-confidence interval is chosen, given by the quartiles 2.5% (lower boundary) and 97.5% (upper boundary). In addition to this, the prediction of DELOS is screened in order to have a reference and, in this way, to establish a comparison between the two predictions.

The sensitivity of the prediction model to the input parameters is important for the following reasons:

- *To validate the behavior of the prediction model.* Depending on the type of structure, the behavior may be different. All parameters can be studied for every type of structure. The process is to vary a certain parameter while other parameters are kept fixed, hence the influence on the transmission coefficient can be examined. The showed influences should agree with the known expectation, or have to be physically possible at least.
- *To analyze the reliability of the prediction model.* For every type of structure a representative structure is selected to carry out the sensitivity analysis. For these structures the prediction model should give accurate results within certain boundaries. With confidence intervals the reliability of the prediction model can be determined. The reliability will be different for every type of structure; because of this representative structures are examined.
- *To find new relations.* For most parameters the influence is well-known and is used to validate the model. There are also parameters present from where the influence on the transmission coefficient is not clear. For these parameters it is interesting to see what tendency the prediction model shows and if this physically can be reasoned. It has already been found in an earlier stage, that all parameters used have influence on the accuracy of the model.

It is important to remark that the model is checked with new structures using this analysis. The new structures are created varying the different possible input parameters from a certain known structure of the database. A representative mound and smooth structure have been selected to carry out the analysis.

Representative structures of the dataset
A total number of 2,795 tests are present to perform a sensitivity analysis on mound structures for 12 governing parameters. The selected breakwater to represent a mound structure belongs to the UPC subset and its characteristics are:

H_{mo} toe	$T_{m-1,0}$ toe	h	h_b	B	R_c	W_c	$\cot\alpha_{df}$	$\cot\alpha_{uf}$	$\cot\alpha_{ub}$	γ	β	P
[m]	[s]	[m]	[m]	[m]	[m]	[m]	[-]	[-]	[-]	[-]	[º]	[-]
0.313	2.331	1.680	0.0	0.0	-0.105	1.825	2.00	2.00	2.00	0.4	0.0	0.500

Table 4-17 Input parameters for specific mound structure

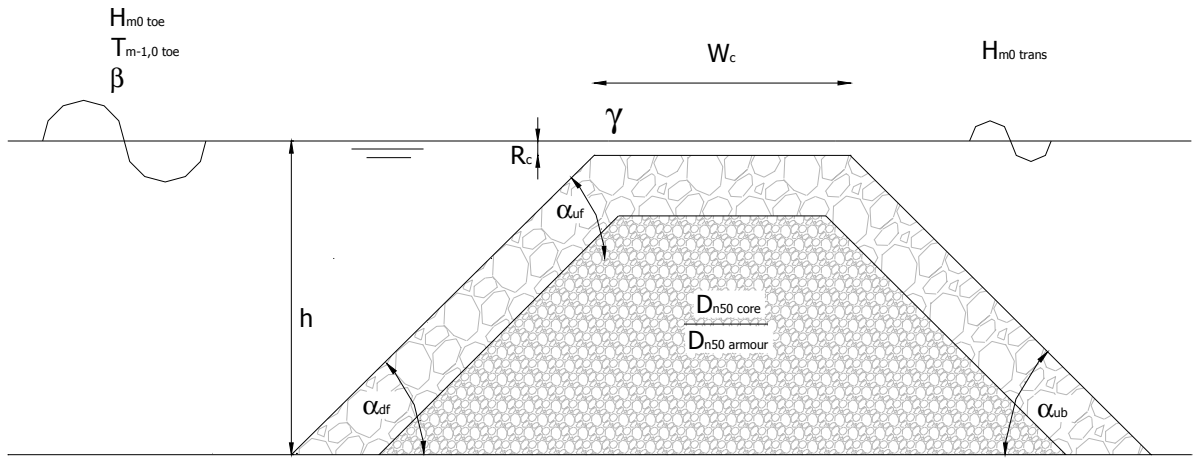

Figure 4-21 Profile of specific mound structure

The wave transmission predictions for the selected breakwater are:

Measured K_t	DELOS prediction	aNN prediction		
		Mean	Std. deviation	Variance
0.416	0.4038	0.4186	0.0165	0.0003

Table 4-18 Predictions of the specific mound structure

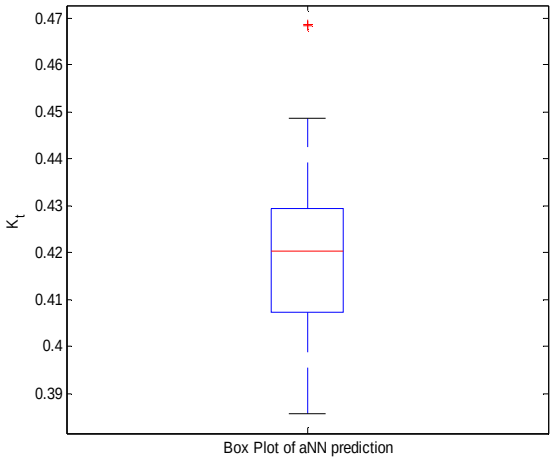

Figure 4-22 Box plot of the prediction model

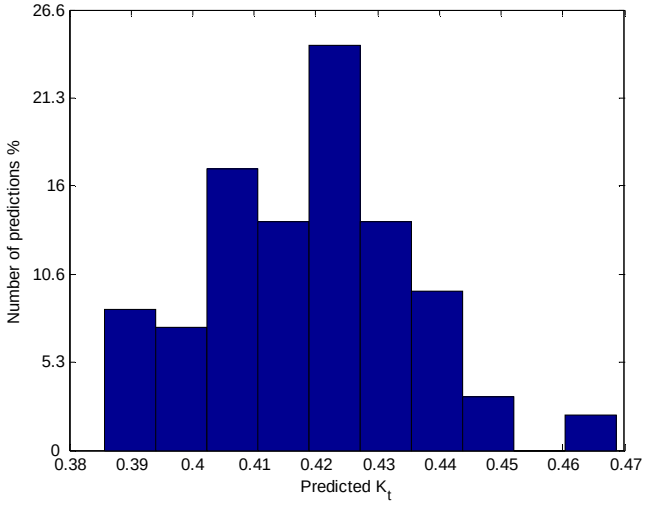

Figure 4-23 Histogram of the prediction model

As for the case of smooth structures, there are a total number of 282 tests to perform a sensitivity analysis for 12 governing parameters. The selected breakwater to represent a smooth structure belongs to the Wang subset and its characteristics are:

$H_{mo\ toe}$	$T_{m-1,0\ toe}$	h	h_b	B	R_c	W_c	$\cot\alpha_{df}$	$\cot\alpha_{uf}$	$\cot\alpha_{ub}$	γ	β	P
[m]	[s]	[m]	[m]	[m]	[m]	[m]	[-]	[-]	[-]	[-]	[º]	[-]
0.100	1.482	0.50	0.0	0.0	0.00	0.20	2.0	2.0	2.0	1.00	0.0	0.100

Table 4-19 Input parameters for specific smooth structure

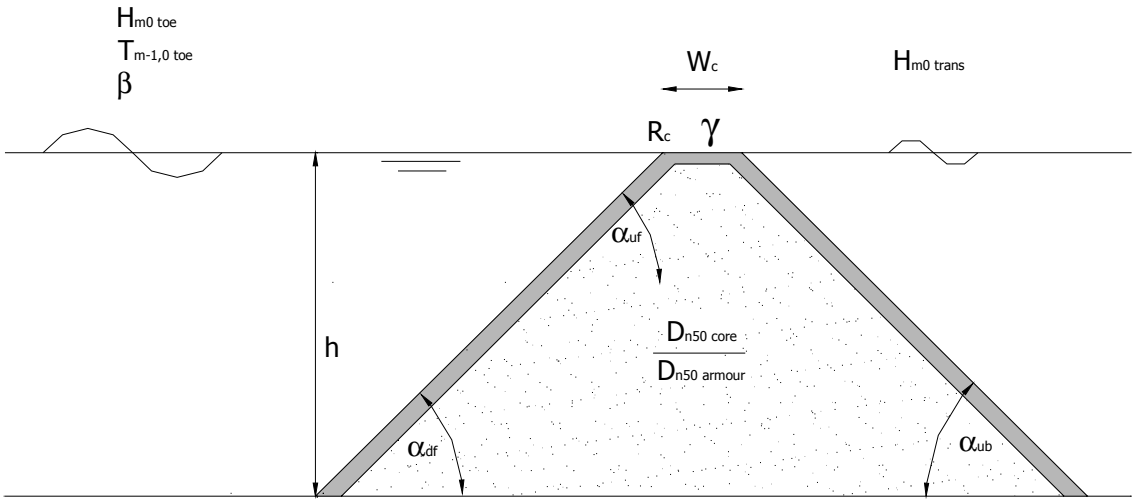

Figure 4-24 Profile of specific smooth structure

The wave transmission predictions for the selected breakwater are:

Measured K_t	DELOS prediction	aNN prediction		
		Mean	Std. deviation	Variance
0.567	0.5765	0.5874	0.0109	0.0001

Table 4-20 Predictions of the specific smooth structure

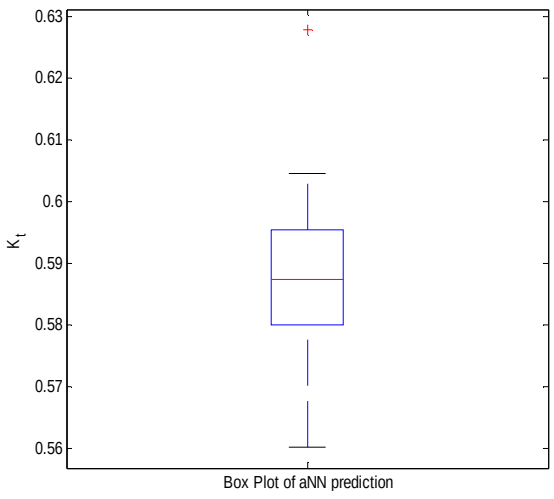

Figure 4-25 Box plot of the prediction model

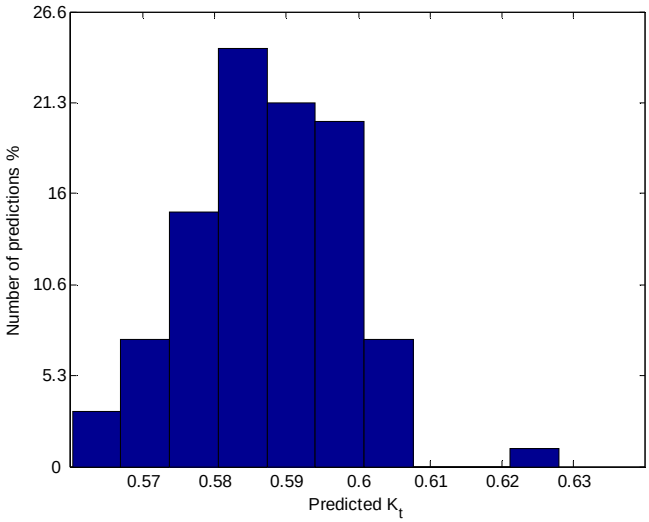

Figure 4-26 Histogram of the prediction model

4.6.2 Applying analyzing techniques

The two analyzing techniques have been performed in this paragraph in order to evaluate the model. The accuracy analysis gives a global indication of the quality of the prediction model, whereas a sensitivity analysis gives insight in the behavior of the model to certain input parameters.

The sensitivity analysis will be done for those parameters that show some problems in Paragraph 4.4: berm parameters (berm width and berm depth) and back slope.

Accuracy analysis

The correlation factor (R^2) and the RMSE represent the quality of the prediction model. The evaluation is carried out for several data sets: all type of structures, mound breakwaters, impermeable structures, smooth structures and breakwaters with berm.

The following table shows a summary of the obtained results:

Dataset	Number of tests	R^2	RMSE
All	3,118*	0.9863	0.0267
Mound	2,795	0.9867	0.0260
Smooth	282	0.9812	0.0307
Impermeable	29	0.9302	0.0672
Berm	1,066	0.9819	0,0231

*Note: the dataset includes 12 caisson tests.

Table 4-21 Overview of prediction model performance for various structures

Using all available data with a $WF \neq 0$ (3,118 tests), good results are obtained by the prediction model if one compares these results with other available prediction methods for wave transmission. For instance, taking as a reference the results of Panizzo et al. (2004), see Section 4.1.2, the prediction model of this study shows a higher R^2 and a lower RMSE. However, almost 800 additional tests are used and more types of structures are being handled within one model.

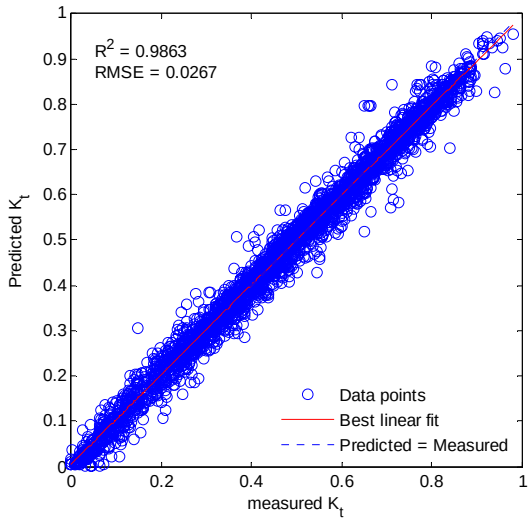

Figure 4-27 Performance using all data

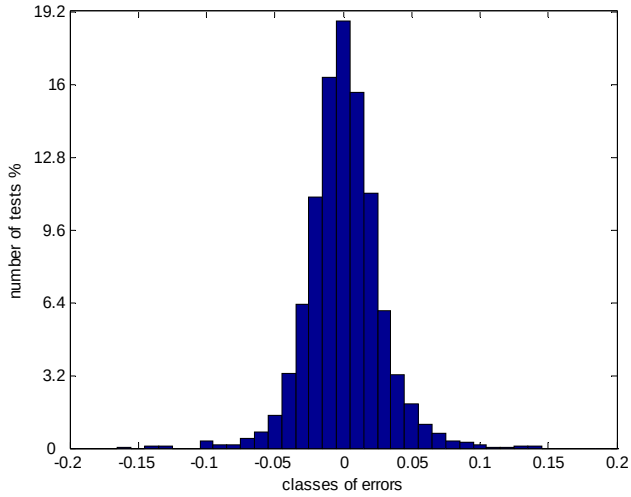

Figure 4-28 Histogram of the error

Figure 4-27 shows that the prediction is very accurate along the whole range of values of K_t, although some points seem to be a bit far from the correlation line. Despite this, according to the histogram, more than 90% of the tests have an error below 0.05 (absolute value). Furthermore, the histogram seems to have a symmetrical distribution, showing no skewness, hence no special over- or under-prediction is found.

Note:
The error is defined as $e = K_{t\ measured} - K_{t\ predicted}$, so a negative value would mean over prediction and positive values under prediction.

A summary of the accuracy for the different methods is shown in the next table: (the results of Panizzo et al. (2004) are obtained with a different database with a different size. Notice that the comparison is not entirely valid).

Dataset	DELOS formulae	Panizzo et al. (2004)	Prediction model
All	0.8851*	-	0.9863
Mound	0.9022*	0.973	0.9867
Smooth	0.8177	-	0.9812
Impermeable	0.8036		0.9302
Berm	0.8484	0.974	0.9819

Table 4-22 Comparison of results between different prediction methods

**Note: the reliable tests of Ahrens (75 tests with WF>0) have been removed because the W_c equals to 0.001 (heap of loose elements with no specific crest width) and the DELOS formulae cannot predict them with proper results.*

The model is able to give more accurate prediction than any of the other available prediction methods.

To sum up, the main advantages of this model in comparison with other methods are:

- High accuracy (the lowest R^2 is 0.9302 for impermeable mound structures and the highest R^2 is 0.9867 for the mound structures).
- No important over- or under prediction and more than the 90% of the predicted K_t have a deviation below 0.05 from the measured K_t in the overall prediction.
- The capacity to predict new low-crested breakwaters is expected to be high, because new low-crested breakwaters will be more or less consisting of the same elements and will have equal shapes.

Sensitivity analysis
This study is only applied for the back slope and berm depth in combination with berm width, in order to solve the uncertainty of their relevance. The back slope is analyzed for a representative mound structure and for a representative smooth structure. The front slope studied as well to ascertain if there is any disturbance in its prediction because of the back slope. The berm parameters are studied with one test from the only set with structures with berm: the Aquareef dataset.

The sensitivity figures contain several lines. The dash lines show the band of the confidence interval, one line for the lower boundary (quartile 2.5%) and another one for the upper boundary (quartile 97.5%). The others two lines are the aNN prediction (mean value) and the DELOS prediction. The legend of the plots is:

Legend of sensitivity figures

aNN prediction

95% confidence interval

DELOS prediction

Back slope for specific mound structure

Parameter validation
The trend line is decreasing until cot α_{ub}=3.5 and then increasing. The influence is small; all values of K_t are around 0.4 (the value of the DELOS prediction). This prediction is physically feasible: the gentler the slope is more dissipation occurs and a lower value of K_t is obtained. However, in the last region (from 3.5 to 5) the trend is to increase, which is a wrong tendency according to the previous statement.

Reliability of prediction model
The model has reliability in the range of 1.75<cot $\alpha_{u\,b}$ < 2.25. Outside this interval the reliability is very low. Despite this, the prediction is always close to the DELOS fixed prediction.

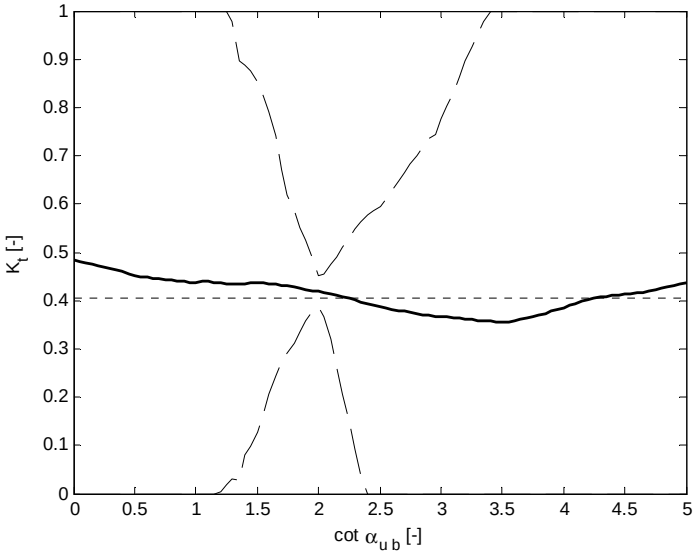

Figure 4-29 Sensitivity of back slope

Front slope for specific mound structure (combined downward and upward slopes)

Parameter validation

The influence of the front slope is not very clear. The mean prediction shows a fluctuating line with a slight influence on the K_t. For $0 < \cot \alpha_f < 1.5$ the transmission coefficient is decreasing and for $1.5 < \cot \alpha_f < 5$ the transmission coefficient is increasing. There is a transition point at $\cot \alpha_f = 1.7$, corresponding to an Iribarren number of $\xi = 3$, which is also the transition point between breaking or non-breaking waves. Wave run-up appears to be in a maximum in this transition point, hence a maximum K_t is expected at the same point, but it is not the case.

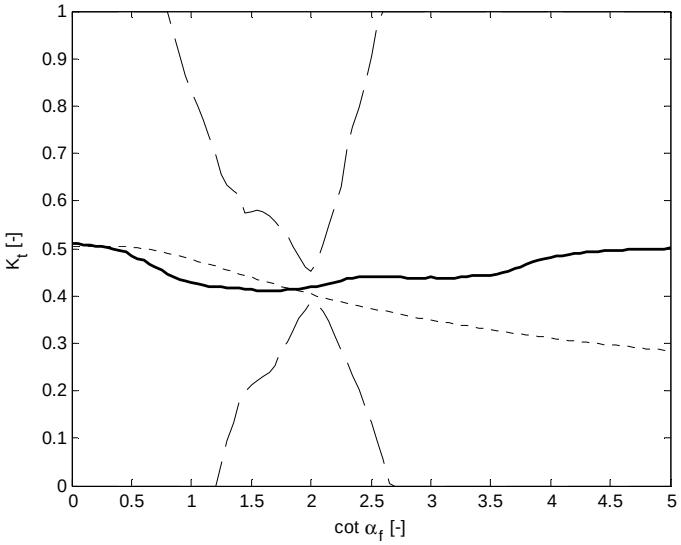

Figure 4-30 Sensitivity of the front slopes

Reliability of prediction model

The figure shows only a narrow point of confidence at $\cot \alpha_f = 2.0$. At this point the predicted value of K_t is equal to the DELOS K_t. For this specific structure the model is only giving a relatively high reliability in the range $1.75 < \cot \alpha_f < 2.25$. Outside this interval the model has a very bad reliability.

To see clearer the possible influence of the back slope on the front slope a symmetrical structure is chosen, where both front- and back slope are varied at the same time to be sure that front- and back slope are fully related.

The figure to the right is made for a symmetrical mound structure. Clearly the confidence band is narrow at values of the slope where also a lot of structures have been tested. It has to be stated that most tests in the database are concerning symmetrical structures, where $\cot \alpha_{uf}$ and $\cot \alpha_{ub}$ are equal. The prediction model shows difficulties to separately detecting the sensitivity of slopes. The figure shows in general a fluctuating line around a K_t=0.4. Therefore, according to the plot, no influence of the slope of the mound structures is noticed, not following the trend of the prediction of DELOS. The prediction model shows a local maximum of K_t for $\cot \alpha = 2$ with a narrow band of confidence (so reliable).

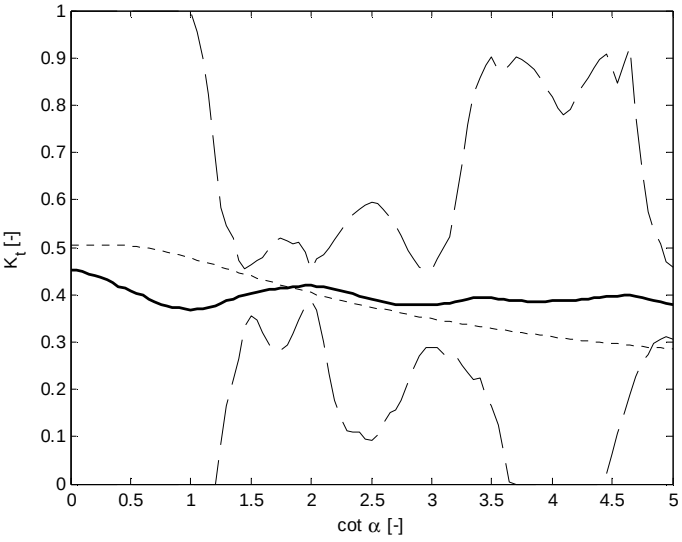

Figure 4-31 Sensitivity for a symmetrical structure

At $\cot \alpha = 2$, the Iribarren number is equal to $\xi = 2.6$, which is again just at the transition between breaking and non-breaking, where wave run-up appears to be in a maximum (see TAW, 2002), hence giving a higher K_t deviating from the trend line. The prediction is only reliable in the range [1.4, 3.25], where is giving physically right results.

Back slope for specific smooth structure

Parameter validation
On a smooth back slope there is nearly no energy dissipation, resulting in low influence on the wave transmission for different back slope angles. However, the figure is showing something totally different, the back slope seems to have a strong influence especially in the region of symmetry of the structure. Such influence on the K_t due to the back slope is physically not possible.

Reliability of prediction model
The prediction has a low reliability over the entire range of values of back slopes, except in the region where the structure is almost symmetrical (cot $\alpha_{u\ b}$=2). This is because the most of the structures are symmetrical or with slight differences between the different slopes.

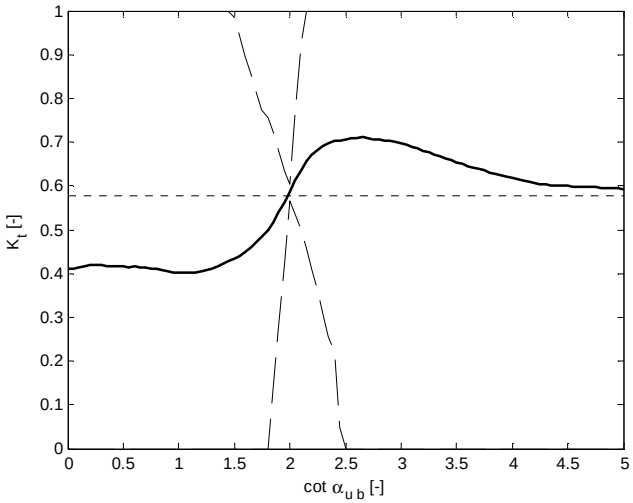

Figure 4-32 Sensitivity of back slope

Front slope smooth structure (combined downward and upward slopes)

Parameter validation
The case of combined front slopes has a decreasing overall trend, although a local maxima is detected at cot α_f = 2.6, the Iribarren number is equal to ξ = 2.25, which is again just at the transition between breaking and non-breaking, where wave run-up appears to be in a maximum, hence giving a higher K_t deviating from the trend line. This last effect is stronger in smooth structures than mound structures due to the run-up (see CUR/TAW, 1992). Therefore same conclusions as mound structures can be taken: the prediction model takes into account wave run-up.

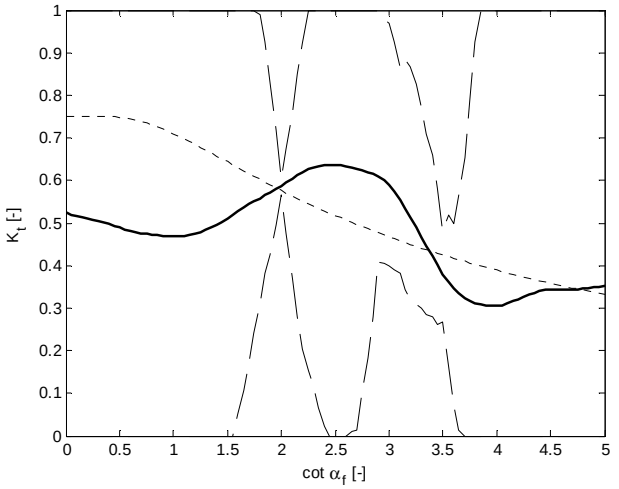

Figure 4-33 Sensitivity of front slopes

For the symmetrical case the results are physically impossible: a variation of 0.4 on the K_t varying the slope from a cot α=1.5 to cot α=2.5 is not possible. It was expected a decreasing line for gentler slopes

Reliability of prediction model
The case of combined front slopes has only a narrow confidence band at cot α_f=2 and cot α_f=3.5, the other regions are rather unreliable. The symmetrical case is reliable from cot α=1.5 to cot α=2.25, but the prediction is physically wrong.

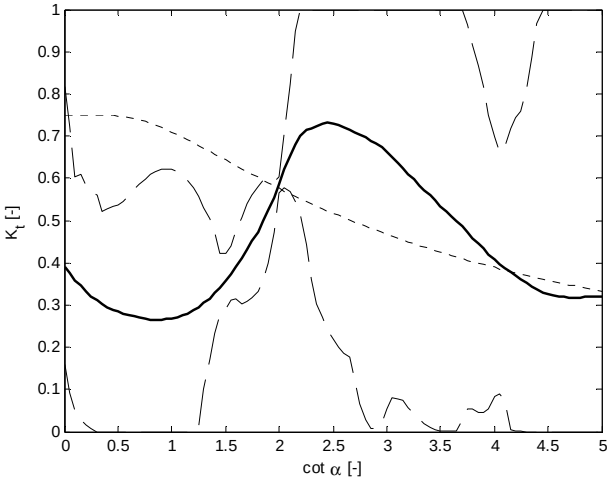

Figure 4-34 Sensitivity for symmetrical structure

Relative berm depth for an Aquareef structure

Parameter validation
Beyond a relative berm depth of 2, the K_t is increasing for increasing depth berm. This region is physically right because the berm is losing its dissipating effect when it is locating deeper (it is moving away from the area of influence of the wave).

For values of the relative berm depth smaller than 2, the behavior in is physically illogical. The K_t is increasing for decreasing h_b / $H_{m0\ toe}$, this is completely the opposite what it should be: the effect of the berm becomes more important if it is closer to the water line. The reason of this illogical result is that the Aquareef structures have a fixed relation between R_c and h_b (the height of the special armour unit) and hence if one varies the berm depth without varying the R_c at the same time, the results will be bad because the network have not learnt about it.

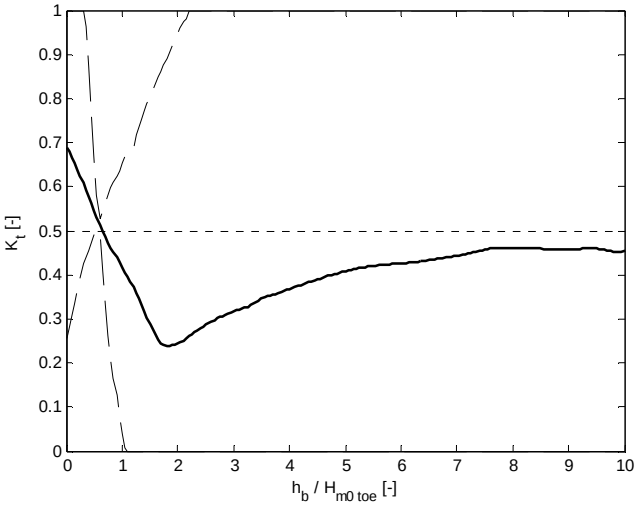

Figure 4-35 Sensitivity of berm depth

Therefore, the behavior of this parameter along its range of possible values is wrong, especially in the most important region where its effect should be more noticeable (are of wave influence).

Reliability of prediction model
The model only shows relative reliable results between the values of relative berm depth of 0.5 and 1.5. However, as it has said before, the results are wrong.

Relative berm width for an Aquareef structure

Parameter validation
Like in the previous case, the prediction shows a wrong trend. According to the physics, a longer berm will cause more dissipation for a given depth berm and hence a decreasing K_t trend line (more or less the same behavior as the wide crest); but in the plot this trend only is visible in the interval (0.5,1) and (1.75,5), describing an important oscillation in between. Besides, this illogical fluctuation is located in the most reliable part of the drawing. On the other hand this region of high reliability the prediction of this model and DELOS is very similar because here the value of B is the original one and of course the model predicts it very well (the model has been trained with that test).

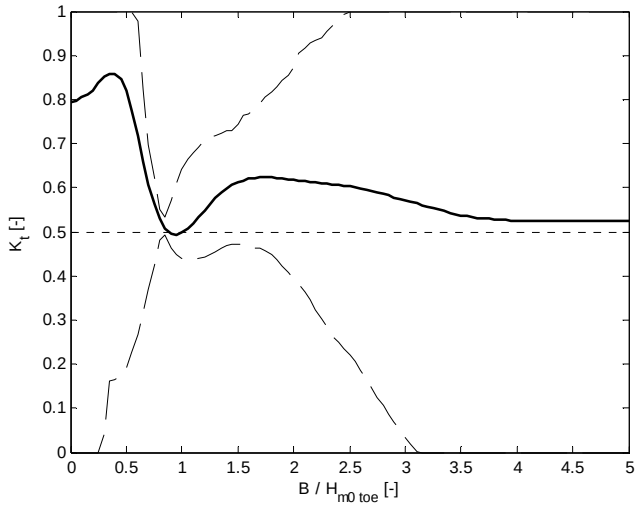

Figure 4-36 Sensitivity of berm width

Reliability of prediction model
The model only seems to be reliable between 0.75 < B / $H_{m0\ toe}$ < 2, outside this range the model has a rather low reliability. Furthermore, the reliable results are physically wrong.

Conclusion about the back slope and the berm
For the case of the slopes, the model predicts physically wrongs trends, especially for the case of smooth structures. The back slope is disturbing the prediction of the front slopes and taking too much importance on the value of K_t when according to the Figure 4-12 and Figure 4-13 the influence of the back slope should be minor to zero. Because of this, it is worth to leave the back slope out of the final prediction model in order to obtain better physical predictions in the front slope, which are the really important ones on the wave transmission phenomenon.

As for the berm matter, unlike it has thought before the sensitivity analysis, the model cannot predict structures with berm; it is only handling Aquareef structures, which have a fixed relation between R_c and h_b. Moreover, low-crested breakwaters are not often applied with a berm, because the goal of both structures is to dissipate the wave energy and the low-crested breakwater can be understood as a berm structure located in front of high-crested breakwater (Figure 4-37) whereas a berm is more typical of being part of a high-crested breakwaters (Figure 4-38). Therefore, in order to improve the overall prediction, the berm parameters will be left out and an immediate consequence of this is the fact that only one slope is needed to represent the front of the structure.

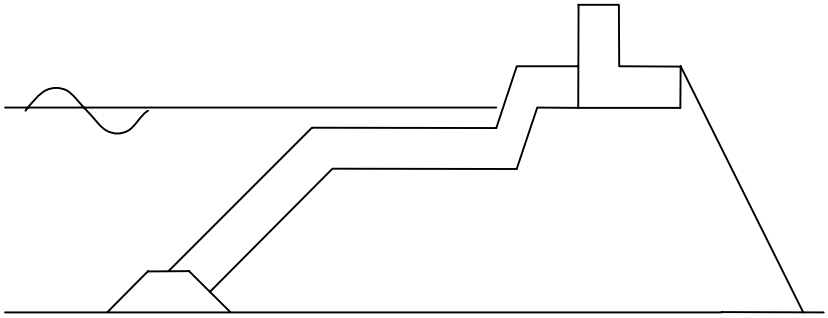

Figure 4-37 High-crested breakwater with berm

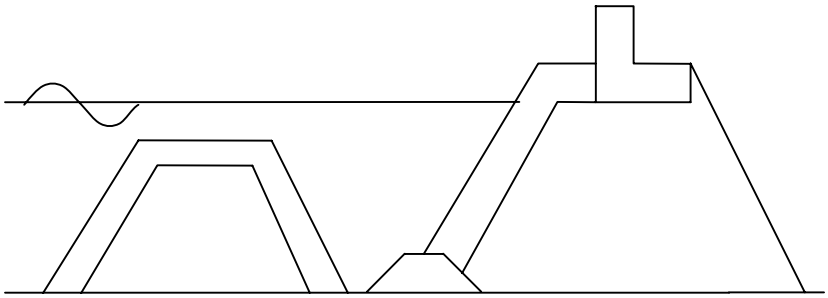

Figure 4-38 High-crested breakwater with low-crested breakwater

Concluding, this model has some problems to predict properly the behavior of the slopes and structures with berm thus, in order to solve this matter and improve the prediction, a new predictive model is required where the back slope and the berm parameters will be left out.

4.7 Final prediction model

Now the set of inputs have been set, the definitive model can be carried out. The steps to obtain the last model are:

- To prepare the database with the final parameters for the network (Section 4.7.1)
- To determine the architecture of the network (Section 4.7.2)
- To gather a committee of networks (Section 0)

Finally, once the model is defined, the results of the final performance are shown (Section 0) by means of an accuracy analysis (explanation of the technique in Section 4.6.1).

4.7.1 Preparing network data

This database receives the same processes as the database of Paragraph 4.2: scaling process, weight factors and training and test composure.

The only changes are on the number of input parameters but also on the size of the database. A new subset has been added with 552 tests of smooth structures, increasing the total number of tests of ROD from 3118 to 3670 tests.

Information new dataset added to database
A new dataset (Taveira-Pinto et al., 1997) is included to the database. It concerns 552 model tests with different impermeable and smooth low-crested breakwaters, under random waves. Water depth, wave period and wave height were varied. The data is implemented to the final prediction model before investigating the influence of parameters. It is assumed this data is not influencing the conclusions of the selection of the final input parameters. The structures have symmetrical shapes for different slopes.

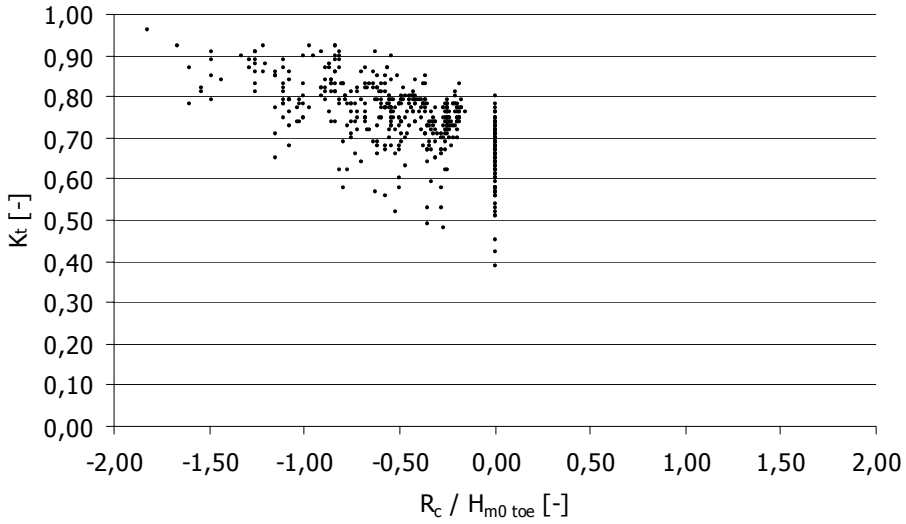

Figure 4-39 Relative crest height versus wave transmission coefficient

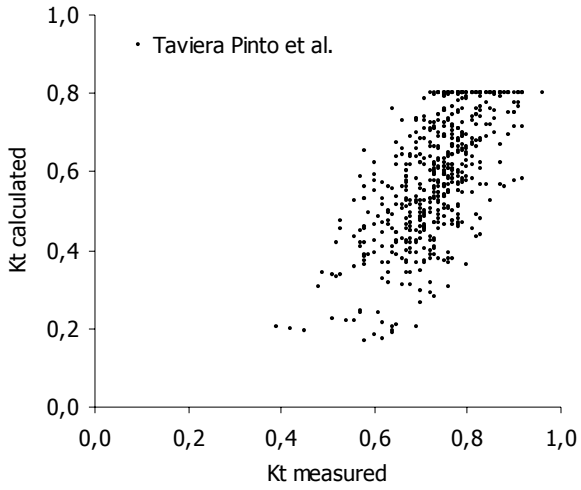

Figure 4-40 Applying the dataset to the DELOS formulae

Taking into account Section 4.6.2, the final 8 input parameters of the definitive model are: $T_{m-1,0\ toe}$, h, R_c, W_c, $\cot\alpha_{uf}$, γ_f, P and β (the wave height is implicitly in all of them because of the scaling process).

The upward slope in front of the structure has been selected to represent the front slope against other alternatives (for instance front slope including berm) because it is a real measurable slope, easy to determine by the user, without calculating.

The final distribution of the scaled parameters is:

Parameter	Mean	Standard deviation	Maximum	Minimum	Unit
$H_{mo\ toe}$	1	0	1	1	m
$T_{m-1,0\ toe}$	5.17	1.96	21.70	2.32	s
h	3.96	2.92	34.43	1.02	m
R_c	-0.41	1.20	8.87	-9.84	m
W_c	6.58	10.72	90.48	0.01	m
$\cot\alpha_{uf}$	1.49	0.98	5.00	0.00	-
γ_f	0.56	0.23	1.00	0.38	-
P	0.44	0.20	0.60	0.10	-
β	1.90	8.72	83.00	0.00	-

Table 4-23 Final input parameter distribution after Froude scaling

4.7.2 Defining the architecture

The procedure to define the architecture is based on Section 4.3. The architecture of the new model remains the same as the first model although the number of hidden units (neurons) will change because the number of input parameters has changed.

With the same method as Section 4.3.5 the following figure is generated:

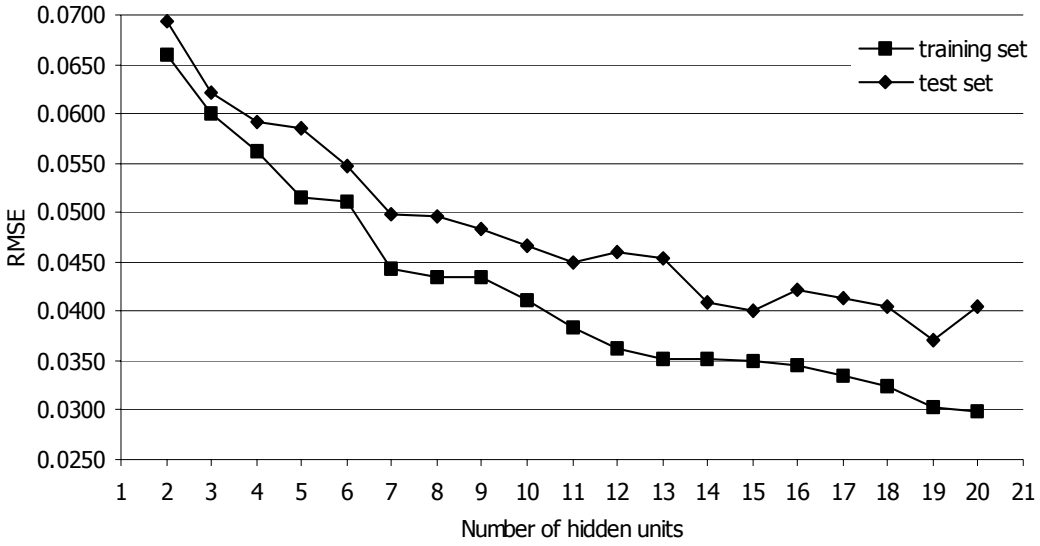

Figure 4-41 Number of neurons versus the RMSE

The trend line of the test set starts to oscillate after the value of 11 neurons in the hidden layer, showing an unstable behavior, typical of the overfitting effect. Therefore, the number of hidden units will be 11 in order to avoid the overfitting problem and obtain relative good results at the same time.

The final set-up for the aNN is:

aNN structure	Transfer Functions	Training method
$I_8 – H_{11}$ - O_1	Log-sigmoid hidden layer) Saturated linear (output layer)	Bayesian Regularization

Table 4-24 Final architecture of neural networks in the prediction model

4.7.3 Gathering a committee of networks

The same procedure as in Paragraph 4.5 is followed here. In this case 100 bootstraps are run for the analysis (the same number as the model of Verhaeghe (2005)), but 500 bootstraps will be run for the final model according to the recommendation of Efron (1982).

The box plot of the 100 bootstraps is:

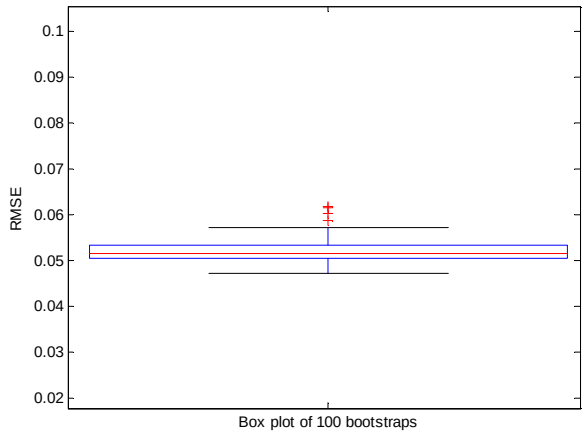

Figure 4-42 Box plot of RMS error distribution

Parameter	Upper whisker	Lower whisker	75 percentile	25 percentile	Median
RMSE	0.057	0.047	0.053	0.050	0.051

Table 4-25 Specific data of box plots

Five outliers have been detected during the resampling and the training. These aNN's give a RMSE of the test set higher than the 1.5*interquartile range above the 75 percentile (RMSE = 0.0575). Therefore the total number of aNN's in the set is L = 95.

Summarizing, the configuration of the prediction model is:

Architecture	Transfer Function	Training algorithm	Number of epochs	Number of bootstraps	Time to calculate
$I_{12} - H_{17} - O_1$	Log sigmoid Saturated linear	Bayesian-regularization	1000	95 (100)	10 hours (Pentium 4)

Table 4-26 Final configuration of the prediction model

4.7.4 Final performance

The correlation factor (R^2) and the RMSE are used here to represent the quality of the prediction model like in Section 4.6.2. The performance is evaluated for several data sets: all type of structures, mound breakwaters, smooth structures and impermeable structures.

The following table shows a summary of the obtained results. Every dataset will be discussed in more detail in following sections.

Dataset	Number of tests	R^2	RMSE
All	3,670*	0.9702	0.0402
Mound	2,795	0.9715	0.0380
Smooth	834	0.9262	0.0364
Impermeable	29	0.9763	0.0391

*Note: the dataset includes 12 caisson tests.

Table 4-27 Overview of prediction model performance for various structures

All type of structures

In general, taking into account that different structures with different physical behavior are been used, the prediction model obtains accurate results.

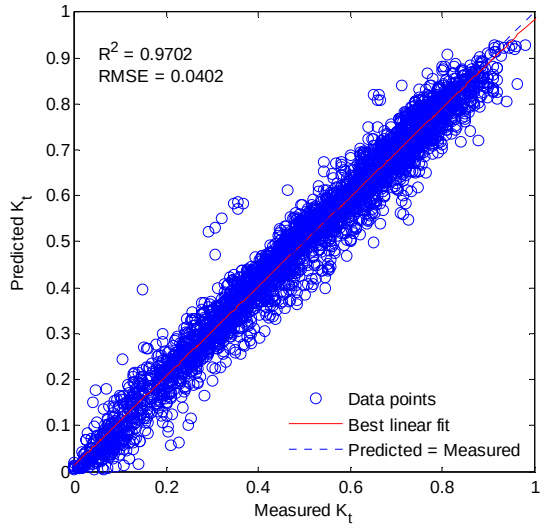

Figure 4-43 Performance using all data

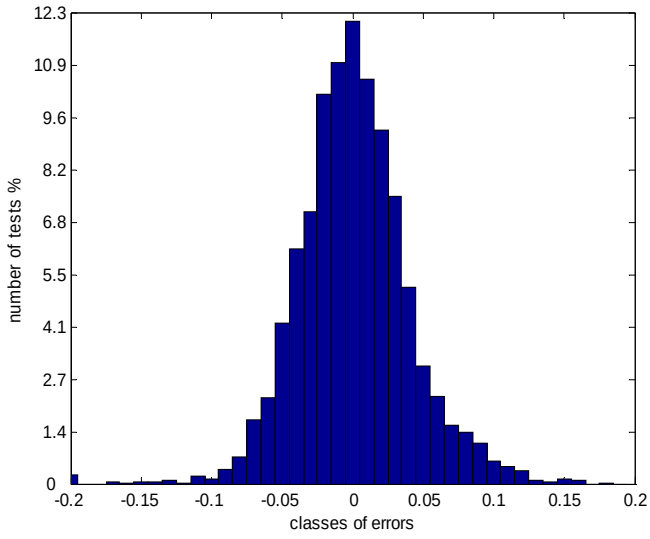

Figure 4-44 Histogram of the error

Figure 4-43 shows that the prediction is very accurate along the whole range of values of K_t, although some points (most of them belong to the new dataset) seem to be a bit far from the correlation line. Despite this, according to the histogram, more than 80% of the tests have an error below 0.05 (absolute value). However, the histogram seems to have a little bit of underprediction in the tail.

Mound structures

The total number of mound structures of the ROD is 2,795. This subset has an important influence on the global results because it represents more than 75%. The results are very similar to the initial model:

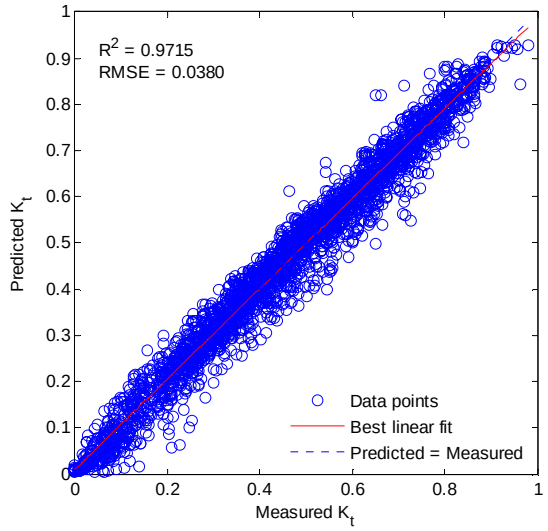

Figure 4-45 Performance of mound data

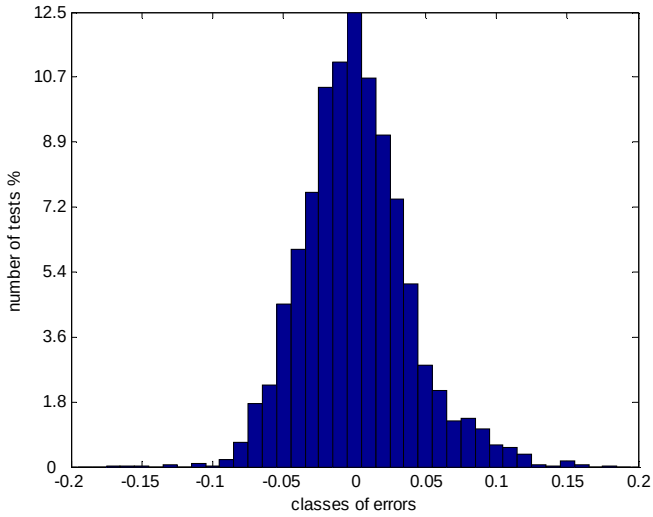

Figure 4-46 Histogram of the error

The prediction along all possible values of K_t is quite accurate (the band of results is very narrow) although there are some points with lower accuracy with a measured K_t between 0.2 and 0.3 and on the other hand 0.6 and 0.8. In any case, more than 85% of the tests have an error below 0.05 expressed as absolute value. Nevertheless, the error distribution shows a slight underprediction in the tail.

Smooth structures

834 tests from the ROD concern smooth structures. The performance is:

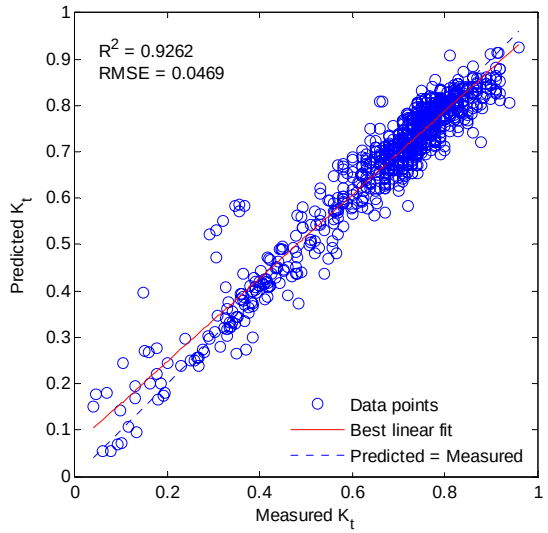

Figure 4-47 Performance of smooth data

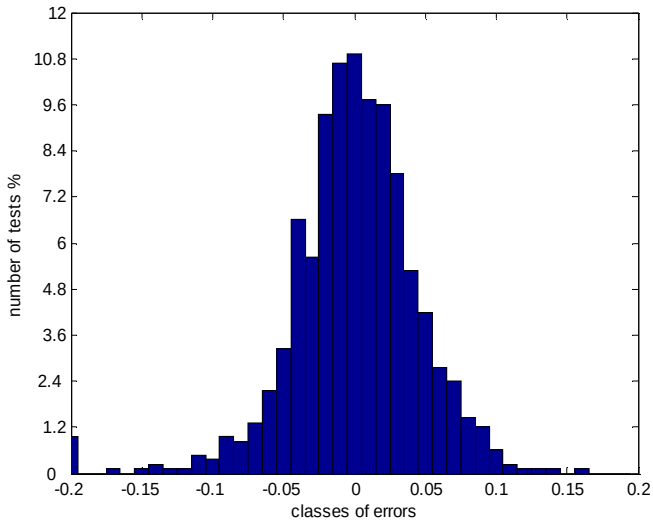

Figure 4-48 Histogram of the error

The prediction is not as accurate as for permeable (mound) structures, but its correlation is relatively high. The most of the smooth test have a K_t between 0.6 and 0.9; this region is well predicted by the model. There are a few points especially deviated from the correlation line with an overprediction of 0.2. Despite this, the histogram shows that more than 80% of the error of the tests is below 0.05 (in absolute value).

Impermeable structures
The impermeable subset (29 tests) consists of only impermeable mound breakwaters, without taking into account smooth structures. Despite the few available tests, the prediction is rather accurate:

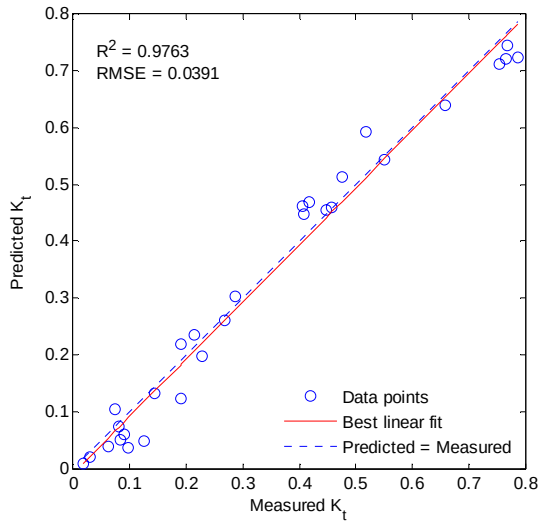

Figure 4-49 Performance of impermeable set

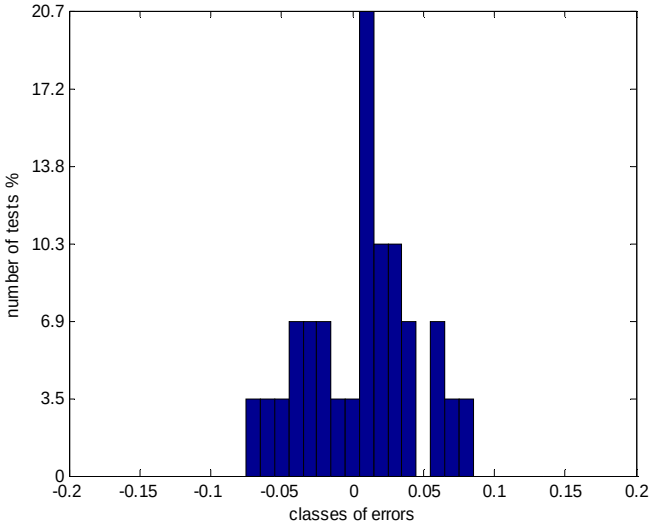

Figure 4-50 Histogram of the error

The prediction is even better than permeable (mound) structures, although this comparison is not entirely valid because of the great difference on the number of tests. The 80% of the prediction has an error below 0.05 (in absolute error). No important over- and underprediction is noticed.

Conclusions
This model is especially accurate for mound (permeable and impermeable) structures. Smooth breakwaters are predicted with a lower reliability by the model, but still useful results are obtained.

On the other hand, using the new available data, the total number of tests to perform with a $WF \neq 0$ is 3,670. The difference with the prediction method of Panizzo et al. (2004) is now around 1300 test, which more than 500 are smooth structures, a difference too large. Consequently the only prediction method available to establish a truly comparison with the model of this research is the Delos formulae.

A summary of the accuracy for the Delos and the current model is exposed in the next table:

Dataset	DELOS formulae	This prediction model
All	0.8201*	0.9702
Mound	0.7906*	0.9715
Smooth	0.6084	0.9262
Impermeable	0.9277	0.9763

**Note: the reliable tests of Ahrens (75 tests with WF>0) have been removed because the W_c is equals to 0.001 (a cone shape) and the DELOS formulae cannot predict them with proper results.*

Table 4-28 Comparison of results between different prediction methods

The model is able to predict more accurate K_t's than the Delos, especially this fact is clearer for smooth structures.

Concluding, the main advantages of this model in comparison with Delos method are:
- High accuracy (the lowest R^2 is 0.9262 for smooth structures and the highest R^2 is 0.9715 for mound structures).
- No important over- or underprediction and more than the 80% of the predicted K_t have a deviation below 0.05 from the measured K_t in the overall prediction.

Therefore, it is possible to state that this model can be used to predict: mound structures (permeable or impermeable) and smooth structures. This is true provided that the new structures have similar characteristics to the structures of the database.

5 Validity and reliability of the prediction model

An optimum of 9 input parameters is found for the prediction model of wave transmission. All parameters relevant for a reliable prediction of the wave transmission coefficient are taken into account, representing different behaviors for various types of breakwater structures. This chapter gains insight in the input boundaries of the prediction model for all 9 parameters. The final input boundary of individual input parameters is based on:

- *Physical boundary.* For every parameter there is a physical range present within a certain parameter may vary. Values outside this range are physically impossible and can logically not be entered to the prediction model.
- *Data distribution.* The data distribution on which the model is based, determines the range where the model is expected to give a reliable prediction. In regions with a lot of data points the model will give reliable predictions, contrary to regions with few or no data points. The boundaries are based on the 2.5%-quantile and 97.5%-quantile data distribution, representing the 95% data interval of the total amount of available data points, because the neural network is able to interpolate within that range.
- *Model validation.* With help of sensitivity analysis of individual parameters, the provided tendencies are validated with earlier findings from different studies on wave transmission. Boundaries are determined where the model predicts physical right tendencies. For the sensitivity figures the follow legend is valid.

Legend of sensitivity figures

Mean prediction
95% confidence interval
DELOS prediction
95% data interval

All three boundaries have resulted in the normative final input boundaries of the prediction model. Within the given ranges the model is capable of providing reliable predictions. Different boundaries are determined for mound and smooth structures as these structures behave very differently to wave transmission. A summery of all input boundaries is given in Section 5.10.2.

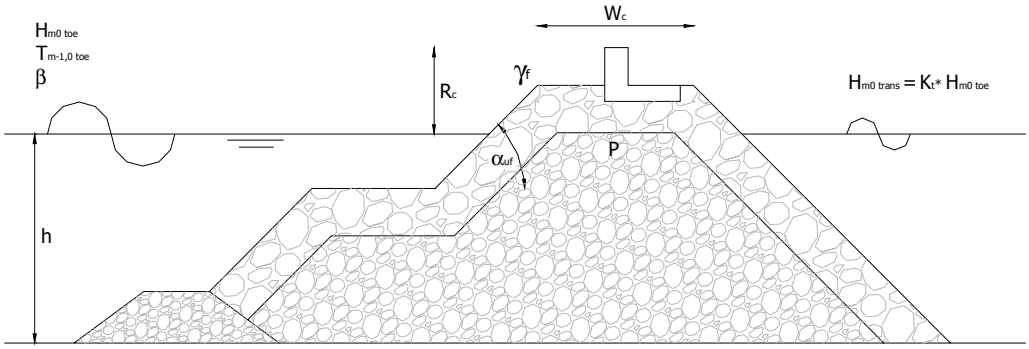

Figure 5-1 Input parameters of the prediction model for a general breakwater section

5.1 Incident wave height

The incident significant wave height, $H_{m0\ toe}$ [m], is defined directly in front of the structure (at the toe). Within the prediction model the incident wave height is used as scaling parameter for applying Froude scaling. All input parameters are scaled to $H_{m0\ toe}$ = 1.0m by the prediction model itself, making it possible to handle all kind of situations: Small-scale models, large-scale models and prototype situations. Therefore, the boundaries of input parameters in this chapter (with a certain dimension) are given as a ratio to the incident wave height $H_{m0\ toe}$ [m].

5.1.1 Physical boundary

Very small waves, with a wave height lower than 0.03m, are very difficult to generate in a wave flume or wave basin and is stated to be a physical lower boundary. The height of the incident waves is restricted to the depth of the foreshore in front the structure. It is recommended to use the following wave height to water depth ratio: $H_{m0} / h < 0.50$. If this condition is exceeded it could be that breaking waves will be present, for which the model is not able to give a reliable prediction.

5.1.2 Data distribution

The available data is obtained from small- and large-scale tests. Scaling effects can therefore influence the predicted transmission coefficient, but this effect is not different from other available prediction methods for which the same is true. In Figure 5-2 and Figure 5-3 the distribution of the wave height is presented. The data distribution is not important for the prediction model as this parameter is scaled to a wave height of 1.0m.

5.1.3 Model validation

A model validation cannot be performed by means of a sensitivity analysis because the incident wave height is used as scaling parameter in the prediction model. The validation of the incident wave height is assumed to be included in the validation of all scaled input parameters. The boundaries of these parameters are based on physically right tendencies and in this way the incident wave height is indirectly taken into account and validated.

5.1.4 Boundary of the prediction model

The following input boundaries for the incident wave height within the prediction model are found. This boundary is equal for both mound and smooth structures and is completely based on the physical boundaries.

The lower boundary of the significant incident wave height:

$H_{m0\ toe} > 0.03m$

The upper boundary of the significant incident wave height:

$H_{m0\ toe} / h < 0.50$

5.2 Incident wave period

The incident mean wave period is like the incident wave height present at the toe of the structure. The spectral mean wave period $T_{m-1,0\ toe}$ [s] is used as input parameter, because it is found most suitable for rather shallow water conditions (Verhaeghe et al., 2003 after TAW, 2002). The following relations can be used as best approximation for $T_{m-1,0\ toe}$ if different characteristic wave periods are known:

$$T_{1/3} \approx 1.20 T_{m0,2},\ T_p \approx 1.05 T_{1/3},\ T_p \approx 1.10 T_{m-1,0}$$

In principle the incident wave period determines the wave steepness of the incident waves. Because all parameters are treated relative to the incident wave height (except for dimensionless parameters), the wave steepness is used to set the input boundary of the incident mean wave period of the prediction model.

5.2.1 Physical boundary

A wave steepness over 0.07 is physically not possible, as the waves should break beyond this point. A wave steepness lower than 0.005 is difficult to generate in a wave flume or wave basin. Therefore the physical boundary of wave steepness (indirectly the wave period for a constant wave height) is stated to be:

$0.005 < s_{0\ m-1,0} < 0.070$

Or expressed like the mean wave period for a constant wave height of $H_{m0\ toe}$ = 1.0m:

$3.27s < T_{m-1,0\ toe} < 11.32s$

5.2.2 Data distribution

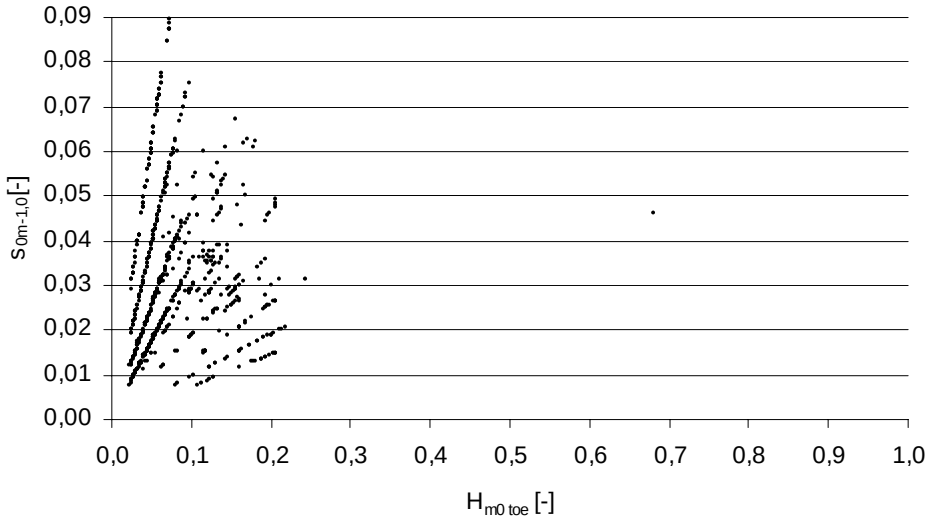

Figure 5-2 Distribution of wave height versus wave steepness for available data (smooth)

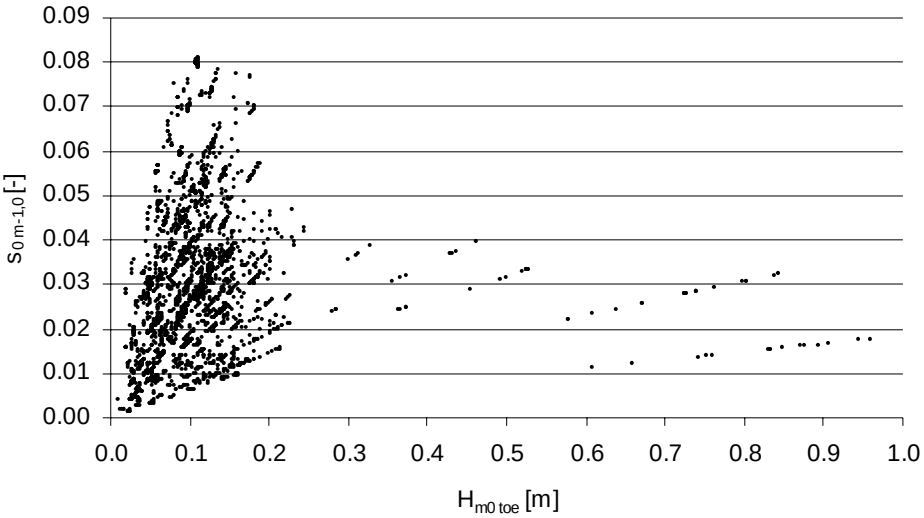

Figure 5-3 Distribution of wave height versus wave steepness for available data (mound)

The distribution of data shows the following boundaries:

Smooth structures:
$0.010 < s_{0\,m-1,0} < 0.076$
$2.90s < T_{m-1,0\,toe} < 7.87s$

Mound structures:
$0.006 < s_{0\,m-1,0} < 0.079$
$2.85s < T_{m-1,0\,toe} < 10.34s$

5.2.3 Model validation

The sensitivity figures below are based on a constant wave height of $H_{m0\,toe}$ = 1.0m.

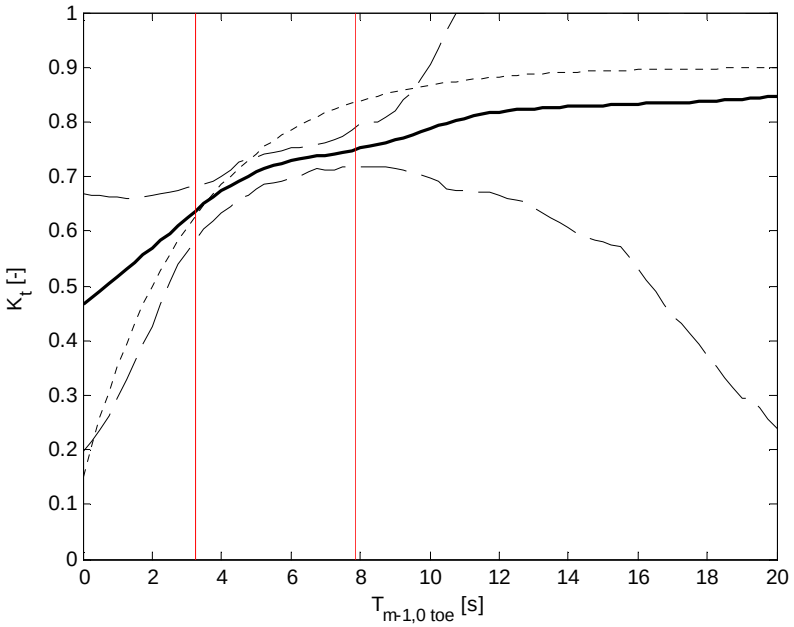

Figure 5-4 Sensitivity of prediction model to mean wave period (smooth & submerged)

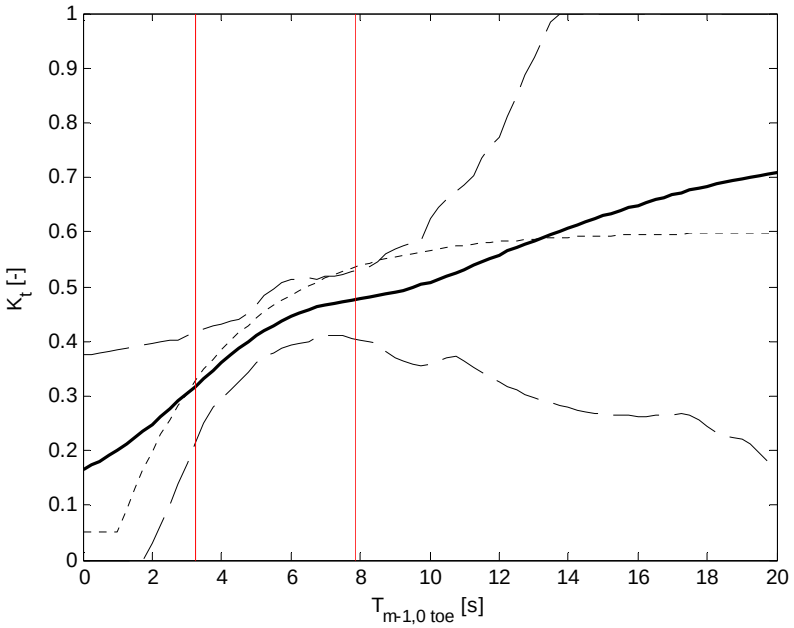

Figure 5-5 Sensitivity of prediction model to mean wave period (smooth & emerged)

The influence of the mean wave period is obvious for a smooth structure. The model shows an increasing transmission coefficient between the shown data boundaries (vertical lines). In case of a smooth structure the influence is clear and valid: a longer wave passes a structure more easily, resulting in a higher transmission coefficient.

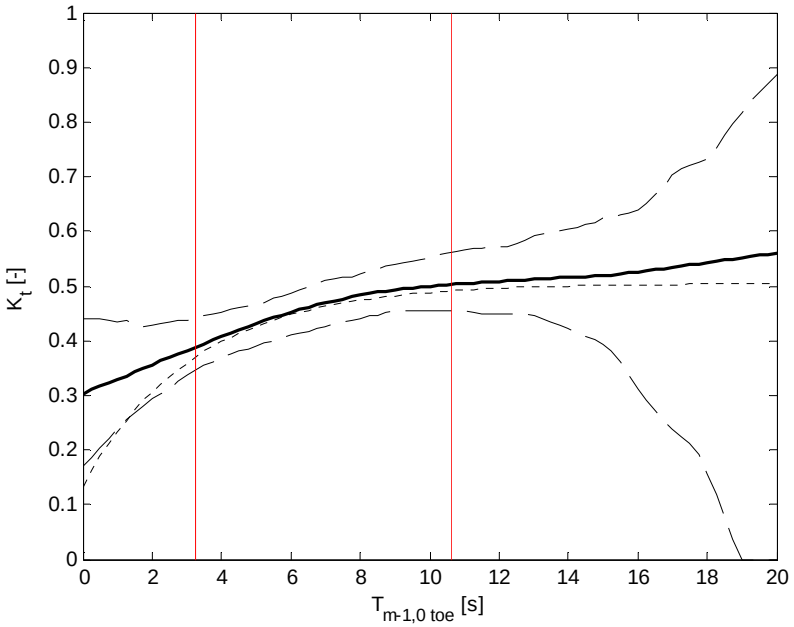

Figure 5-6 Sensitivity of prediction model to mean wave period (mound & submerged)

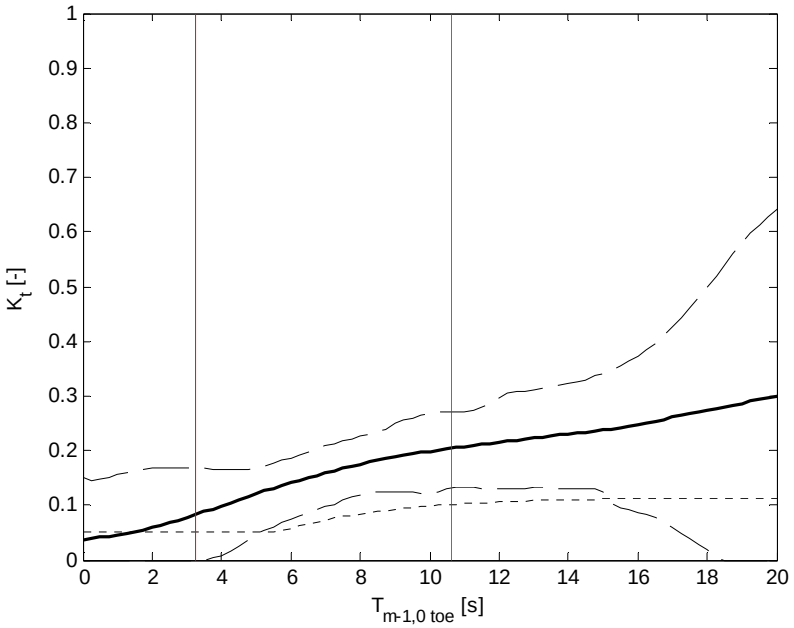

Figure 5-7 Sensitivity of prediction model to mean wave period (mound & emerged)

The prediction model shows the expected tendency for both submerged and emerged mound structures too. The confidence band is narrow for both cases between the data boundaries, indicating the prediction model is unambiguous in predicting the transmission coefficient. Clearly, for an emerged mound structure the predicted transmission coefficient deviates considerable from the DELOS formulae, contrary to a submerged mound structure, where the prediction of both methods is nearly equal. Apparently the prediction model is more capable to deal with relative higher crest freeboards than the DELOS formulae.

5.2.4 Prediction model boundary

The boundary of the prediction model for the wave steepness (indirectly the wave period), is based on the distribution of the data points, leading to the following boundaries:

Smooth structures:
$0.009 < s_{0\ m-1,0} < 0.060$

Mound structures:
$0.006 < s_{0\ m-1,0} < 0.080$

5.3 Mean angle of wave incidence

The mean angle of wave incidence β [°] is defined as the angle of the incident waves to the normal of the breakwater structure. An angle of $\beta = 0^o$ means that waves are propagating perpendicular to the structure. An angle of incidence of $\beta = 90^o$ means that waves are propagating parallel to the structure.

5.3.1 Physical boundary

Because the angle of wave incidence is restricted between a direction perpendicular and parallel to the structure, the angle of wave incidence has the following physical boundary: $0^o < \beta < 90^o$. It is clear that for $\beta = 90^o$ there will be no wave transmission, because there is no transfer component present to the lee side of the structure.

5.3.2 Data distribution

93.3% of the available data concerns tests with an angle of incidence to the normal of the structure ($\beta = 0^o$). Only a small amount of data is tested with a deviating angle. For mound structures 95.4% has no angle of incidence and for smooth structures this is 90.8%.

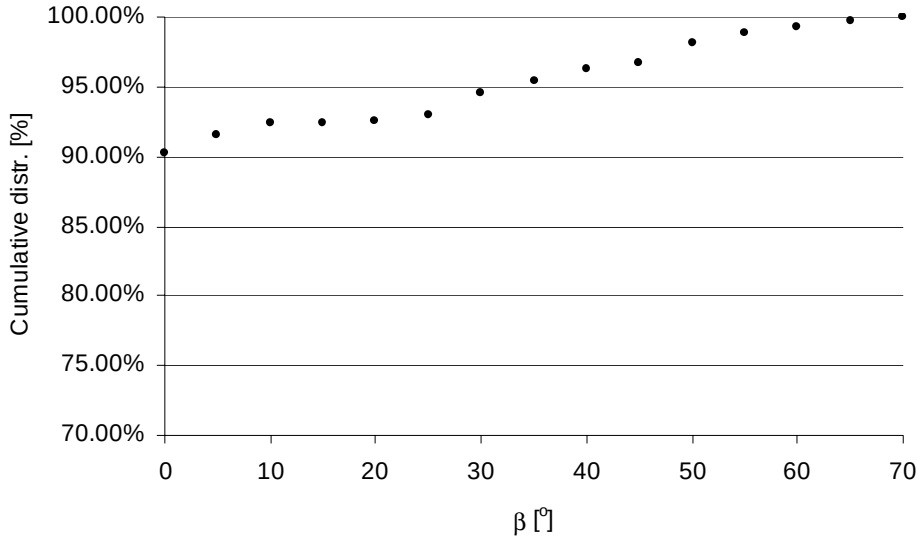

Figure 5-8 Distribution of angle of incidence for the available data (smooth)

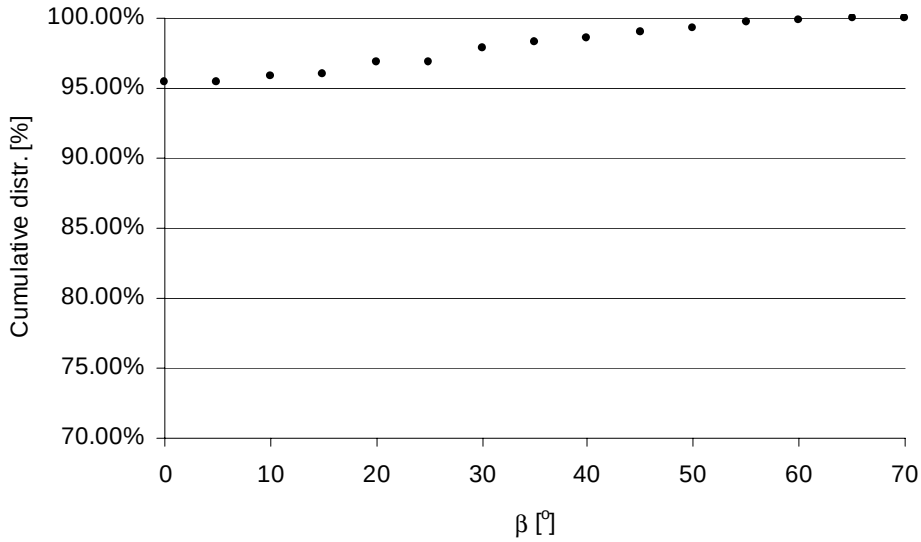

Figure 5-9 Distribution of angle of incidence for the available data (mound)

The distribution of the angle of incidence shows the following boundaries:

Smooth structures: $0^o < \beta < 70^o$
Mound structures: $0^o < \beta < 45^o$

5.3.3 Model validation

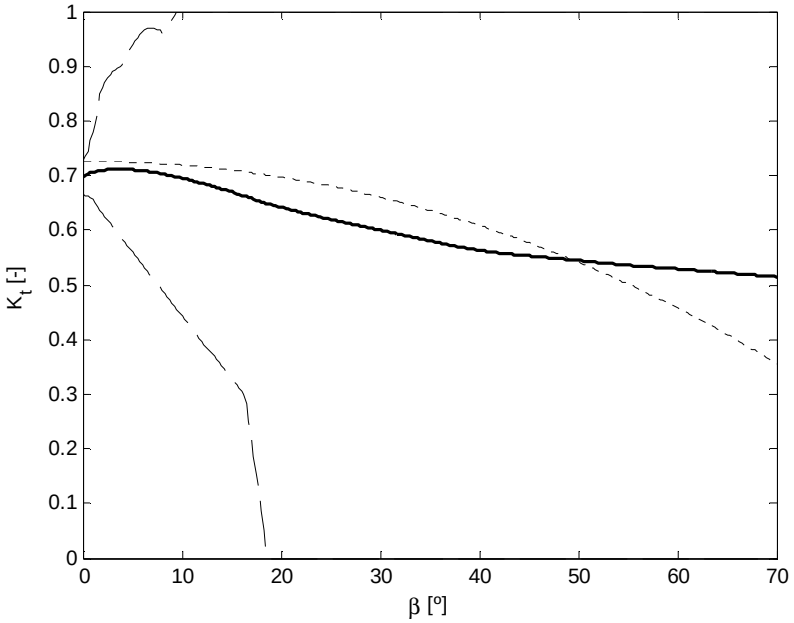

Figure 5-10 Sensitivity of prediction model to angle of incidence (smooth & submerged)

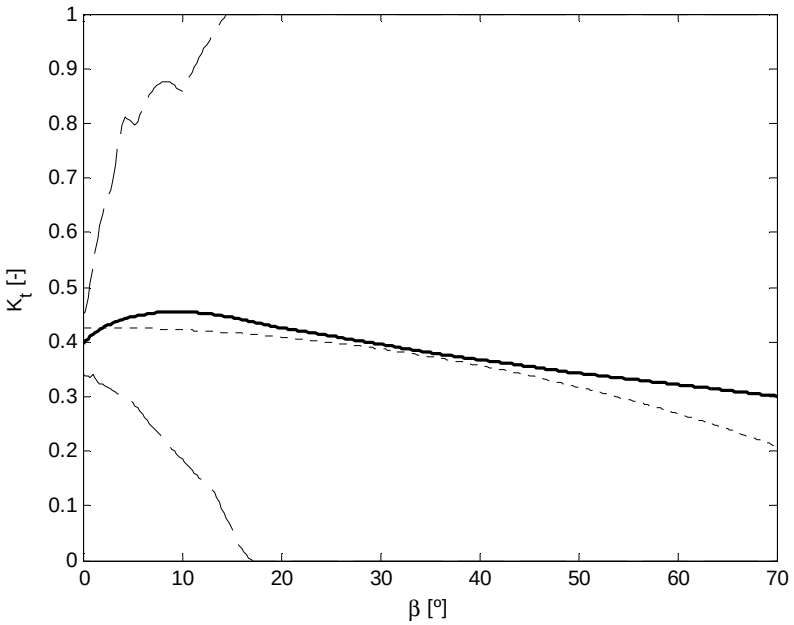

Figure 5-11 Sensitivity of prediction model to angle of incidence (smooth & emerged)

The influence of the angle of incidence is of significant influence for a smooth breakwater structure as found in earlier studies (Van der Meer et al., 2004). The model shows more or less the same tendency as the formula of Van der Meer et al. (2004). An increasing angle of incidence results in a decreasing transmission coefficient. Unlike the formula of Van der Meer et al. (2004) there is a maximum present for a small angle of incidence for both a submerged as an emerged structure. This maximum cannot be validated, because a decrease is expected for the whole range. A reason can

possibly be overfitting of this specific parameter, as the total number of tests for smooth structures with an angle of influence is small.

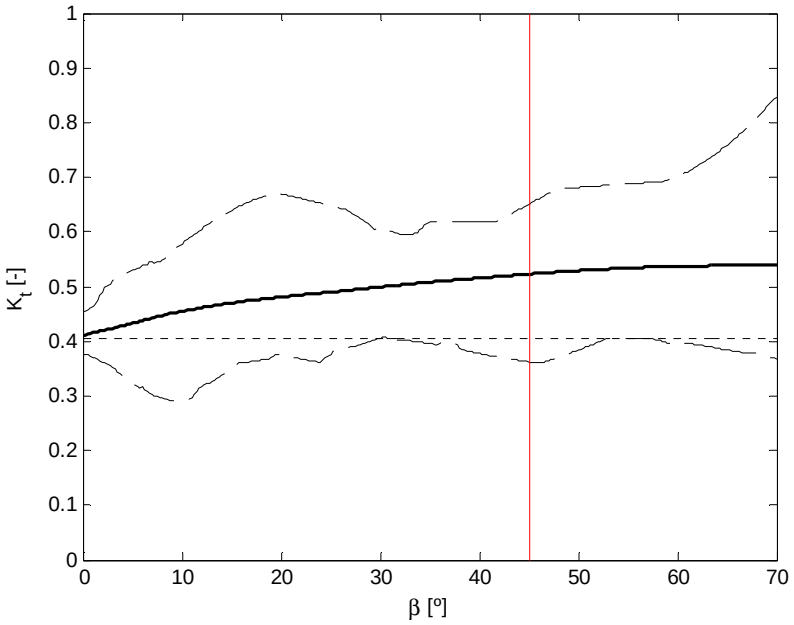

Figure 5-12 Sensitivity of prediction model to angle of incidence (mound & submerged)

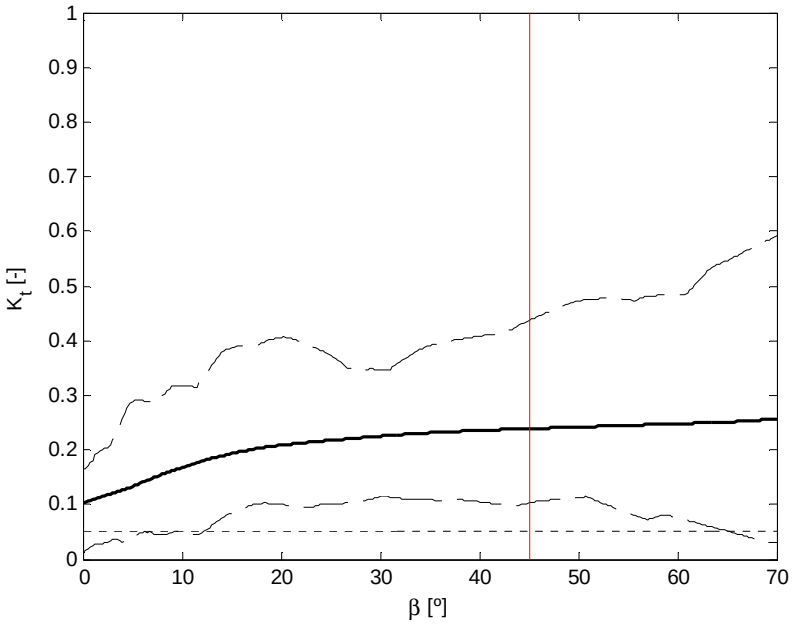

Figure 5-13 Sensitivity of prediction model to angle of incidence (mound & emerged)

The angle of incidence is found to be of minor importance for mound structures in earlier studies (Van der Meer et al., 2004) and was not taken into account. The predicted transmission coefficient increases for an increasing angle of incidence for both submerged and emerged mound structures. This tendency is physically not right. A possible explanation is again the presence of overfitting of prediction model, caused by the limited amount of data points for this parameter. Therefore, it is recommended to apply $\beta = 0^o$ in every case, like the formula of Van der Meer et al. (2004). In this way the model predicts the most reliable wave transmission coefficient for mound structures. The range is equal to the boundaries given for the distribution of data.

5.3.4 Prediction model boundary

The use of the angle of incidence within the prediction model is limited for mound structures. The following boundary is found for the prediction model, based on the given data range.

Smooth structures:
$0^o < \beta < 70^o$

Mound structures:
$0^o < \beta < 45^o$, but enter as input value: $\beta = 0^o$

5.4 Depth in front of the structure

The depth in front of the structure h [m] has to be determined at the toe of the structure. At this depth the hydraulic parameters $H_{m0\ toe}$, $T_{m-1,0\ toe}$, and β are present.

5.4.1 Physical boundary

The physical boundary of the water depth in front of the structure is given by:

$h > 0$

Of course no waves can exist if there is no water depth present. Therefore only positive values can be entered to the prediction model.

5.4.2 Data distribution

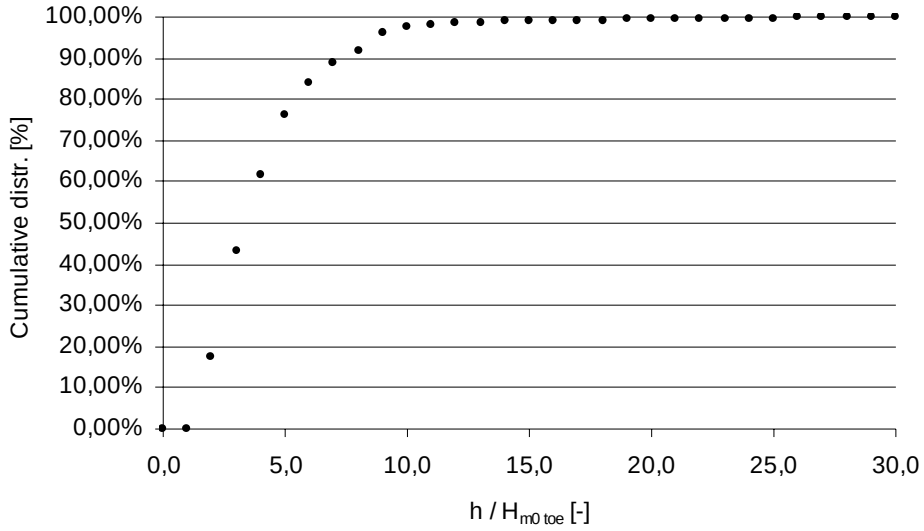

Figure 5-14 Distribution of relative water depth for the available data (smooth)

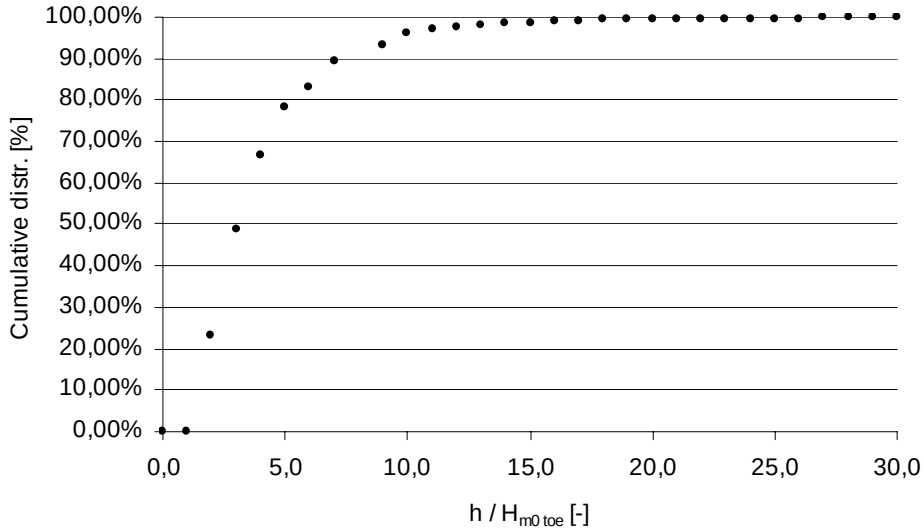

Figure 5-15 Distribution of relative water depth for the available data (mound)

From the distribution figures the follow data boundaries are found:
Smooth structures: $1.18 < h / H_{m0\ toe} < 9.79$
Mound structures: $1.55 < h / H_{m0\ toe} < 10.92$

5.4.3 Model validation

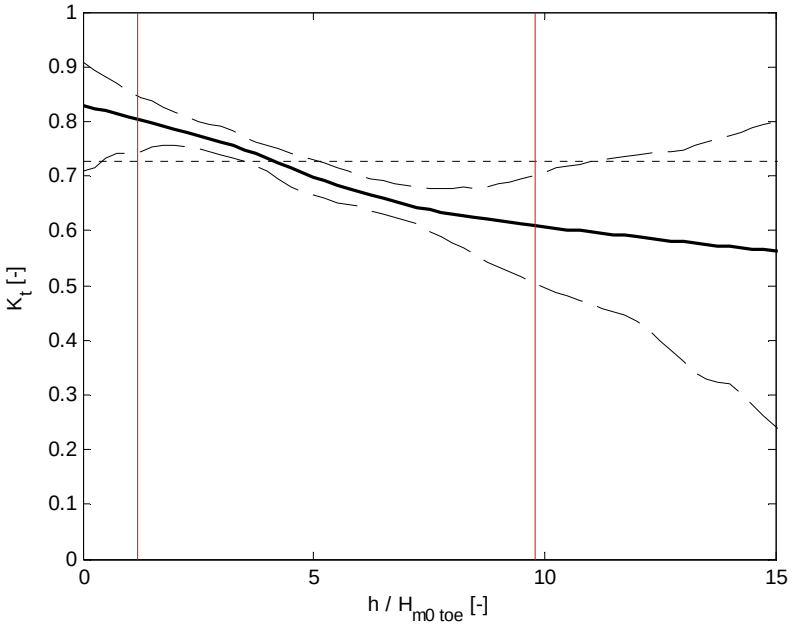

Figure 5-16 Sensitivity of prediction model to relative water depth (smooth & submerged)

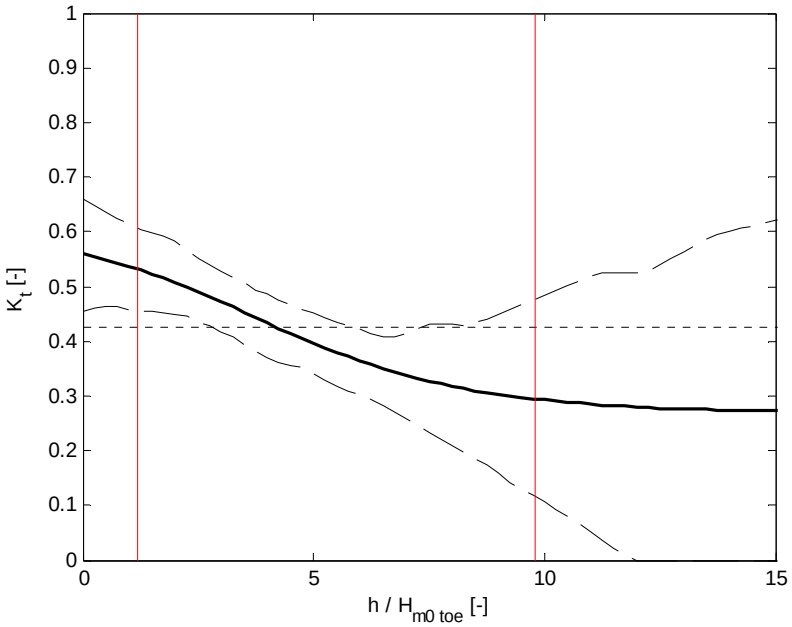

Figure 5-17 Sensitivity of prediction model to relative water depth (smooth & emerged)

The prediction model shows to be very sensitive to the value of the water depth in front of a smooth structure. In earlier studies the influence was not taken into account, but for smooth structures (submerged and emerged) the model is showing a strong decrease of wave transmission as the water depth at the toe of the structure increases. The confidence band is narrow within the 95%-data confidence range, indicating the ensemble of neural networks is reliable in its prediction. An explanation of this strong influence cannot be given at this moment. A possible explanation could be that shallower water conditions result in a steep front of the incident waves, having influence on the type of breaking and therefore also on the wave transmission coefficient.

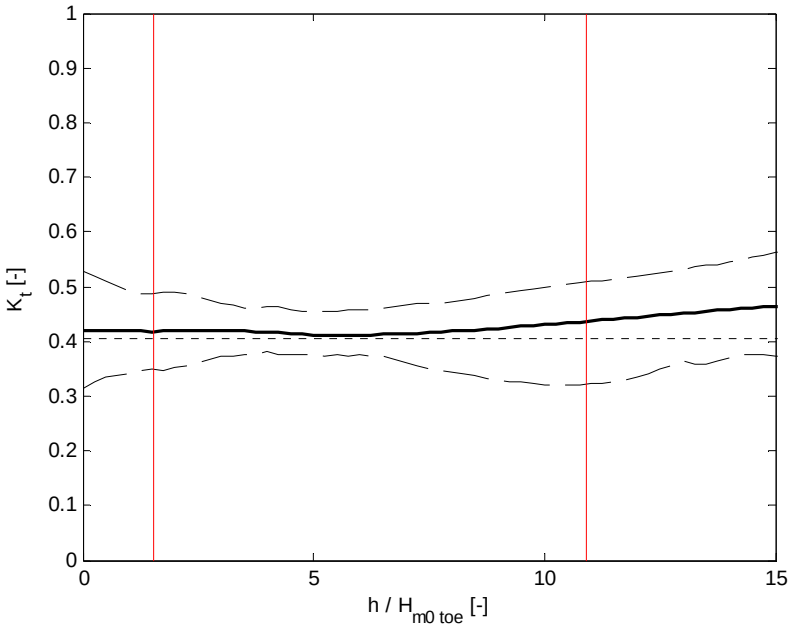

Figure 5-18 Sensitivity of prediction model to relative water depth (mound & submerged)

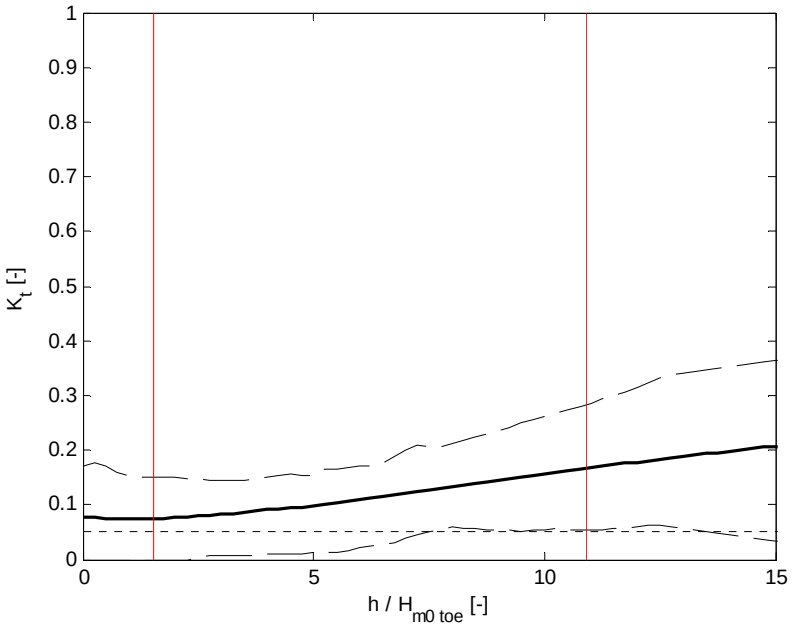

Figure 5-19 Sensitivity of prediction model to relative water depth (mound & emerged)

The influence of the relative water depth seems to be less important for submerged mound structures, where the tendency is more of less constant indicating there is no influence. For a emerged mound structure the tendency is different from smooth structures and the prediction model shows an increasing transmission coefficient for an increasing water depth, for a rather wide band of confidence. No possible explanation of this last mentioned tendency can be given at this moment, but assumed is the influence should be small too.

5.4.4 Prediction model boundary

The prediction model boundary is based on the data distribution for smooth and mound structures:

Smooth structures:
$1.20 < h / H_{m0\ toe} < 9.80$

Mound structures:
$1.55 < h / H_{m0\ toe} < 11.00$

5.5 Crest freeboard

The crest freeboard R_c [m] is the vertical distance between sea water level and the crest of the breakwater structure.

5.5.1 Physical boundary

There is no physical boundary of the relative crest freeboard present as the parameter can be either positive (emerged) or negative (submerged).

5.5.2 Data distribution

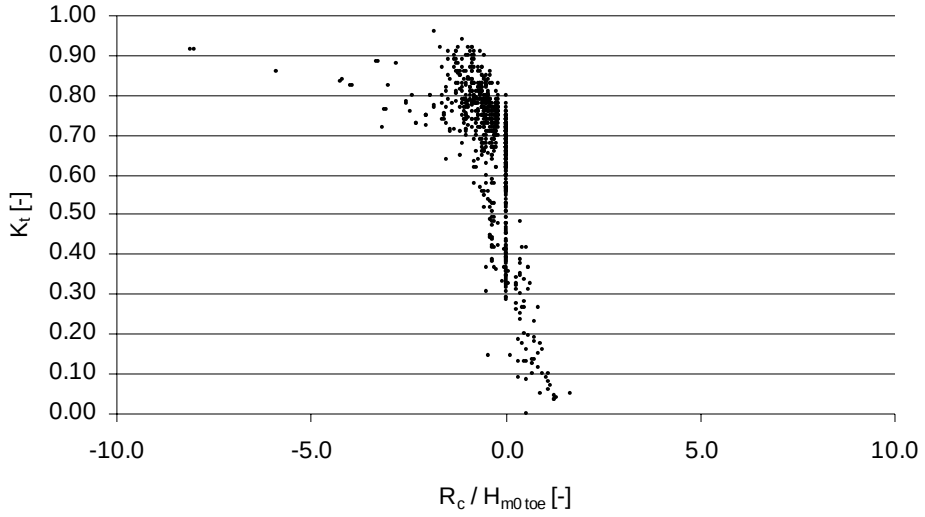

Figure 5-20 Distribution of relative crest freeboard for the available data (smooth)

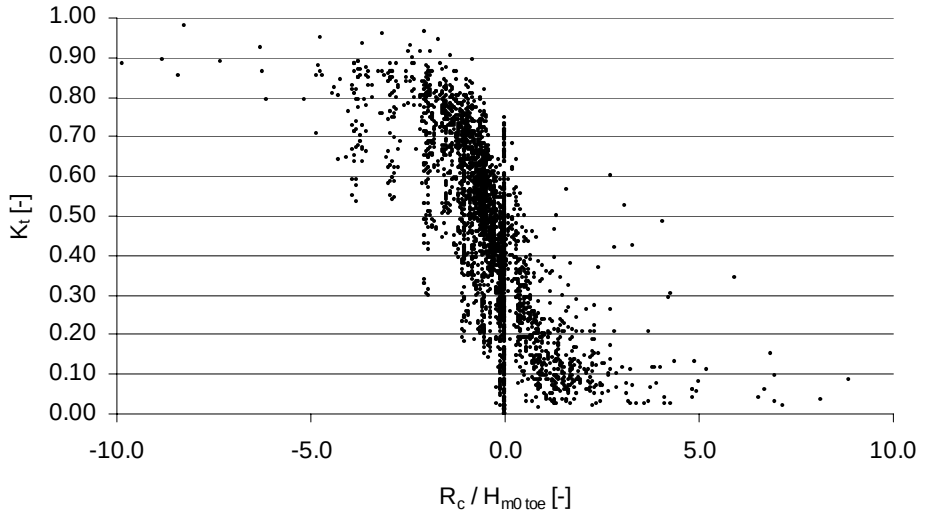

Figure 5-21 Distribution of relative crest freeboard for the available data (mound)

From the distribution figures the follow data boundaries are found:

Smooth structures: $-2.04 < R_c / H_{m0\ toe} < 0.70$
Mound structures: $-3.48 < R_c / H_{m0\ toe} < 2.27$

5.5.3 Model validation

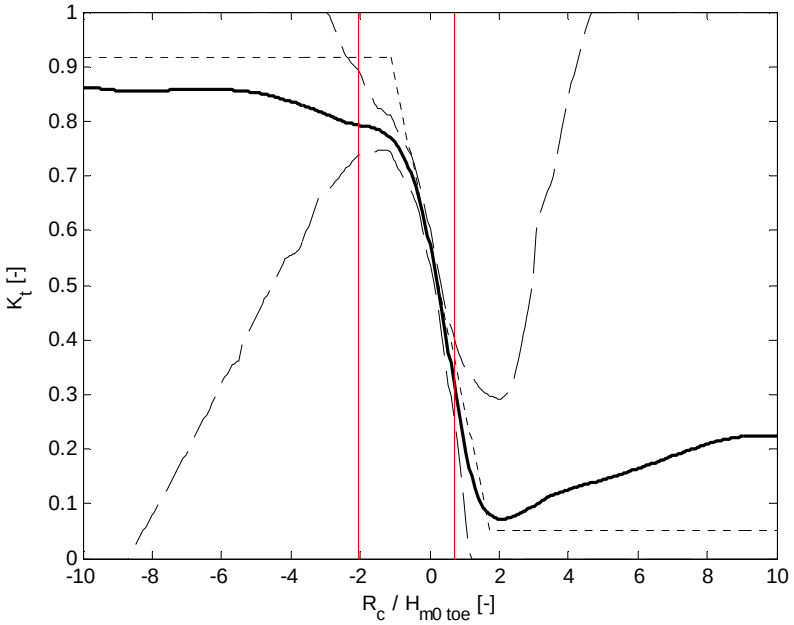

Figure 5-22 Sensitivity of prediction model to relative crest freeboard (smooth)

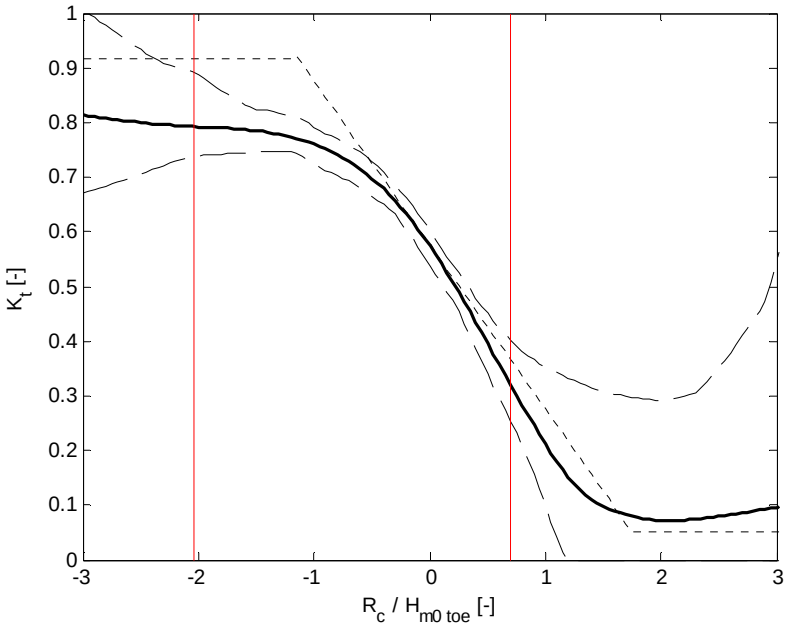

Figure 5-23 Zoom in on Figure 5-22 for the range –3.0 < R_c / $H_{m0\ toe}$ < 3

The influence of the relative crest freeboard is very clear. An increasing relative crest freeboard results in a decreasing transmission coefficient, which is physically expected. Within the range of the test data this tendency is very strong and the confidence band is very narrow. The prediction model is even able to predict a right tendency outside the range of data, indicating the model is adapting the strong influence of the relative crest freeboard of mound structures as well. For the range -7.0 < R_c / $H_{m0\ toe}$ < 2.0 the tendency is still valid.

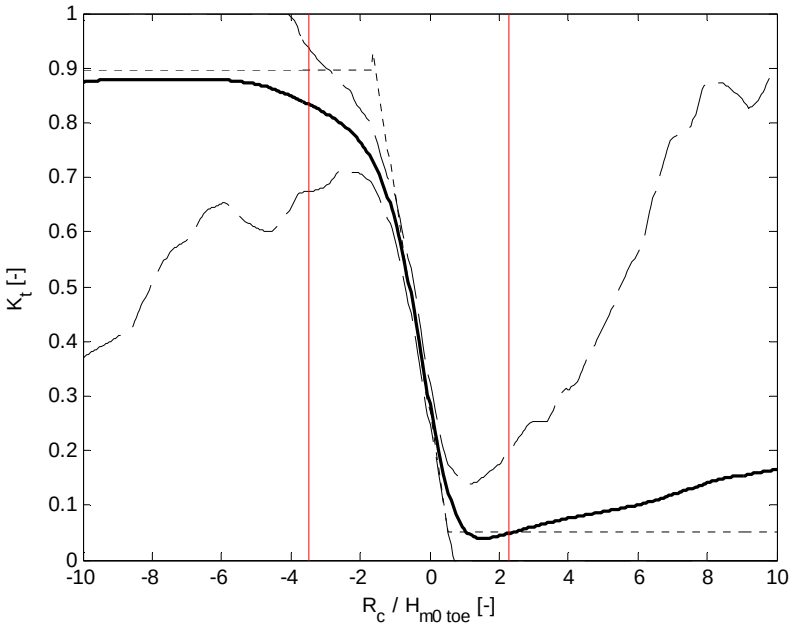

Figure 5-24 Sensitivity of prediction model to relative crest freeboard (mound)

Also for mound structures is expected that an increasing relative crest freeboard always results in a decreasing transmission coefficient. Within the range of $-8.0 < R_c / H_{m0\ toe} < 1.8$ this tendency is shown by the prediction model. For $R_c / H_{m0\ toe} > 1.8$ the model shows a deviating prediction, which is caused by the limited number of data points within this region.

5.5.4 Prediction model boundary

The lower boundary of the prediction model is based on the distribution of the available data, although the prediction model is showing a right tendency (but with a wide confidence band) for even smaller values of the relative crest freeboard. The upper boundary of the prediction model for the relative crest height is determined by the tendency which is physically wrong beyond $R_c / H_{m0\ toe} = 1.8$.

Smooth structures:
$-2.00 < R_c / H_{m0\ toe} < 0.70$

Mound structures:
$-3.50 < R_c / H_{m0\ toe} < 1.80$

5.6 Crest width

The total crest width W_c [m] is the horizontal distance between front- and back slope at the crest of the structure.

5.6.1 Physical boundary

Crest widths with a value of zero are physically possible if the shape of a breakwater structure is like a heap of loose elements (the case for a reef breakwater, like Ahrens).

5.6.2 Data distribution

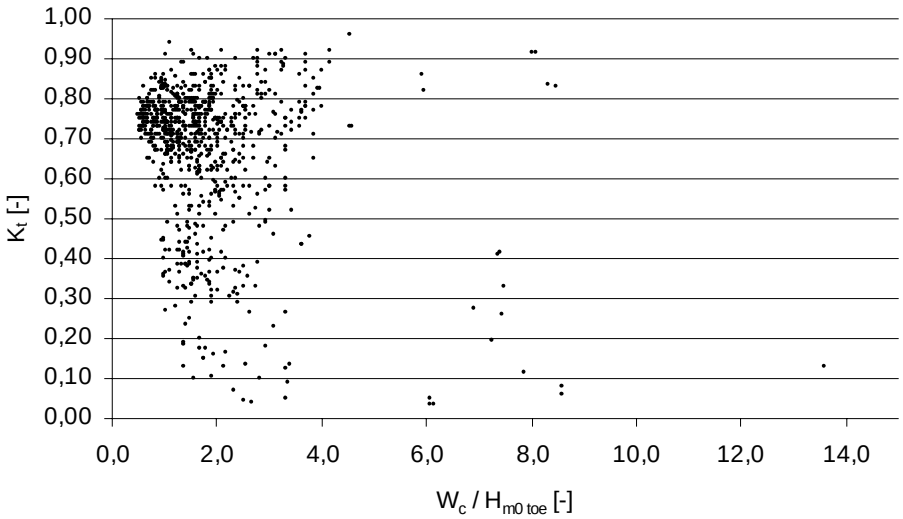

Figure 5-25 Distribution of relative crest width for the available data (smooth)

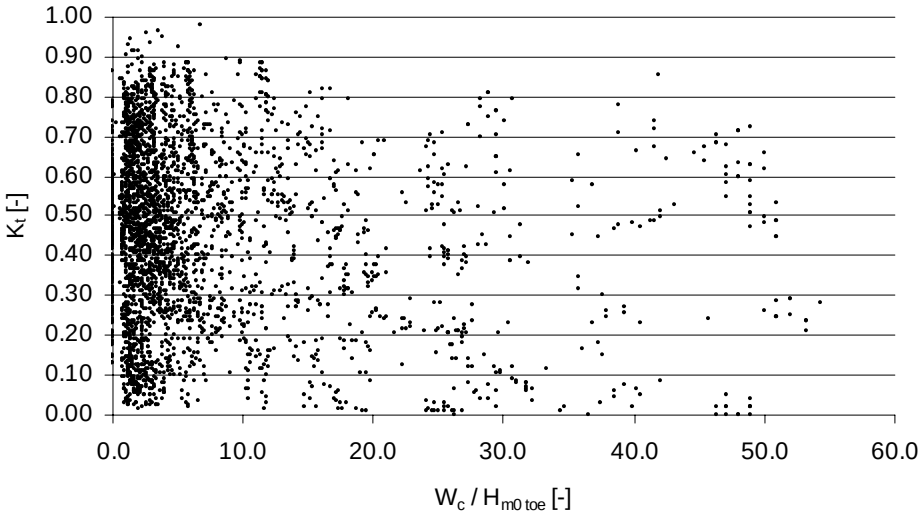

Figure 5-26 Distribution of relative crest width for the available data (mound)

From the distribution figures the follow data boundaries are found:

Smooth structures: $0.62 < W_c / H_{m0\ toe} < 5.96$
Mound structures: $0.009 < W_c / H_{m0\ toe} < 47.17$

5.6.3 Model validation

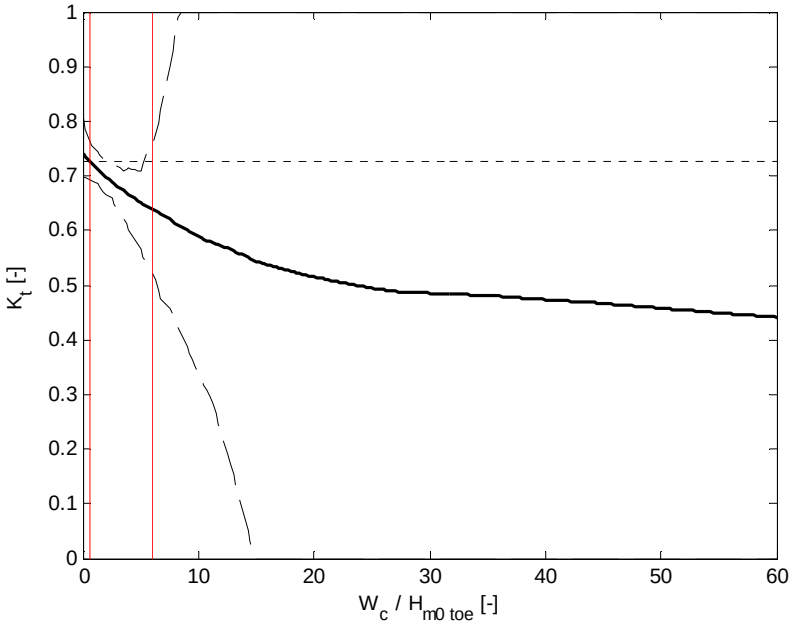

Figure 5-27 Sensitivity of prediction model to relative crest width (smooth & submerged)

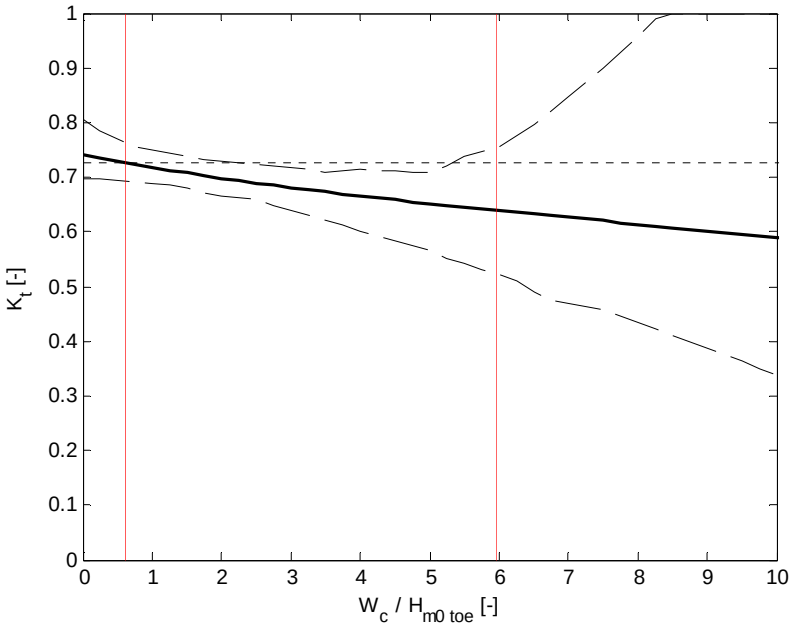

Figure 5-28 Zoom in on Figure 5-27 for the range 0 < Wc / $H_{m0\ toe}$ < 6

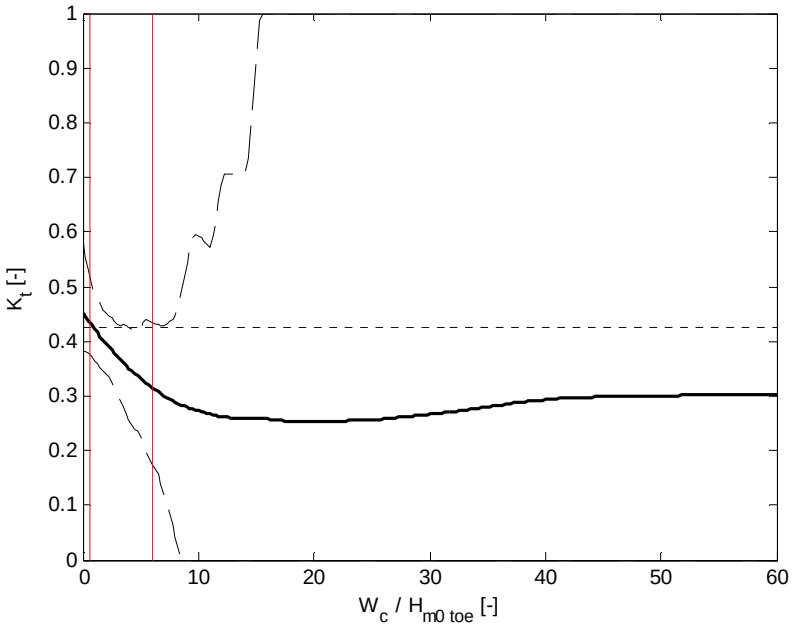

Figure 5-29 Sensitivity of prediction model to relative crest width (smooth & emerged)

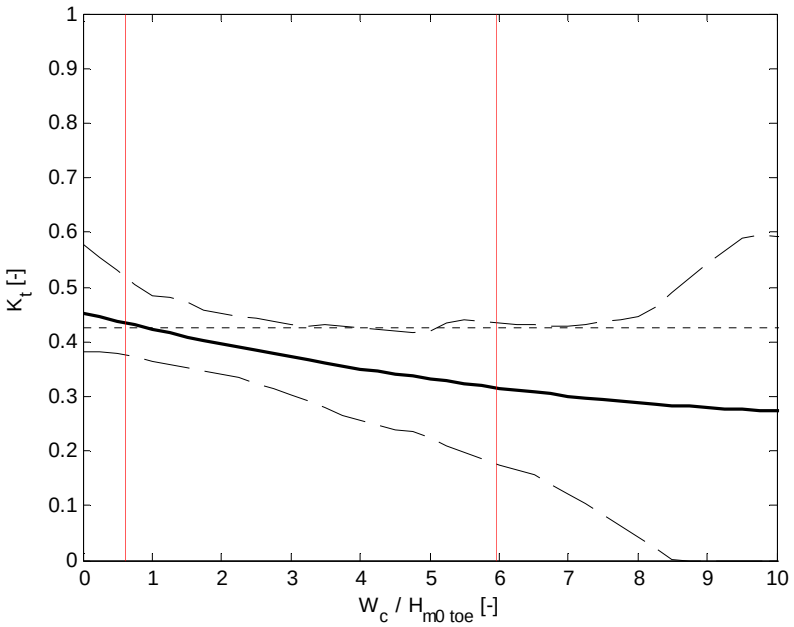

Figure 5-30 Zoom in on Figure 5-29 for the range 0 < W_c / $H_{m0\ toe}$ < 6

The prediction models shows for both submerged and emerged smooth structures a decreasing transmission coefficient as the relative crest width increases. This decreasing tendency becomes smaller as the relative crest width increases. The confidence band is only narrow within the range of data: 0.62 < W_c / $H_{m0\ toe}$ < 5.96. This is completely deviating from mound structures, where the confidence band is very narrow over a much wider range and showing a stronger decreasing tendency. This indicates that the prediction model clearly separates the behavior of smooth structures from mound structures concerning the influence of the relative crest width. Additionally, the influence of the relative crest width is much smaller for smooth structures compared to mound structures. This difference is explained in earlier studies by the fact that no energy dissipation is present at the crest of a smooth structure, contrary to mound structures where energy dissipation is present due to friction and permeability effects of the rough and permeable crest.

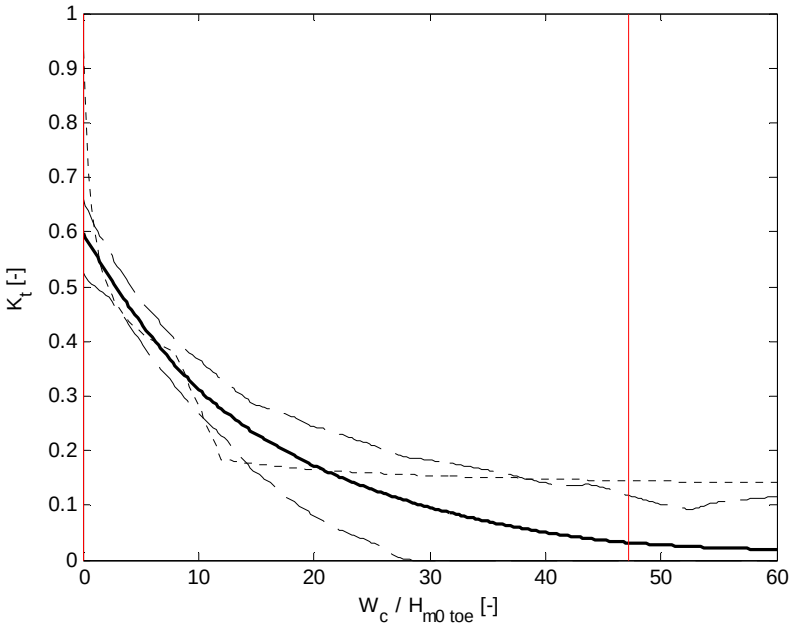

Figure 5-31 Sensitivity of prediction model to relative crest width (mound & submerged)

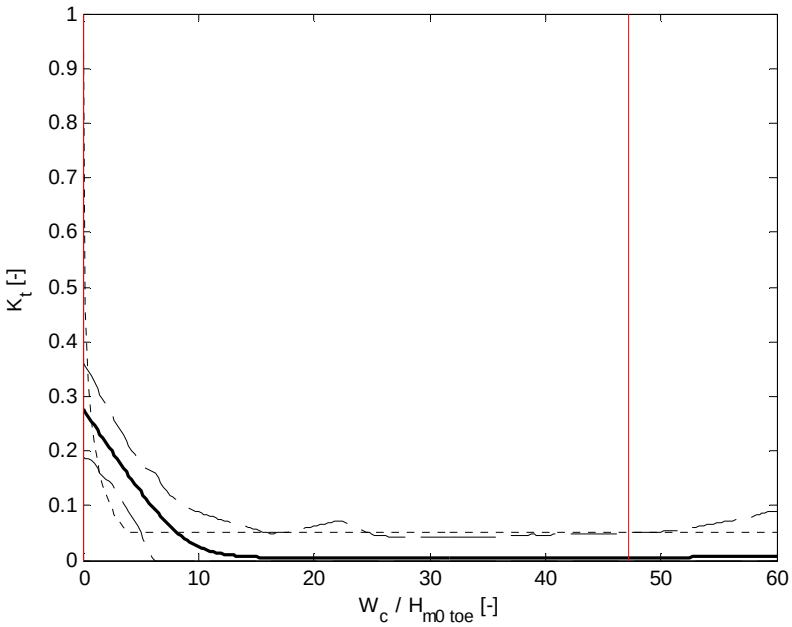

Figure 5-32 Sensitivity of prediction model to relative crest width (mound & emerged)

The prediction model shows a decreasing transmission coefficient for an increasing relative crest width for both emerged and submerged mound structures, which is physically right. This tendency continues for both cases till a constant transmission coefficient is reached. Note that for an mound structures the transmission coefficient is decreasing to zero, which is to be expected as the rough crest keeps causing wave energy dissipation as a wave travels over the crest. The confidence band is most narrow in case a mound structure is emerged. The range of validity of the prediction model to this relative crest width is equal to the boundary of the data distribution.

5.6.4 Prediction model boundary

The prediction model boundary is based on the data distribution for both smooth and mound structures:

Smooth structures:
$0.60 < W_c / H_{m0\ toe} < 6.00$

Mound structures:
$0.01 < W_c / H_{m0\ toe} < 47.00$

5.7 Upward front slope

The upward front slope is described as the cotangent front slope cot α_{uf} [-]. This is the slope from toe to the crest of the structure, or if a berm is present from berm to the crest. The cotangent is defined as the ratio of the horizontal distance over the vertical distance.

5.7.1 Physical boundary

The upward front slope can vary between 0 < cot α_{uf} < 5. A lower boundary of cot α_{uf} = 0 means a completely vertical structure, while an upper boundary of cot α_{uf} = 5 is a very gentle slope. Gentler slopes are close to a sloping beach and cannot be entered to the prediction model.

5.7.2 Data distribution

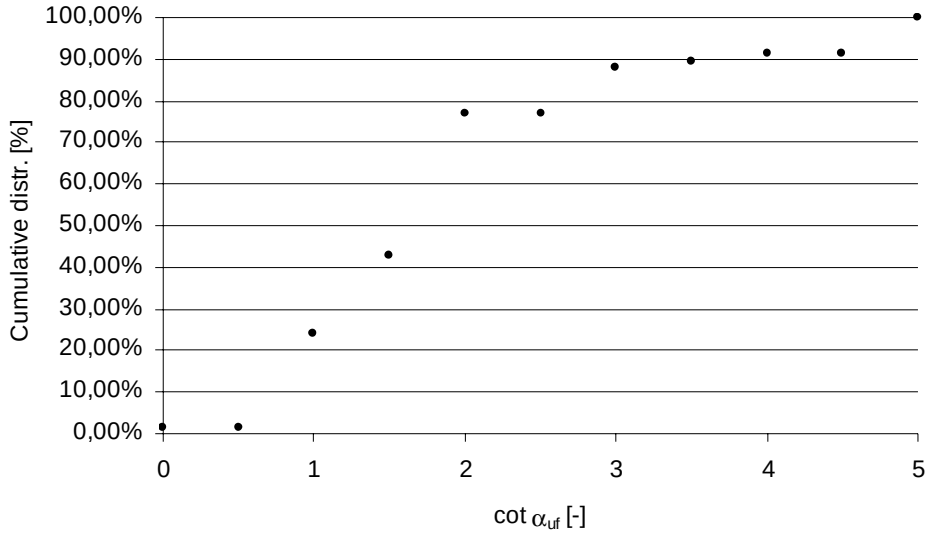

Figure 5-33 Distribution of upward front slope for the available data (smooth)

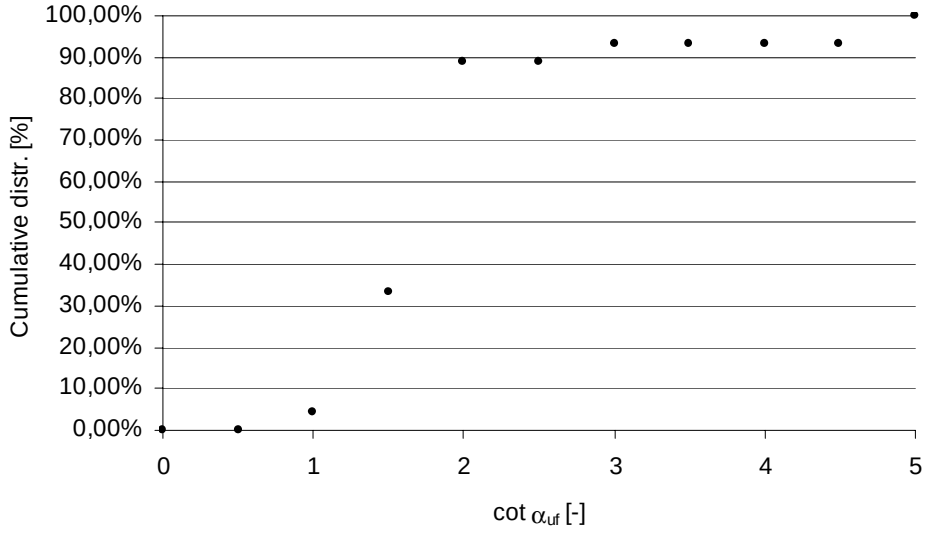

Figure 5-34 Distribution of upward front slope for the available data (mound)

From the distribution figures the follow data boundaries are found:

Smooth structures: 1.0 < cot α_{uf} < 5.0
Mound structures: 1.0 < cot α_{uf} < 5.0

5.7.3 Model validation

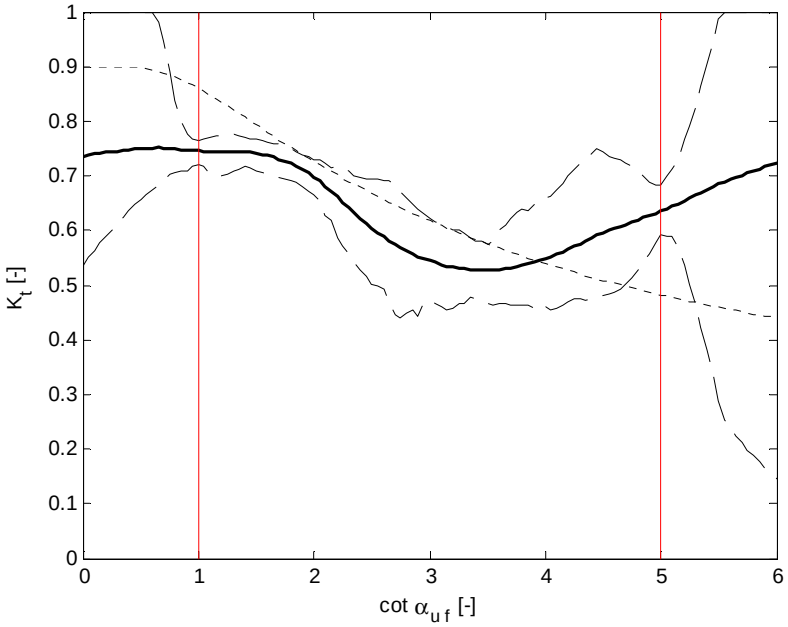

Figure 5-35 Sensitivity of prediction model to upward front slope (smooth & submerged)

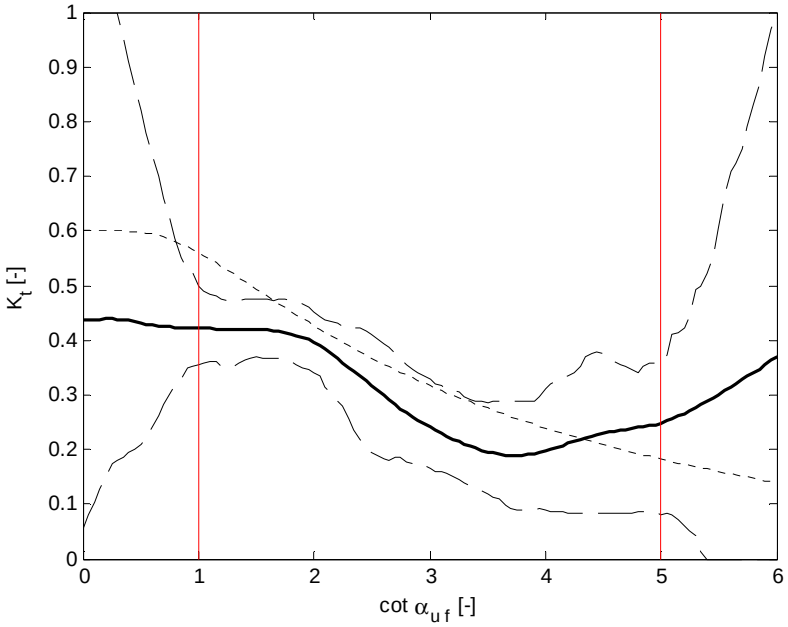

Figure 5-36 Sensitivity of prediction model to upward front slope (smooth & emerged)

A strong tendency of the influence of the upward front slope to the wave transmission coefficient is found for both submerged and emerged smooth structures. The decreasing trend line of the transmission coefficient for a milder slope is physically expected as waves are influenced over a longer distance and more wave energy dissipation is present. The found tendency is more or less equal to the DELOS formula of Van der Meer et al. (2004), although there is more fluctuation present for the prediction model. The increase of the transmission coefficient for cot α_{uf} > 3.8 are physically not expected and will determine the upper boundary for smooth structures.

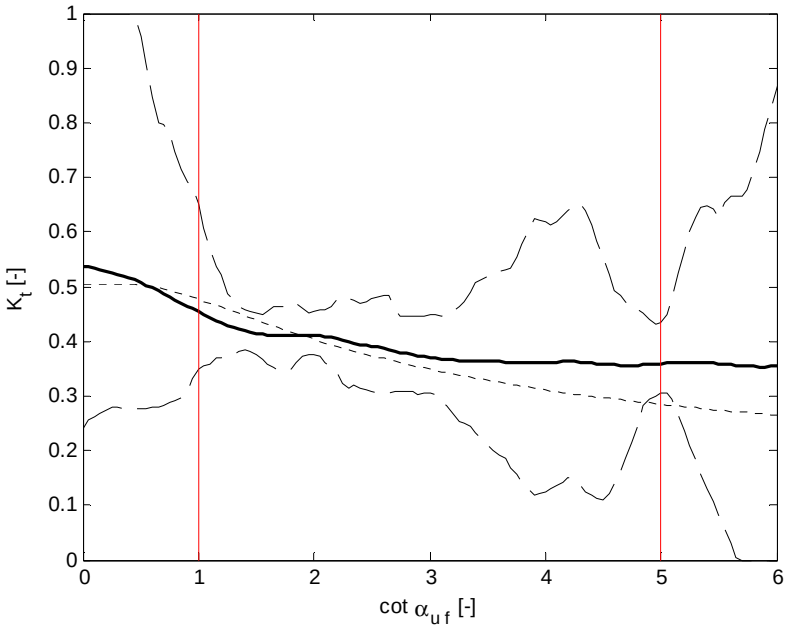

Figure 5-37 Sensitivity of prediction model to upward front slope (mound & submerged)

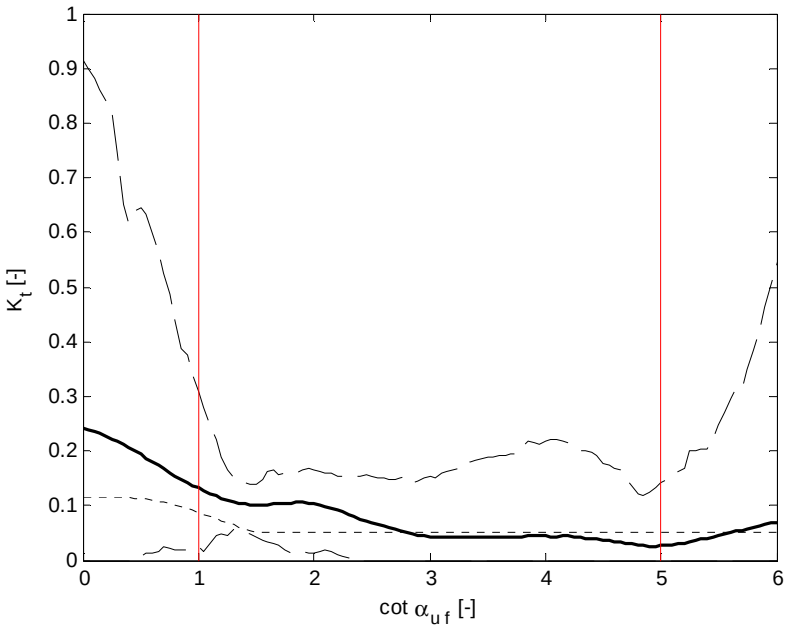

Figure 5-38 Sensitivity of prediction model to upward front slope (mound & emerged)

The prediction model is showing a decreasing tendency of the transmission coefficient for a gentler slope, within the range of the distribution of data points. The prediction model is showing some fluctuations due to interpolations between the rounded values (1.5, 2.0, 3.0, etc.) of the upward front slope. These fluctuations are stated to be of minor importance as in practice front slopes are also given a rounded value. For an emerged mound structure the transmission coefficient is even approaching a value of zero, as in case of a submerged mound structure the transmission coefficient is getting constant.

5.7.4 Prediction model boundary

The prediction model boundary is based on the data distribution for both smooth and mound structures. The upper boundary for smooth structures is adapted to the range of a physically right tendency.

Smooth structures:
$1.0 < \cot \alpha_{uf} < 3.8$

Mound structures:
$1.0 < \cot \alpha_{uf} < 5.0$

5.8 Roughness factor

The roughness factor γ_f [-] is introduced to characterize the roughness of the surface of a breakwater structure. The roughness factor is used within the empirical formula of wave run-up (TAW, 2002), but shows to be of use for the prediction of wave transmission as well to describe the roughness of the surface of breakwater structures for various types of armour material (see Table 3-8)

5.8.1 Physical boundary

Till this moment the roughness factor is only defined within the range: $0.3 < \gamma < 1.0$. In order to make a distinction between the roughness/permeability of different types of armour units, a lot of values between 0.40 and 0.50 are found, describing very well the difference in behavior to wave transmission. Because most structures concern rubble mound, the value of 0.45 is frequently present.

5.8.2 Data distribution

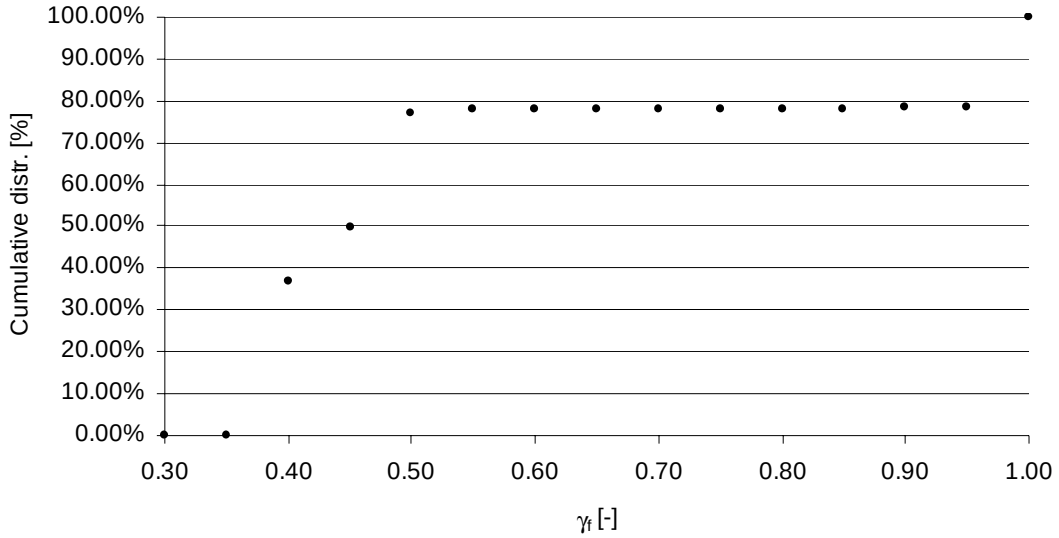

Figure 5-39 Distribution of the roughness factor for all available data

From the distribution figures the follow data boundaries are found:

Smooth structures: $\gamma_f = 1.00$
Mound structures: $0.38 < \gamma_f < 0.90$

In order to avoid confusion about the transition of rough and smooth surfaces, a structure is only defined rough if the roughness factor $\gamma_f = 1.0$.

5.8.3 Model validation

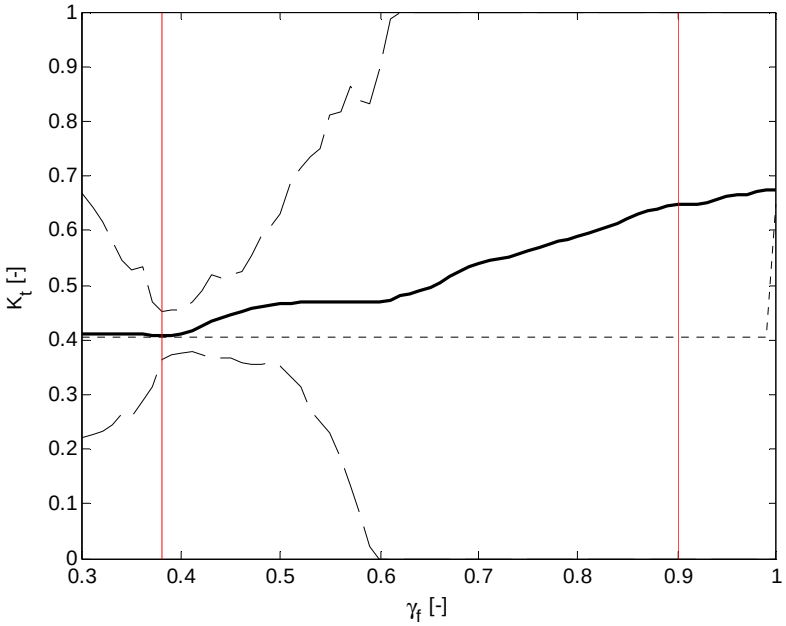

Figure 5-40 Sensitivity of prediction model to roughness factor (mound & submerged)

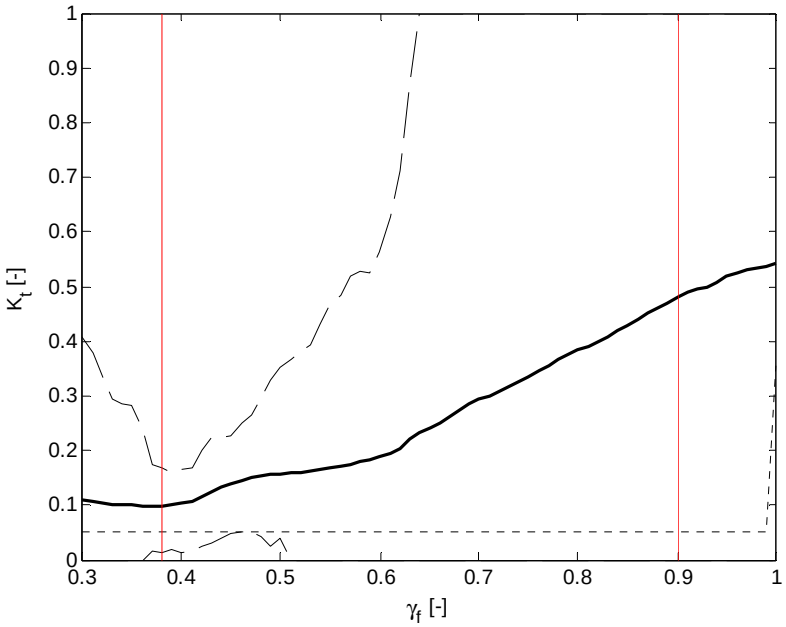

Figure 5-41 Sensitivity of prediction model to roughness factor (mound & emerged)

For both mound submerged and emerged structures is found that a smoother structure's surface causes less wave energy dissipation, resulting in more wave transmission. Note the confidence band is most narrow for $0.40 < \gamma_f < 0.50$, because most structures in the available data are rubble mound. Nevertheless, the prediction model is able to find a clear relation of the roughness factor for the whole range of data. The roughness factor mainly influences wave run-up, which is only present for an emerged structure. Therefore the influence of the roughness factor is smaller for a submerged structure. A rougher surface will cause more wave energy dissipation along the surface of the structure and will therefore reduce the wave transmission.

5.8.4 Prediction model boundary

The prediction model boundary is based on the data distribution for both smooth and mound structures:

Smooth structures:
$\gamma_f = 1.00$

Mound structures:
$0.38 < \gamma_f < 0.90$

5.9 Notional permeability factor

The notional permeability factor P [-] is well known from the stability formulae of Van der Meer (1988a). This input parameter represents the permeability for waves underneath the armour layer, but in this study the permeability of the core is taken into account as well. P is defined in the prediction model for describing four different composures of a breakwater structure:

Value	Definition
P = 0.1	Impermeable structure, mound armour layer with filter on clay or sand
P = 0.4	Low permeable structure, mound armour layer with filter on a rip-rap core
P = 0.5	Medium permeable structure, mound armour layer on a rip-rap core
P = 0.6	High permeable structure, homogeneous mound armour

Table 5-1 Value for P [-] for various types of structures

The notional permeability factor is introduced to take into account transmission through the breakwater structure for permeable structures and to distinguish in this way impermeable and permeable structures. In combination with the roughness factor all structures of the available data could be described.

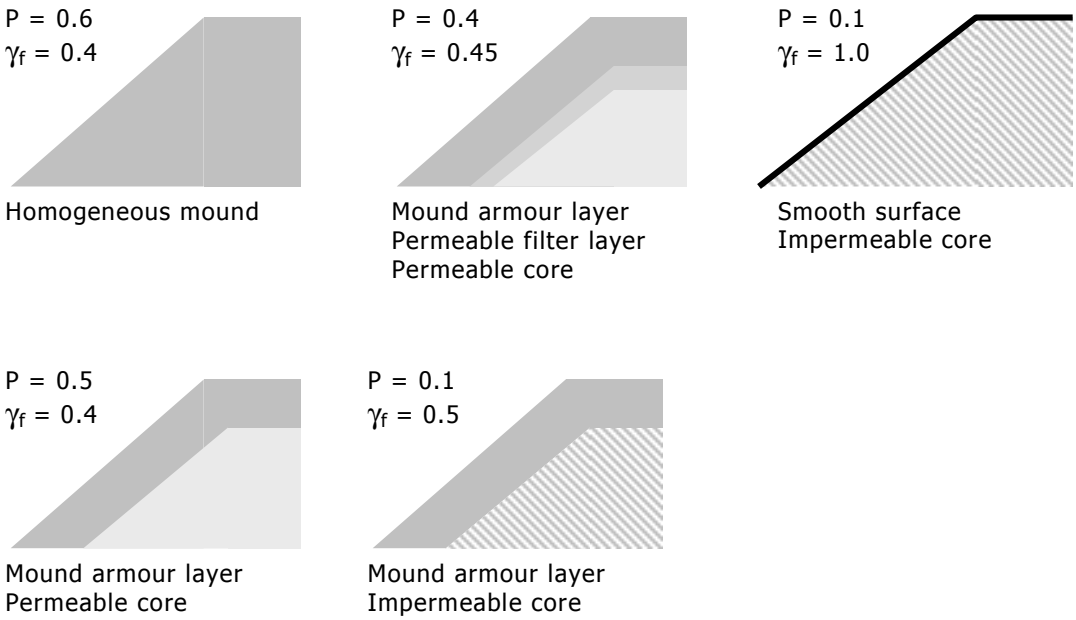

Figure 5-42 Examples of the notional permeability factor in combination with the γ_f

5.9.1 Physical boundary

As mentioned before, the notional permeability can adopt values between 0.1 and 0.6. Within the prediction model for simplicity reasons, only four different values are used. The values P = 0.1, 0.4, 0.5 and 0.6 can be entered to the model.

5.9.2 Data distribution

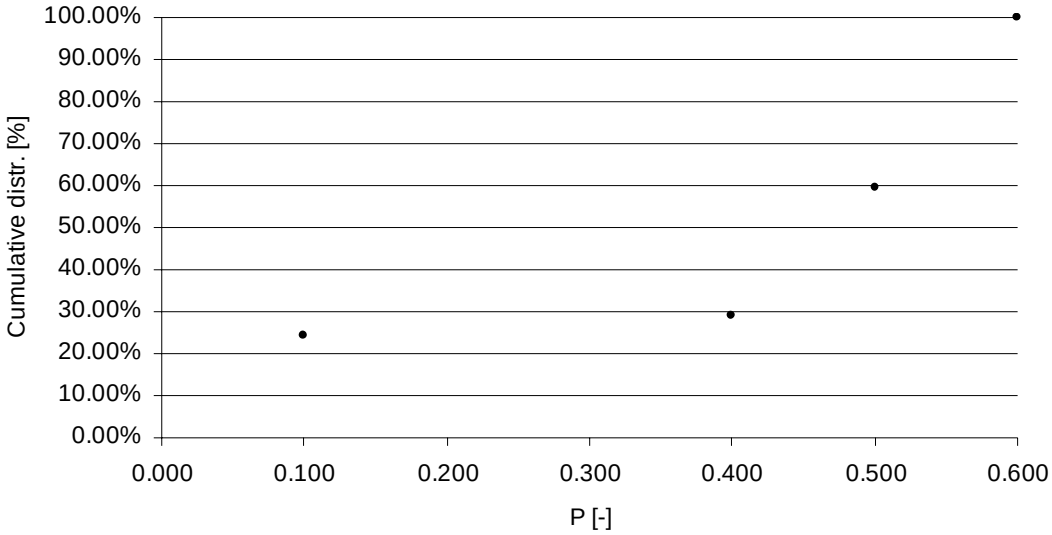

Figure 5-43 Distribution of the notional permeability factor for all available data

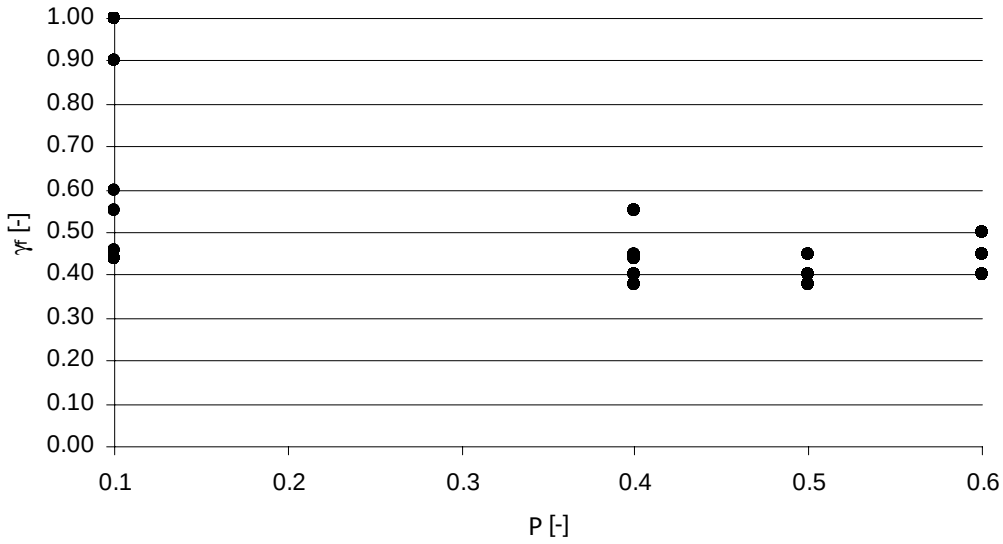

Figure 5-44 Notional permeability factor versus roughness factor for all available data

Mound structures can be either permeable or impermeable. Smooth structures are always impermeable and should be given a notional permeability of P = 0.1 in combination with a roughness factor of γ_f = 1.0.

5.9.3 Model validation

A model validation of the notional permeability factor is be made for a roughness factor of γ_f = 0.45. The prediction model proves that it is capable of detecting smooth from mound structures and permeable from impermeable structures.

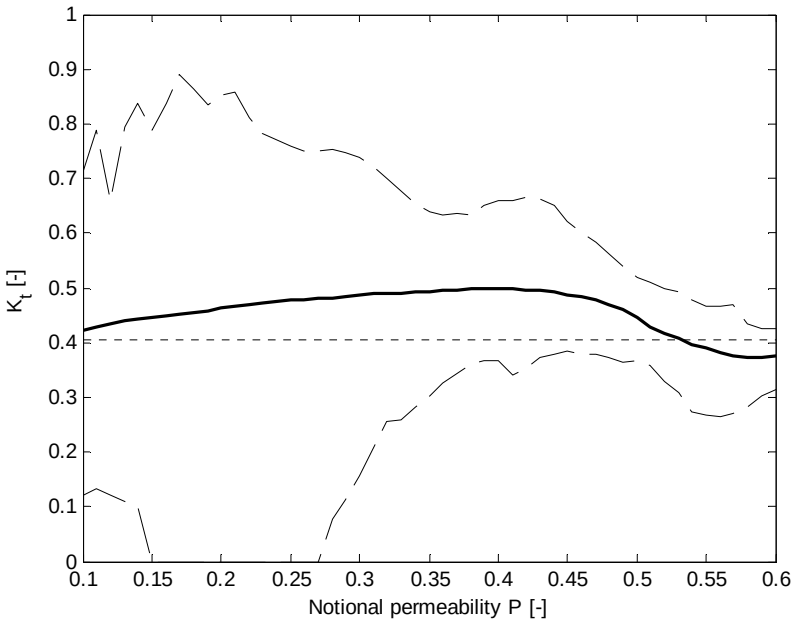

Figure 5-45 Sensitivity of prediction model to the notional permeability (mound & submerged)

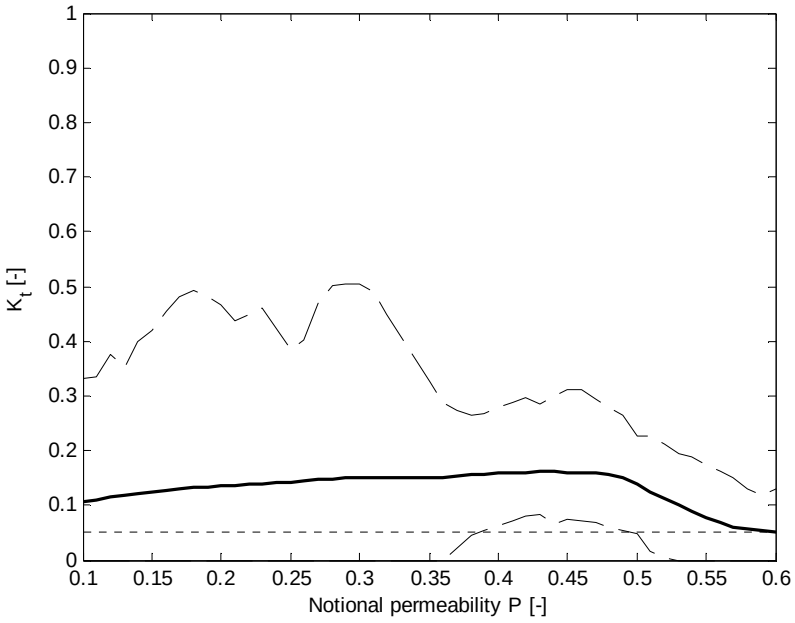

Figure 5-46 Sensitivity of prediction model to the notional permeability (mound & emerged)

The wave transmission coefficient is maximum for a notional permeability factor around P = 0.4. For a notional permeability factor of P = 0.1, there is an impermeable core present giving a lower transmission coefficient. For a homogeneous type of breakwater (P = 0.6) the wave transmission is lowest, apparently much of the wave energy is dissipated inside the core of the structure.

5.9.4 Prediction model boundary

The following boundaries are given for the notional permeability factor P [-], based on the data range and physical boundary.

Smooth structures:
P = 0.10

Mound structures:
0.10 < P < 0.60

5.10 Conclusion for the validity of the prediction model

5.10.1 Structure types

The prediction model has proven to be capable of handling both smooth and mound structures, although their behavior to wave transmission is completely different. The advantaged of handling both structures in one prediction model is that also structures in the transition between smooth and mound structure can be handled. Examples for instance are an impermeable mound structure or a reduced smooth structure. Clearly the neural networks used have proven to be powerful tools and very useful to this study.

5.10.2 Parameter boundaries

The following boundaries of input parameters have found to give reliable and valid predictions.

Input Parameter	Prediction model input boundary
Incident significant wave height, $H_{m0\ toe}$ [-]	$H_{m0\ toe} > 0.03$m $H_{m0\ toe} / h < 0.50$
Mean wave steepness, $s_{0\ m-1,0\ toe}$ [-]	$0.009 < s_{0\ m-1,0} < 0.060$
Angle of wave incidence, β [^{o}]	$0^o < \beta < 70^o$
Relative water depth, $h / H_{m0\ toe}$ [-]	$1.20 < h / H_{m0\ toe} < 9.80$
Relative crest freeboard, $R_c / H_{m0\ toe}$ [-]	$-2.00 < R_c / H_{m0\ toe} < 0.70$
Relative crest width, $W_c / H_{m0\ toe}$ [-]	$0.60 < W_c / H_{m0\ toe} < 6.00$
Front slope, cot $\alpha_{u\ f}$ [-]	$1.0 < \cot \alpha_{uf} < 3.8$
Roughness factor, γ_f [-]	1.0
Notional Permeability factor, P [-]	0.10

Table 5-2 Prediction model input boundaries for smooth structures

Parameter considered	Prediction model input boundary
Incident significant wave height, $H_{m0\ toe}$ [-]	$H_{m0\ toe} > 0.03$m $H_{m0\ toe} / h < 0.50$
Mean wave steepness, $s_{0\ m-1,0\ toe}$ [-]	$0.006 < s_{0\ m-1,0} < 0.080$
Angle of wave incidence, β [^{o}]	$0^o < \beta < 45^o$, but enter as input value: $\beta = 0^o$
Relative water depth, $h / H_{m0\ toe}$ [-]	$1.55 < h / H_{m0\ toe} < 11.00$
Relative crest freeboard, $R_c / H_{m0\ toe}$ [-]	$-3.50 < R_c / H_{m0\ toe} < 1.80$
Relative crest width, $W_c / H_{m0\ toe}$ [-]	$0.01 < W_c / H_{m0\ toe} < 47.00$
Front slope, cot $\alpha_{u\ f}$ [-]	$1.0 < \cot \alpha_{uf} < 5.0$
Roughness factor, γ_f [-]	$0.38 < \gamma_f < 0.90$
Notional Permeability factor, P [-]	$0.10 < P < 0.60$

Table 5-3 Prediction model input boundaries for mound structures

6 Recommendations

In this final chapter some recommendations are presented for the use of the model as well for some future studies to improve the prediction of wave transmission in a later stadium.

6.1 Use of the recent prediction model

The recent prediction model is made with Matlab® 7, including the Neural Network Toolbox. Guidance to the use the prediction model is given in the following sections. Three basic steps are presented to obtain a prediction of the wave transmission coefficient for a specific case:

- Introducing the specific characteristics of the designed breakwater structure and its hydraulic conditions by means of setting the right parameters in the input file (Section 6.1.1)
- Running the Matlab M-files: 'Prediction.m' and / or 'Sensitivity.m' (see Section 6.1.2)
- Analyzing the given results of the prediction model (Section 6.1.3)

It is recommended to follow the guideline described in this paragraph to obtain a valid and reliable prediction of the wave transmission coefficient.

6.1.1 Making the input file

It is very important to apply the same definitions of parameters as used in this report. The reliability of the prediction of the wave transmission coefficient is very much depending on the right determination of the input parameters according to the definitions in Paragraph 3.3. Unreliable input parameters will cause in principle an unreliable prediction of the wave transmission coefficient.

Hydraulic parameters
All inputs of hydraulic parameters are defined at the toe of the considered structure. It is at this position were the prediction model is based on for all spectral wave parameters. It is recommended to use only wave characteristics from deeper water if at the toe of structure relative deep-water relations are valid. If not, it is recommended to simulate the waves to the toe of the structure like this is done in this study with the numerical model SWAN (free downloadable at: www.fluidmechanics.tudelft.nl/swan/). The input boundaries of the hydraulic parameters are given in Paragraph 5.10.

Structural parameters
The more easily the considered structure section can be described with the structural parameters present for the input file (h [m], R_c [m], W_c [m], cot $\alpha_{u\ f}$ [-], P [-], γ_f [m]), the more reliable the prediction of the wave transmission coefficient will be. The input boundaries of the structural parameters are given in Paragraph 5.10.

Input file
The user has to introduce the structural characteristics of the designed breakwater as well as the hydrodynamic conditions into the model with use of an input file called 'Input-LCS.xls'. This file is a simple Excel® sheet (see Figure 6-1) where the user can introduce easily the data of the structure. The file has to be saved with the original name 'Input-LCS.xls' (it will be necessary to overwrite the

file for each time changes are made). Scaling is done automatically by the program, so a user can enter either model- and prototype values to this file.

	A	B	C	D	E	F	G	H	I
1	**Hmo toe**	**Tm-1,0 toe**	**h**	**Rc**	**Wc**	**cotα u f**	**β**	**P**	**γ;f**
2	[m]	[s]	[m]	[m]	[m]	[-]	[-]	[-]	[-]
3									
4	0.313	2.331	1.680	-0.105	1.825	2.000	0.000	0.500	0.450
5									

Figure 6-1 Example of the input file 'Input-LCS.xls' within MS Excel

6.1.2 Running the prediction model

The prediction model can be opened with Matlab 7. There are two files present called 'Prediction.m' and 'Sensitivity.m'. The file 'Prediction.m' results a prediction for the wave transmission coefficient for the specific case entered to the file 'Input-LCS.xls'. When running the file 'Prediction.m', Matlab returns a predicted K_t and some additional information about the reliability of this predicted transmission coefficient. The file 'Sensitivity.m' can be used to perform a sensitivity analysis on individual parameters, to obtain insight of the influence of these parameters. For design purposes, the sensitivity analysis can be a helpful tool to optimize a design for the case of wave transmission.

Using the file 'Prediction.m'
After starting up Matlab 7, the file 'Prediction.m' can be opened. In the command screen must be typed: Prediction. Automatically, the program will read the input file 'Input-LCS.xls' for the specific case of the user and generates a prediction of K_t. Matlab will automatically calculate the predicted transmission coefficient and replies a K_t with additional information about the reliability of the prediction. Matlab returns the following results:

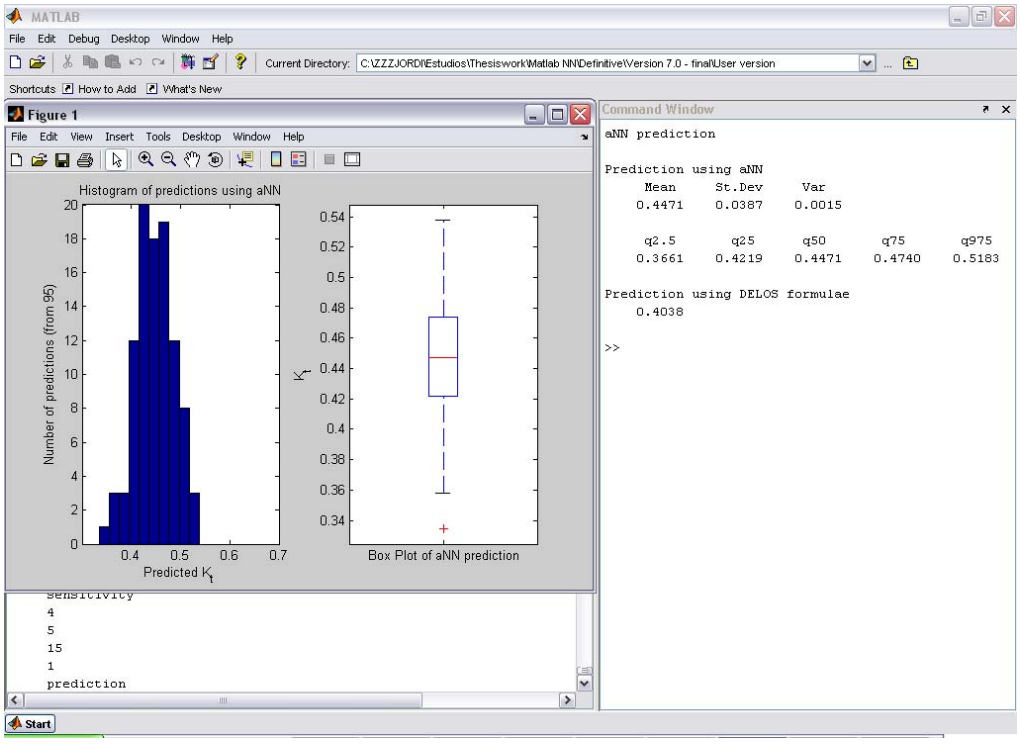

Figure 6-2 Example of the Matlab interface with prediction results

Figures
- Histogram of the distribution of the predicted transmission coefficient K_t
- Box plot of the predicted transmission coefficient K_t

Numerical values

- Mean K_t: This is the mean predicted wave transmission coefficient by the ensemble of neural networks for the user's case and should be used as the official prediction of K_t.
- Standard deviation of the predicted K_t
- Variance of the predicted K_t
- The following quintiles of the predicted K_t: $q_{2.5\%}$, $q_{25\%}$, $q_{50\%}$, $q_{75\%}$, $q_{97.5\%}$. The $q_{2.5\%}$ and $q_{97.5\%}$ are used to give the 95% confidence interval for the sensitivity file.

Using the file 'Sensitivity.m'
After starting up Matlab 7, the file 'Sensitivity.m' can be opened. This file predicts a transmission coefficient for a given range of an individual parameter to examine the influence or sensitivity. In the command screen must be typed: Sensitivity. The command screen shows all parameters that can be selected to perform a sensitivity analysis. Only one parameter can be varied while all other parameters remain constant as given to the file 'Input-LCS.xls'. To select one parameter one has to type in its corresponding number.

Matlab will ask the lower- and upper boundary of the range of the sensitivity analysis. Also the step size has to be entered. A smaller step size will make the calculation slower, but the produced sensitivity figure shows a gentler line. The sensitivity figure shows the mean prediction of the transmission coefficient (thick black line), the 95%-confidence band (big-dashed lines), the prediction of the DELOS formulae as term of comparison (small-dashed line) and the valid input boundaries (vertical red lines). Of course results outside the valid input boundaries are very unreliable and results cannot be used. A wide confidence means an unreliable prediction, so results for these regions should be interpreted with care. Help about this matter is given in Section 6.1.3.

6.1.3 Interpretation of results

The statistical values of the predicted wave transmission coefficient give insight in the reliability of the predicted transmission coefficient. In general can be stated, that the larger the standard deviation, the more unreliable the prediction is. The $q_{50\%}$ gives the median of all predicted transmissions coefficients by the ensemble of neural networks. In most case the $q_{50\%}$ will be very close to the mean predicted transmission coefficient. If these two values deviate much, the prediction should be interpreted as unreliable too.

6.2 Future use of the prediction model

Because the model is made within Matlab 7, also the use of the prediction model is at this moment only possible if Matlab 7 is available for a user. Like the classical empirical formulae it is recommended to make this model available for all users in the field of coastal engineering in the nearby future. Some possibilities are found to make the model accessible worldwide.

6.2.1 PHP in combination with Matlab

PHP is a server-side, cross-platform, HTML embedded scripting language that creates dynamic web pages. PHP-enabled web pages are treated just like regular HTML pages and can be created and edited the same way like regular HTML pages are normally created. It is possible to connect a web page to a server-installed Matlab interface. Every user with access to the internet can use the prediction model everywhere at any time.

A user would be able to enter his parameter to a website, submit the settings and a Matlab program on the web page server can easily read the information from the web page and perform the prediction calculation. After this, Matlab returns a file with the prediction of the transmission coefficient and PHP makes it possible to return the results this on the web page.

A disadvantage of this method is the fact that a user cannot modify the model to its own preference, because the model itself cannot be entered. Secondly, problems concerning the license of using Matlab for this kind of purposes should be taken into account as well.

6.2.2 Compiling the Matlab interface

The Matlab interface can be compiled to another computer language (for instance the c-language) in order to obtain a stand-alone version of the prediction model. This stand-alone executable could be placed on a website making it possible for future users to download it from the Internet and use it

on their own computer. In principle a wave transmission prediction program is programmed in that case.

6.2.3 Excel interface

In principle is the final prediction model not more than a giant empirical formula, which consists of large matrices and some appliances of functions to these matrices. If the sizes of the matrices are not too large, it is possible to let Excel perform the calculation. It is questionable if Excel is capable of carrying out such a big calculation without any problems. It is worthwhile to examine this possibility having in mind that Excel is widely applied program and simple to use for most future users.

6.3 Improvements of the prediction performance

Some recommendations are given below to improve the prediction model performance in the future.

6.3.1 Collecting more data with an angle of incidence

The sensitivity figures for the parameter β: angle of incidence show a wide band of confidence indicating the reliability of using this parameter can be improved. It is recommended to collect more data for smooth structures with a varying angle of incidence in order to train the prediction model again with this data. Especially because the angle of incidence showed to be important for wave transmission for smooth structure there is a possibility to make the prediction model more useful for this kind of structures. For mound structures, the angle of incidence is found to be less important but with more data with a varying angle of incidence this finding can be made clearer and a wider boundary can be given than valid for the present model.

6.3.2 Increasing the number of tests for smooth structure

Still the total number of smooth structures is only 21.5% of the data where the prediction model is based on. The model proves to be able to distinguish smooth from mound structures, however the prediction of the mound structures is more reliable (smaller bands of confidence) and the input boundaries for the input parameters are wide, so the range of applicability is larger. Increasing the number of tests for smooth structures would make the prediction model better for the case of predicting smooth structure. The prediction will be more reliable (narrower confidence bands over the whole data range) and a wider boundary will be present.

6.3.3 Increasing the number of tests for artificial reefs

The Aquareef dataset is describing an artificial reef breakwater structure, deviating very much from other available test sections within the database. It is recommended to include more datasets of artificial reefs made from other reef type armour units than Aquareef. A widely applied artificial reef armour unit is the Reefball from which is known that tests are performed in the past. As term of comparison it would be right to include more of this kind of structures to give lower weight to the characteristics of the Aquareef armour units for wave transmission on artificial reefs.

6.3.4 Investigating deviating prediction of certain datasets

For a small number of datasets, the prediction model showed to find a deviating wave transmission coefficient than measured. These datasets have been examined but no clear explanation can be found. It is recommended to valid these tests with new tests. The performed tests are old compared to new data and measure techniques have improved during the years. It could be that a more accurate transmission coefficient will be found at this moment, resulting in a better fit.

6.4 Future studies to wave transmission

6.4.1 Wave period

The wave period showed to be more important for smooth structures than for mound structures. Within this study no strong explanation can be given. It is therefore worthily to gather of perform more tests to find a possible explanation and check the found influence.

6.4.2 Water depth

The water depth in front the structure is found to be very important for smooth structures. It can physically be explained that the water depth influences the shape of the incident waves. It is very interesting to examine the influence of a foreshore on the shape of the incident waves and the type of breaking / transmission at the breakwater structure.

7 References

Ahrens, J.P. (1987). "Characteristics of reef breakwaters, CERC, Vicksburg, Technical Report CERC-87-17

Allsop, N.W.H. (1983), "Low-crest breakwaters, studies in random waves", Proc. Coastal Structures '83, Arlington, Virginia, pp. 94-107

d'Angremond K., van der Meer J.W., de Jong R. J. (1996). "Wave transmission at low crested structures", Proc. 25th Int. Conf. on Coastal Engineering, ASCE, 3305-3318.

Barron, A.R. (1993). "Universal approximations bounds for superposition of a sigmoidal function", IEEE Transactions on Information Theory, Vol. 39, No. 3, pp. 930-945.

Bishop, C.M. (1995). "Neural networks for pattern recognition", Oxford University Press, Oxford.

Battjes, J.A. and H.W. Groenendijk, 2000. "Wave height distributions on shallow foreshores". J. of CE, No. 40, 161-182.

Booij, N., Ris, R.C., Holthuijsen, L.H. (1999). "A third generation wave model for coastal regions, Part I, Model description and validation, Journal of Geophysical Research, 104, C4, pp. 7649-7666.

Briganti R, Van der Meer J.W., Buccino M., Calabrese M. (2003). "Wave transmission behind low crested structures", Proc. 3rd Coastal Structures Conference.

Calabrese M., Vicinanza V., Buccino M. (2002). "Large scale experiments on the behavior of low-crested and submerged breakwaters in presence of broken waves". Proc. 28th Int. Conf. On Coastal Engineering, ASCE, pp. 1900-1912.

Daemen, I. F. R. (1991). "Wave transmission at low crested structures". MSc thesis, Delft University of Technology, Delft, The Netherlands.

Daemrich, K.F. and Kahle, W. (1985). Schutzwirkung von Unterwassenwellen brechern unter dem einfluss unregelmässiger Seegangswellen. Eigenverslag des Franzius-Institutes fur Wasserbau und Kusteningenieurswesen, Heft 61. (In German)

Daemrich, K.F., Mai, S., Ohle, N., (2002), "Wave transmission at rubble mound structures", Proc. Of the 1st German-Chinese Joint Symposium on Coastal and Ocean engineering, pp. 299-310, Rostock Germany.

Delft Hydraulics (1985). "Laem Chabang Harbour: Report on model investigation. Two dimensional tests on breakwater stability and overtopping". Report no. M2090-07 (Confidential)

Delft Hydraulics, (1990), "Berm breakwater study for Karwar, India: Model investigation with oblique and multi-directional seas", Report no. H524 (Confidential).

Delft Hydraulics (1993). "Stability of breakwater truck, Kerith breakwater: Two-dimensional model tests", Report no. H1872 (Confidential)

Delft Hydraulics (1994), "Kerith breakwater: Three-dimensional model tests", Report no. H1872 (Confidential)

Delft Hydraulics (1994), "Stabiliteit van lage golfbreker met tetrapods: meetverslag". Report no H2014 (In Dutch)

Delft Hydraulics (1994), "Waterkering Harlinge: kruinhoogtes en belastingen op de keermuur", Report no. H2014 (In Dutch)

Delft Hydraulics (1994), "Ennore Coal Port Project, India: 3-D stability tests ", Report no. H1974

Delft Hydraulics (2003), "Stabiliteit van kruinmuur en steenzetting op Zuiderpier van Harlingen: Verslag Deltagootonderzoek.", Report no. H4171.

Delft Hydraulics (2002), "AmWaj Island Development, Bahrein; Physical modeling of submerged breakwaters", Report no. H4087

Efron, B. (1982). "The Jackknife, the Boostraps and Other Resampling Plans", Philadelphia: SIAM

Efron, B. Tibshirani, R.J. (1993). "An introduction to the bootstrap", Chapman&Hall, New York.

Foresee, F. D., M. T. Hagan, "Gauss-Newton approximation to Bayesian regularization," Proceedings of the 1997 International Joint Conference on Neural Networks, pages 1930-1935, 1997.

Hagan, M. T., M. Menhaj, "Training feedforward networks with the Marquardt algorithm," IEEE Transactions on Neural Networks, vol. 5, no. 6, pp. 989-993, 1994.

Hagan, M. T., H. B. Demuth, and M. H. Beale, Neural Network Design, Boston, MA: PWS Publishing, 1996.

Hirose, N., Watanuki A. and Saito M. (2002). "New types Units for Artificial Reef Development of Ecofriendly Artificial Reefs and the Effectiveness Thereof", Proc. 30th International navigation congress, PIANC 2002.

Hearn, J.K. (1987), "An analysis of stability of and wave field modification due to low-crested sacrificial breakwaters", University of Florida, Report UFL/COEL/MP-87/1

Heijn, K.M. (1997). "Wave transmission at vertical breakwaters", MS thesis, Delft University of Technology, Delft, The Netherlands.

Hornik, K., Stinchcombre, M., White, H., 1989. "Multilayer feedforward networks are universal approximators", Neural networks, Vol. 2, pp. 359-366.

Gironella, X., Sanchez-Arcilla, A., Briganti R., Sierra, J.P>, and Moreno, L., (2002), "Submerged detached breakwaters: towards a functional design", Proc. 28th Int. Conf. On Coastal Engineering, ASCE, pp. 1768-1777.

Mase, H., Sakamoto, M., Sakai, T. (1995). "Neural network of stability analysis of rubble-mound breakwaters", Journal of waterway, Port, Coastal, and Ocean Engineering div., ASCE Vol. 121(6), pp. 294-299.

MacKay, D. J. C., "Bayesian interpolation," Neural Computation, vol. 4, no. 3, pp. 415-447, 1992.

MacKay, D.J.C. (1992). "A practical Bayesian framework for backpropagation networks, Neural Computation, 4(3), pp. 448-472.

Marquardt, D., "An Algorithm for Least-Squares Estimation of Nonlinear Parameters," SIAM J. Appl. Math. Vol. 11, pp 431-441, 1963.

Mase, H., Sakamoto, M., Sakai, T., (1995). "Neural network for stability analysis of rubble-mound breakwaters", ASCE J. of waterway, Port, Coastal Engineering div., 121(6), pp. 294-299

Medina, J.R., (1999). "Neural network modelling of run-up and overtopping", Proc. 2nd Coastal Structures Conference, pp. 421-429.

Medina, J.R., González Escrivá, J.A. Garrido, J., de Rouck, J., (2002). "Overtopping analysis using neural networks", Proc. 28th Int. Conf. on Coastal Engineering, Cardiff, Wales, Vol. 2, pp. 2165-2177.

Melito, I., and Melby, J.A., (2002), "Wave runup, transmission, and reflection for structures armoured with CORE-LOC". J. of Coastal Engineering 45, pp. 33-52, Elsevier.

Padova, University of., Ruol, P., Faedo, A., Paris, A., "Physical model study of water piling up behind low-crested structures", Proc. 29th Inr. Conf. On Coastal Engineering, ASCE.

Panizzo, A., Briganti, R., Van der Meer, J.W., Franco, L., (2003). "Analysis of wave transmission behind low crested structures using neural networks", Proc. 4th Int. Coastal Structures Conference 2003, Portland, Oregon, pp. 555-566.

Powell, K.A. and Allsop, N.W.H (1985), "Low-crest breakwaters, hydraulic performance and stability", Hydraulic Research, Wallingford, Report SR 57

Pozueta, B., Van Gent, M.R.A., Van den Boogaard, H., Medina, J.R. (2004), "Neural network modelling of wave overtopping at coastal structure", Proc. 29th Int. Conf. on Coastal Engineering, ASCE.

Roeleveld, B.J. (1997). "Eigenschappen van gabionboxen onder golfaanval", MSc.-Thesis, Technische University Delft, Delft. (In Dutch)

Rojas, R. (1996). "Neural networks – A systematic introduction", Springer-Verlag, Berlin, New York.

Seabrook S.R. and Hall K.R. (1998). "Wave transmission at submerged rubble-mound breakwaters", Proc. 26th Int. Conf. on Coastal Engineering, ASCE, pp. 2000-2013.

Seelig, W.N. (1980). "Two-dimensional tests of wave transmission and reflection characteristics of laboratory breakwaters", WES, CERC, Fort Belvoir, Technical Report No.80-1.

Steendam, G. J., van der Meer, J. W., Verhaeghe, H., Besley, P., Franco, L. and M. van Gent, 2004. "The international database on wave overtopping", ASCE, Proc. ICCE 2004, Lisbon

Taveira-Pinto, F., Veloso-Gomez, F., Avilez Valente, P., (1997), "Energy Dissipation of Low-crested Breakwaters", Proc. Of the 3rd Int. Symposium Waves, Virginia 1997

TAW (2002). *Technisch rapport golfoploop en golfoverslag bij dijken* (Technical report on wave runup and wave overtopping at dikes - in Dutch). Technical Advisory Committee on Water Defences.

Van den Boogaard, H., Mynett, A.E. and Heskes, T. (2000), "Resampling techniques for the assessment of uncertainties in parameters and predictions of calibrated models", Proc. Hydroinformatics Conference, IOWA.

Van der Meer, J.W. (1988a). "Rock slopes and gravel beaches under wave attack", Phd-Thesis, Delft University of Technology. Also: Delft Hydraulics Communication No. 396

Van der Meer, J.W. (1990a). "Data on wave transmission due to overtopping, Delft Hydraulics Report no. H986, prepared for CUR C 67.

Van der Meer, J.W. (1990b). "Low-crested and reef breakwaters", Delft Hydraulics Report no. H986II, prepared for CUR C 67.

Van der Meer, J.W. and Daemen, I.F.R. (1994). "Stability and wave transmission at low crested rubble-mound structures", Journal of Waterway, Port, Coastal, and Ocean Engineering, Vol. 1, pp. 1-19.

Van der Meer, J.W. (2000). "Golfrandvoorwaarden voor dijkontwerp in door dammen afgeschermde gebieden:, Band B. Beschrijving van golftransmissie en dubbeltoppige spectra", ref: no: IJA 2069, Infram.

Van der Meer, J.W., Briganti, R., Wang, B. and Zanuttigh, B. (2004), "Wave transmission at low-crested structures including oblique wave attack", Proc. 29th Int. Conf. on Coastal Engineering, ASCE.

Van der Meer, J.W., M.R.A. van Gent, B. Pozueta, H. Verhaeghe, G.J. Steendam and J.R. Medina, 2004. "Applications of a neural network to predict wave overtopping at coastal structures". ICE, Proc. Coastlines, Structures and Breakwaters 2005, London.

Van Gent, M.R.A., van der Boogaard, H.F.P. (1998). "Neural network modelling of forces on vertical structures", Proc. 26th Int. Conf. on Coastal Engineering, ASCE, pp. 2096-2109.

Van Gent, M.R.A., Pozueta, B., Van den Boogaard, H., Medina, J.R., (2004). "Neural network modelling of wave overtopping at coastal structures", CLASH WP8 Neural Network, Delft Hydraulic, Delft, The Netherlands.

Verhaeghe, H. (2005). "Neural network prediction of wave overtopping at coastal structures", PhD thesis, Ghent University, Ghent, Belgium. ISBN 90-8578-018-7.

Verhaeghe, H., Van der Meer, J.W., Steendam, G.-J., Besley, P., Franco L. And Van Gent, M.R.A. (2003). "Wave overtopping database as the starting point for a neural network prediction method" ASCE, Proc. Coastal Structures 2003, Portland.

Wang, B. (2003), "Oblique wave transmission at low-crested structures", MSc-Thesis, IHE Delft, The Netherlands.

Zanuttigh, B., and Lambertini, A., (2000), "3D Hydrodynamic tests at Aalborg University", DELOS report no. EVK3-CT-2000-00041, Denmark.